PB84-153204

Pilot Demonstration of Magnetic Filtration with Continuous Media Regeneration

Research Triangle Inst.
Research Triangle Park, NC

Prepared for

Industrial Environmental Research Lab.
Research Triangle Park, NC

Feb 84

U.S. Department of Commerce
National Technical Information Service
NTIS

PB84-153204

EPA-600/7-84-011
February 1984

PILOT DEMONSTRATION OF MAGNETIC FILTRATION WITH CONTINUOUS MEDIA REGENERATION

by

Carroll E. Ball
and
David W. Coy

Research Triangle Institute
Post Office Box 12194
Research Triangle Park, North Carolina 27709

Contract No. 68-02-3142

EPA Project Officer: William B. Kuykendal
Particulate Technology Branch
Industrial Environmental Research Laboratory
Research Triangle Park, NC 27711

Prepared for

U.S. Environmental Protection Agency
Office of Research and Development
Washington, D.C. 20460

REPRODUCED BY
NATIONAL TECHNICAL
INFORMATION SERVICE
U.S. DEPARTMENT OF COMMERCE
SPRINGFIELD, VA. 22161

TECHNICAL REPORT DATA

(Please read Instructions on the reverse before completing)

1. REPORT NO.
EPA-600/7-84-011

2.

3. RECIPIENT'S ACCESSION NO.
PB8 4 153204

4. TITLE AND SUBTITLE
Pilot Demonstration of Magnetic Filtration with Continuous Media Regeneration

5. REPORT DATE
February 1984

6. PERFORMING ORGANIZATION CODE

7. AUTHOR(S)
Carroll E. Ball and David W. Coy

8. PERFORMING ORGANIZATION REPORT NO.

9. PERFORMING ORGANIZATION NAME AND ADDRESS
Research Triangle Institute
P.O. Box 12194
Research Triangle Park, North Carolina 27709

10. PROGRAM ELEMENT NO.

11. CONTRACT/GRANT NO.
68-02-3142

12. SPONSORING AGENCY NAME AND ADDRESS
EPA, Office of Research and Development
Industrial Environmental Research Laboratory
Research Triangle Park, NC 27711

13. TYPE OF REPORT AND PERIOD COVERED

14. SPONSORING AGENCY CODE
EPA/600/13

15. SUPPLEMENTARY NOTES IERL-RTP project officer is William B. Kuykendal, Mail Drop 61, 919/541-7865.

16. ABSTRACT

The report describes the design and construction of a continuous High Gradient Magnetic Filtration (HGMF) mobile pilot plant, as well as some of the background work in HGMF at Research Triangle Institute. The field start-up and performance characterization of the mobile pilot plant are discussed in detail. Experimental data and data analysis are given, as well as an economic evaluation and comparison of HGMF with other particulate control devices. The mobile pilot plant, with a nominal flow capacity of 3,060 cu m/hr, was designed and built to evaluate the use of HGMF for particulate emission control on an electric arc furnace. A 5-month program was conducted at Georgetown Steel Corporation's plant in Georgetown, SC, to test the performance of HGMF. A 500-hr long-term test was scheduled, and later changed to permit additional characterization studies. The pilot plant collection efficiency was less than expected for the stainless steel wool matrix packed to a density of 1.5% by volume. The matrix was then changed to an expanded metal packed to a density of 3.5% by volume, which resulted in much lower pressure drops, but even lower collection efficiencies. The expanded metal matrix was then packed to a density of 6.0% by volume, which gave higher collection efficiencies (94-96%) than the steel wool and a slightly lower pressure drop.

17. KEY WORDS AND DOCUMENT ANALYSIS

a. DESCRIPTORS		b. IDENTIFIERS/OPEN ENDED TERMS	c. COSATI Field/Group	
Pollution	Aerosols	Pollution Control	13B	
Filtration	Electric Arc Furnaces	Stationary Sources	07D	13A
Magnetic Separators		High Gradient Magnetic Separators	13I	
Magnetic Fields			20C	
Particles		Particulate	14G	
Dust			11G	

18. DISTRIBUTION STATEMENT
Release to Public

19. SECURITY CLASS *(This Report)*
Unclassified

20. SECURITY CLASS *(This page)*
Unclassified

21. NO. OF PAGES
130

22. PRICE

EPA Form 2220-1 (9-73)

NOTICE

This document has been reviewed in accordance with U.S. Environmental Protection Agency policy and approved for publication. Mention of trade names or commercial products does not constitute endorsement or recommendation for use.

ABSTRACT

A mobile pilot plant with a nominal flow capacity of 3,060 m^3/hr (1,800 cfm) was designed and built to evaluate the use of High Gradient Magnetic Filtration (HGMF) for particulate emission control on an electric arc furnace (EAF). A five-month test program was conducted at Georgetown Steel Corporation's plant in Georgetown, South Carolina, to test the performance of the HGMF. A 500 hour long-term test was scheduled and later changed in order to perform additional characterization studies.

The pilot plant collection efficiency was less than expected for the stainless steel wool matrix packed to a density of 1.5 percent by volume. The matrix was then changed to an expanded metal packed to a density of 3.5 percent by volume, which resulted in much lower pressure drop measurements but even lower collection efficiencies. The expanded metal matrix was then packed to a density of 6.0 percent by volume which gave higher collection efficiencies than the steel wool and a slightly lower pressure drop.

During the field test operations, there were no significant problems with the HGMF mobile pilot plant equipment.

The report describes the design and construction of the continuous HGMF mobile pilot plant, as well as some of the background work in High Gradient Magnetic Filtration done at RTI. The field start-up and performance characterization of the mobile pilot plant are discussed in detail. The experimental data and data analysis are given as well as an economic evaluation and comparison of the HGMF with other particulate control devices.

TABLE OF CONTENTS

Page

ABSTRACT iii
FIGURES vi
TABLES. viii
ACKNOWLEDGEMENT x

1.0 SUMMARY. 1

2.0 CONCLUSIONS. 3

3.0 RECOMMENDATIONS. 5

4.0 BACKGROUND DEVELOPMENT 6
  4.1 BASIC CONCEPT 6
  4.2 HGMF DEVELOPMENT AND APPLICATIONS 6
  4.3 POTENTIAL APPLICATION TO PARTICULATE EMISSION CONTROL . 8
  4.4 PRELIMINARY DESIGN AND DEVELOPMENT. 10
  4.5 MATHEMATICAL MODEL. 13
  4.6 SITE SELECTION FOR CURRENT FIELD TESTS. 13

5.0 DETAILED DESIGN AND CONSTRUCTION OF THE HGMF MOBILE PILOT PLANT. 24

6.0 FIELD OPERATIONS 31
  6.1 DESCRIPTION OF THE ELECTRIC ARC FURNACE AT GEORGETOWN, SOUTH CAROLINA. 31
  6.2 INSTALLATION OF STARTUP OF THE PILOT PLANT. 34
    6.2.1 Temperature Control. 34
    6.2.2 Filter Cleaning. 34
    6.2.3 Magnet Operation 35
    6.2.4 Flow Measurement and Control 35
    6.2.5 Final Site Setup 36

7.0 PERFORMANCE CHARACTERIZATION 39
  7.1 TEST PLAN 39
    7.1.1 Performance Charcterization and Optimization . . . 39
    7.1.2 Performance Data for Principal Variables 39
  7.2 TEST PROCEDURES 42
    7.2.1 Sampling Procedures. 42
    7.2.2 Filter Operating Procedures. 44
  7.3 COARSE GRADE STAINLESS STEEL WOOL MATRIX. 44
  7.4 EXPANDED METAL MATRIX 53
    7.4.1 Packing Density of 2.5 Percent by Volume 53
    7.4.2 Packing Density of 6.0 Percent by Volume 61
    7.4.3 Additional Testing 63

8.0 DATA ANALYSIS 70
  8.1 PERFORMANCE DATA 70
    8.1.1 Overall Performance 70
      8.1.1.1 Steel Wool-Packing Density 1.5 Percent . . . 71
      8.1.1.2 Expanded Metal-Packing Density 3.5 Percent 73
      8.1.1.3 Expanded Metal-Packing Density 6.0 Percent 73
      8.1.1.4 Performance Summary--All Matrices, All Packing Densities 78
    8.1.2 Performance By Particle Size 82
  8.2 CHEMICAL AND MAGNETIC CHARACTERISTICS OF ELECTRIC ARC FURNACE DUST 89
    8.2.1 Magnetic Analysis 89
    8.2.2 Chemical Analysis 93
  8.3 MODEL DISCUSSIONS 97
  8.4 DISCUSSION OF RESULTS 103

9.0 ECONOMICS 111
  9.1 CAPITAL COSTS 113

10.0 REFERENCES 116

FIGURES

Number		Page
1	Magnetic analysis of dust samples from HGMF pilot plant tests	11
2	Particle size distribution, preliminary tests	15
3	Particle size distribution, average of runs 2, 3, and 4	16
4	Georgetown Steel HGMF test--preliminary sampling program	18
5	HGMF--Collection efficiency vs. particle size	20
6	Magnetic analysis of EAF dust samples	21
7	Flow schematic of continuous HGMF system	25
8	HGMF mobile pilot plant	26
9	HGMF pilot plant under construction	28
10	HGMF pilot plant under construction	29
11	Material balance of electric arc furnace based on 1,000 kg of steel produced	32
12	Rough site map	33
13	HGMF pilot plant at Georgetown Steel	37
14	HGMF pilot plant at Georgetown Steel	38
15	HGMF test points	41
16	Filter train for determination of mass efficiency	43
17	Georgetown Steel HGMF test--steel wool matrix (packing density 0.015)	47
18	Georgetown Steel HGMF test--steel wool matrix (packing density 0.015)	48
19	Georgetown Steel HGMF test--steel wool matrix (packing density 0.015)	49
20	Georgetown Steel HGMF test--steel wool matrix (packing density 0.015)	50
21	Georgetown Steel HGMF test--steel wool matrix (packing density 0.015)	51
22	Georgetown Steel HGMF test--steel wool matrix (packing density 0.015)	52
23	Georgetown Steel HGMF test--expanded metal matrix (packing density 0.035)	55
24	Georgetown Steel HGMF test--expanded metal matrix (packing density 0.035)	56
25	Georgetown Steel HGMF test--expanded metal matrix (packing density 0.035)	57
26	Georgetown Steel HGMF test--expanded metal matrix (packing density 0.035)	58
27	Georgetown Steel HGMF test--expanded metal matrix (packing density 0.035)	59
28	Georgetown Steel HGMF test--expanded metal matrix (packing density 0.035)	60
29	Georgetown Steel HGMF test--expanded metal matrix (packing density 0.06)	64
30	Georgetown Steel HGMF test--expanded metal matrix (packing density 0.06)	65
31	Georgetown Steel HGMF test--expanded metal matrix (packing density 0.06)	68
32	Georgetown Steel HGMF test--expanded metal matrix (packing density 0.06)	69

33 Georgetown Steel HGMF test--expanded metal matrix (packing density 0.06). 79
34 Georgetown Steel HGMF test--penetration vs. regression function (all matrices and packing densities) 80
35 Georgetown Steel HGMF test--penetration vs. particle size (steel wool matrix 0.015). 83
36 Georgetown Steel HGMF test--penetration vs. particle size (expanded metal matrix 0.035). 84
37 Georgetown Steel HGMF test--penetration vs. particle size (expanded metal matrix 0.06) 85
38 Georgetown Steel HGMF test--penetration vs. particle size (expanded metal matrix 0.06) 86
39 Georgetown Steel HGMF test--penetration vs. particle size (steel wool matrix 0.015). 87
40 Georgetown Steel HGMF test--penetration vs. particle size (expanded metal matrix 0.035). 88
41 Georgetown Steel HGMF test--specific magnetization vs. particle size, steel wool matrix (packing density 0.015). 92
42 Georgetown Steel HGMF test--particle size elemental analysis, expanded metal matrix (packing density 0.06) 98
43 Georgetown Steel HGMF test--particle size elemental analysis, expanded metal matrix (packing density 0.06) 99
44 Georgetown Steel HGMF test--iron penetration vs. particle size (packing density 0.06) 100
45 Georgetown Steel HGMF test--zinc penetration vs. particle size expanded metal matrix (packing density 0.06) 101
46 Illustration of particle capture by a single wire. 102
47 Georgetown Steel HGMF test--theoretical and actual penetration vs. particle size, expanded metal matrix (packing density 0.06). 106
48 Georgetown Steel HGMF test--theoretical and actual penetration vs. particle size, expanded metal matrix (packing density 0.06). 107

TABLES

Number   Page

1 HGMF APPLICATIONS BEING INVESTIGATED. 7

2 EXTENDED CHARACTERISTICS OF UNCONTROLLED GAS STREAMS FROM SEVERAL SOURCES 9

3 COMPONENT MASS BALANCES BASED ON CHEMICAL ANALYSIS . . 12

4 ELEMENTS (PERCENT BY MASS)(OBTAINED BY ATOMIC ADSORPTION 17

5 BAGHOUSE DUST ANALYSIS 19

6 GEORGETOWN STEEL HGMF TESTS (STEEL WOOL MATRIX-PACKING DENSITY 0.015) 45

7 GEORGETOWN STEEL HGMF TESTS (EXPANDED METAL MATRIX-PACKING DENSITY 0.035) 54

8 GEORGETOWN STEEL HGMF TESTS (EXPANDED METAL MATRIX-PACKING DENSITY 0.06). 62

9 GEORGETOWN STEEL HGMF TESTS (EXPANDED METAL MATRIX-PACKING DENSITY 0.06, NO RECYCLE). 67

10 HGMF OVERALL PERFORMANCE REGRESSION COEFFICIENTS, STEEL WOOL MATRIX. 72

11 HGMF OVERALL PERFORMANCE REGRESSION COEFFICIENTS EXPANDED METAL MATRIX, 3.5 PERCENT 74

12 HGMF OVERALL PERFORMANCE REGRESSION COEFFICIENTS EXPANDED METAL MATRIX, 6 PERCENT 75

13 COMPARISON OF REGRESSION STATISTICS EXPANDED METAL MATRIX - 6 PERCENT 77

14 REGRESSION COEFFICIENTS FOR EACH FILTER MATRIX AND PACKING DENSITY. 81

15 PREDICTED FILTER PERFORMANCE FOR EACH FILTER MATRIX AND PACKING DENSITY. 81

16 SPECIFIC MAGNETIZATION OF BULK DUST SAMPLES. 91

17 CHEMICAL ANALYSES OF BULK DUST SAMPLES - WEIGHT PERCENT. 94

18 ELEMENTAL PENETRATION PERCENT - BULK SAMPLES 95

Number		Page
19	CORRELATION OF REENTRAINMENT CORRECTION.	104
20	CORRELATION OF REENTRAINMENT CORRECTION FOR THE HGMF TESTS AT GEORGETOWN STEEL.	105
21	COSTS OF VARIOUS CONTROL OPTIONS FOR EAF PARTICULATE EMISSION	112
22	DIRECT OPERATING COSTS	115

ACKNOWLEDGEMENTS

The authors wish to acknowledge the assistance and support of the following individuals in various segments of this work.

William Kuykendal, Norman Plaks, and Dennis C. Drehmel from EPA-IERL, who provided support and direction throughout the project; Charles Gooding from Clemson University for his expert assistance during all phases of the project.

The author would like to thank Georgetown Steel Corporation for allowing us to perform the field testing at their electric arc furnace steel plant in Georgetown, South Carolina, and Roscoe Hinson for his invaluable support and assistance throughout the program.

Douglas VanOsdell and J. Spivey from RTI, were very helpful in the design, construction, and operation of the pilot plant and the resultant data analysis. Technicians Daryl Smith, David Carter, and Don O'Neal, also from RTI, were key participants in the construction and field operation of the pilot plant.

1.0 SUMMARY

Since the commercialization of High Gradient Magnetic Filtration (HGMF) in the clay industry 10 years ago, the applications of magnetic separation of process streams have been steadily increasing. Some of the applications are mineral beneficiation, coal deashing, coal desulfurization, wastewater treatment, and blood component separation. The application of HGMF to air pollution, however, is a recent development. From 1975 to 1977 RTI conducted experimental work, funded by the U.S. Environmental Protection Agency, in the application of HGMF to air pollution control. Magnetic separation was tested in the laboratory on several dusts from the iron and steel industry. There were promising results from the following iron and steel industry sources; basic oxygen furnace (BOF); electric arc furnaces (EAF); blast furnace (BF); open hearth furnace; scarfing machine; and the sinter machine.

Tests run on the laboratory pilot plant demonstrated high collection efficiencies on the BOF and EAF dusts and identified the effects of important operating variables. A mathematical model was also developed to correlate the data and aid in the field pilot plant design.

A mobile pilot plant with a nominal flow capacity of 5,100 m^3/hr (3,000 cfm) was designed and built by RTI and tested on a Pennsylvania Sintering Plant.

The pilot plant was a cyclic design composed of two complete systems that permitted filtering of the gas stream by one system while the other was cleaning itself by backflushing. The overall efficiency data were low for these tests, however, due to the low specific magnetization of the sinter plant dust.

It was then decided to design and build a pilot plant with continuous media regeneration and test it on a dust with higher specific magnetization such as BOF or EAF dust.

A presentation was given to the American Iron and Steel Institute in November, 1980 describing prior HGMF work and the present objectives. At this time, Georgetown Steel Corporation offered to let us conduct field tests at their electric arc furnace steel plant in Georgetown, South Carolina. The

Georgetown steel plant was picked as the site for our pilot plant field test work after performing magnetization studies and chemical analyses on dust obtained from the EAF air pollution control system.

The mobile pilot plant is a continuous HGMF system which is designed for a nominal flow capacity of 3,060 m^3/hr (1,800 cfm). The pilot plant contains a Sala-HGMS® Carousel Model 120-05-00 (Sala Magnetics Inc., Cambridge, Mass.), which is a continuous device that incorporates a magnet head and a filter cleaning station mounted 180° apart on a rotating carousel.

In June, 1981 the pilot plant was moved to Georgetown, South Carolina and connected to a slipstream from the exhaust of the three EAF's just upstream of a baghouse. After startup and debugging, the test program was begun to give results on the effects of filter density, applied magnetic field, and gas velocity on overall and fractional collection efficiency. A 500 hour long term test was planned at optimum operating conditions and later cancelled due to the lower than expected collection efficiencies. It was decided to use the remaining time for additional performance characterization tests with changes in the pilot plant recycle stream. Total mass and fractional collection efficiency tests were conducted and samples of the dust entering, exiting, and captured by the pilot plant were collected for magnetic and chemical analysis.

The results of the field tests were used to make technical and economic assessments of the application of HGMF to EAF's, and to compare HGMF to other types of pollution control devices. In particular, capital and operating cost were developed to compare HGMF to fabric filters, electrostatic precipitators, and venturi scrubbers.

The following sections of this report present the background work done at RTI in HGMF as applied to air pollution control and the detailed design, construction, and operation of the continuous HGMF mobile pilot plant. The results and analyses of the data from the field tests are presented along with the economic analysis and comparison of a full scale HGMF system to the generic pollution control systems, and conclusions.

2.0 CONCLUSIONS

The following list of conclusions was drawn from the field operation of the HGMF mobile pilot plant:

1. While no long term continuous 500 hour test was performed, the continuous cleaning system for the filter was capable of maintaining a stable pressure drop through the matrix at each of the velocity conditions during one to two week periods of performance characterization.
2. Test series were performed on two types of matrices at three levels of matrix packing density. The best overall performance of the HGMF unit was achieved with the expanded metal matrix at a packing density of 6 percent. The highest efficiency level achieved was 96.4 percent with five of nine tests (excluding zero applied magnetic field tests) in the range of 93.9 to 96.4 percent.
3. Pressure drop through the filter matrices varied directly with the superficial gas velocity through the filter, approximately as the square of the velocity. In the velocity range of 4 to 8 m/s, the expanded metal matrix at 6 percent had lower pressure drops (10 cm H_2O to 46 cm H_2O) than the steel wool matrix (16 cm H_2O to 50 cm H_2O). Given the better overall performance (both efficiency and pressure drop) with the expanded metal at 6 percent packing density, it was the preferred filter matrix.
4. Fractional penetration curves show performance of the HGMF to be relatively poor (85 percent efficiency or less) in the particle size range below 1 μm.
5. Elemental chemical analyses show iron removal efficiencies are higher than overall mass efficiencies as determined from thimble dust samples. However, elemental analyses performed on cascade impactors samples show the iron penetration to be as much as 6 percent when overall mass penetration is 9 percent.

Potential explanations for inadequate capture of iron-bearing particles include the following:

a. magnetic forces acting on the fine particles are not sufficent to effect capture as the gas passes through the filter due to insufficient residence time,

b. some of the iron occurs in complex compounds with zinc that is not sufficiently magnetic to be captured; this is supported by work done at Lehigh University on waste dusts from electric arc furnaces, and

c. reentrainment.

6. The overall penetration of electric arc furnace dust through HGMF measured in this program must be reduced by a factor of 2 or 6 to compete with the performance of conventional particulate control devices applied to new sources. Standards for existing sources in some states might permit the retrofit of an HGMF.

7. Assuming HGMF performance can reach a competitive level in the configuration and operating mode tested in this program (e.g. 99 percent efficiency), comparative annualized costs for HGMF, fabric filters, ESPs, and venturi scrubbers show that HGMF can compete economically with venturi scrubbers, but is more expensive than fabric filters and ESPs. Since to achieve that level of performance on EAF dust, it would be necessary to reduce the gas velocity and/or increase filter length, it will be difficult for HGMF to compete as a control device for EAFs.

3.0 RECOMMENDATIONS

It appears that high gradient magnetic filtration's potential as an alternate particulate control device is limited. While the high gradient magnetic filtration achieved on electric arc furnace (EAF) dust was significantly better than on sinter plant dust, it did not reach a level that would compete with conventional pollution control devices. The cost estimates presented in this report suggest that HGMF might compete best in applications in which venturi scrubbers are usually applied. Basic oxygen furnaces (BOF), particularly those of closed hood design yielding combustible waste gas, may be an appropriate source. Magnetic susceptability data have shown BOF dust to be more susceptible than EAF dust. The reason that a BOF was not chosen for this program was lack of a host plant willing to accept the pilot plant and associated risk of explosion from seal leaks and occupational exposures to carbon monoxide. There is some risk, however, that BOF dust might exhibit some properties of complex particles seen in the EAF dust in this study depending on the type and amount of scrap used. Another application that might prove more appropriate is the waste gas stream from steel scarfing. The particles from this operation are expected to be virtually all iron oxide.

An alternative use not explored in this study is to separate magnetic and non-magnetic components of EAF waste dust. EAF dust is classified as a hazardous waste due to heavy metal contamination. Recovery of the iron bearing portion for recycle would reduce the quantity for disposal. If the residue were sufficiently rich it might be treated to recover zinc or other metals.

4.0 BACKGROUND DEVELOPMENT

4.1 BASIC CONCEPT

The fundamental concept of the HGMF process is the interaction between paramagnetic or ferromagnetic particles and ferromagnetic fibers while in the presence of an applied background magnetic field. The applied magnetic field induces a magnetic dipole in the particle and magnetizes the wire. This creates a convergence of the field near the wire resulting in a net force being applied to the particle. The magnetic force, in competition with the viscous, inertial, and gravitational forces, causes the particle to be attracted to the wire and held there until the applied field is removed.

The high gradient magnetic filter consists of several cassettes packed with ferromagnetic fibers (such as stainless steel wool or expanded metal) which are moved into a magnetic field as the particle laden gas is being passed through. The particle laden gas is cleansed as the particles are attracted to and held by the fibers. When the matrix is loaded, the cassette is then moved out of the magnetic field and the particles are flushed from the fibers.

4.2 HGMF DEVELOPMENT AND APPLICATIONS

The experimental work in high gradient magnetic filtration, with the exception of the EPA sponsored development begun in 1975, has been most concerned with the magnetic separation of particles in a slurry. Oberteuffer,[1] Kolm, et al.,[2] Oder,[3] and Iannicelli[4] have published excellent reviews of the process and its chronological development. A brief review of HGMF development can also be found in the EPA report "Application of High Gradient Magnetic Separation to Fine Particle Control" by Dr. C. H. Gooding.[5]

The most extensive development of HGMF has been within the last decade in the clay industry. Here, the HGMF is used to separate small paramagnetic color bodies from kaolin clay. The successful demonstration of this process in the clay industry has sparked investigations of HGMF for many different applications. Table 1 lists some of the HGMF applications being investigated.

TABLE 1. HGMF APPLICATIONS BEING INVESTIGATED

Application	References
Mineral beneficiation-general	Kelland, 1973[6] Murray, 1976[7]
Taconite beneficiation	Kelland and Maxwell, 1975[8]
Coal deashing and desulfurization	Ergun and Bean, 1968[9] Trindade and Kolm, 1973[10] Vives, et al., 1976[11] Maxwell, et al., 1976[12] Maxwell, et al., 1977[13] Liu, et al., 1978[14] Maxwell and Kelland, 1978[15] Hise, et al., 1979[16]
Wastewater treatment-general	Mitchell, et al., 1975[17] Petrakis and Ahner, 1978[18]
Steel mill wastewater treatment	Oberteuffer, et al., 1975[19] Harland, et al., 1976[20]
Municipal wastewater treatment	deLatour and Kolm, 1975[21] Yadidia, et al., 1977[22]
Blood component separation	Melville, et al., 1975[23]
Catalyst recovery	Whitesides, et al., 1976[24]
Particulate emission control from steel mill sinter plant	Gooding, 1980[25]
Aluminum extraction	Friedlander, et al., 1980[26]

4.3 POTENTIAL APPLICATION TO PARTICULATE EMISSION CONTROL

The presence of iron in the waste gas particulate from several sources in the iron and steel industry makes HGMF a potential candidate for air pollution control. Table 2 lists the waste gas characteristics of several widely used processes in the iron and steel industry.

A sinter plant is used to combine iron ore with flux and with other iron-bearing materials such as flue dust, mill scale, turnings, and borings to form a blast furnace feed. The blast furnace reduces the iron ore, pellets, and sinter. The basic oxygen furnace, electric arc furnace, and open hearth furnace are used to refine the iron to steels of various composition. The scarfer is a surface improvement process which volatilizes a thin layer of the hot steel slab by blasting it with oxygen. In each of these processes, iron bearing particles are entrained in the waste gas stream and must be collected by some air pollution control device. The control devices currently in use are cyclones, baghouses, wet scrubbers, and electrostatic precipitators.

The iron content of the dust, the large throughput velocities, and current magnet technology combine to make HGMF potentially competitive with other pollution control devices. Also, if the HGMF matrix is cleaned by backflushing with air, the process can remain completely dry and avoid water pollution problems.

Consideration of application of HGMF to any of the above processes must take into account magnetic susceptability, particle size distribution, and waste gas composition. Presuming magnetic susceptability to be proportional to iron content, the BOF, open hearth furnace, and scarfing operations seem to be better candidates for HGMF than the others. The blast furnace with more coarse dust and lesser iron content could be nearly as good.

The declining use of open hearths limits that potential application. Blast furnaces and BOFs present problems relative to gas stream composition. Closed hood BOFs (the recent trend) generate a gas stream rich in carbon monoxide which would require the development of a sealing or containment system more complex than used in the pilot plants. Blast furnaces likewise generate a waste gas stream with carbon monoxide, but present the additional complicating problem of pressurized operation. The advantage of dry dust collection that HGMF could provide for blast furnaces might make seal development a worthwhile effort.

TABLE 2. EXTENDED CHARACTERISTICS OF UNCONTROLLED GAS STREAMS FROM SEVERAL PROCESSES.*

Process	Dust concentration g/m^3	Mass median diameter μm	Iron composition % total Fe	Noteworthy gas characteristics
Sinter machine				
Windbox	1-2	10	25-50	5-15% H_2O, Hydrocarbons, Flourides, SO_x, 120-180° C
Discharge end	5-12	10	25-50	120-180° C
Blast furnace	10-25	20	35-50	20-40% CO, 2-6% H_2, 200-300° C
Basic oxygen furnace				
Open system	10-25	1	55-70	250-300° C
Closed system	40-70	2	55-70	75% CO, 250-300° C
Electric arc furnace	0.2-7	1	15-40	40-120° C
Open hearth furnace	4-7	5	55-70	7-15% H_2O, 250-300° C
Scarfing machine	0.5-1	0.5	50-70	H_2O Satruated, 50-60° C

*Compiled from numerous references including Hardison and Greathouse (1972)[27], Dulaney (1974)[28], Steiner (1976)[29], Jaasund (1977)[30], and Whitehead (1977)[31].

4.4 PRELIMINARY DESIGN AND DEVELOPMENT

A laboratory pilot plant was constructed and operated by Research Triangle Institute for EPA in order to demonstrate the feasibility of HGMF as an air pollution control device on various iron and steel industry processes.[5] Using the data obtained during the operation of the laboratory pilot plant and the mathematical model developed during this time, a mobile HGMF pilot plant was designed and constructed. The pilot plant was connected to a slipstream from the waste gas duct at a Pennsylvania sintering plant and operated for 4.5 months. The detailed design and resulting data from the operation of this pilot plant are given in a prior report.[25] This earlier mobile pilot plant was a 5,100 m^3/hr (3,000 cfm) cyclic system housed in a 12.8 m (42 ft) freight van. The cyclic design was actually two 5,100 m^3/hr systems that allowed one system to be filtering the waste gas stream while the other system was cleaning itself by backflushing with compressed air through a cyclone.

The operation of the pilot plant on the sinter plant gas resulted in lower than expected mass efficiencies. Chemical anaysis of the dust samples showed that the low efficiencies were due to the low iron content (7-11% Fe) of the sinter plant dust and resultant low specific magnetization.

Figure 1 shows the specific magnetization (magnetization/unit mass, measurement method described in Section 8.2.1) values of the sinter plant dust samples collected at the inlet, outlet, and cyclone hopper. Table 3 shows the component mass balances based on the chemical analysis of the samples. Samples at the inlet and outlet were collected by isokinetic sampling. The cyclone hopper was grab sampled.

Although the collection efficiency of the pilot plant on the sinter dust was not satisfactory, earlier laboratory work showed that HGMF might be practical for operations such as the basic oxygen furnace (BOF), the electric arc furnace (EAF), and the blast furnace. These operations have dusts with specific magetizations from 10 to 20 times higher than the sinter dust.

There were also problems with the cyclic HGMF design. The redundancy of magnets necessary to achieve continuous operation would result in a severe cost penalty when scaled up to a full size system.

For these reasons it was decided to design and build a new pilot plant with continuous media regeneration and locate a test site at either a BOF, EAF, or blast furnace.

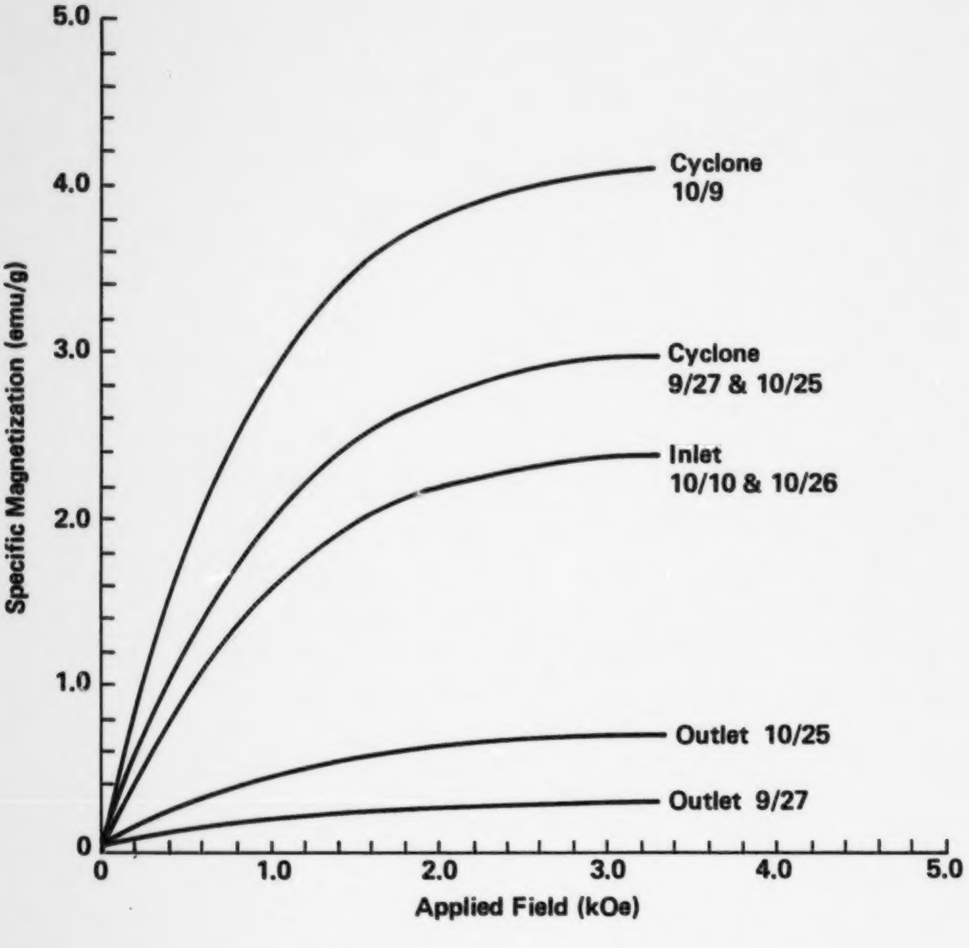

Figure 1. Magnetic analysis of dust samples from sinter plant HGMF pilot plant tests.

TABLE 3. COMPONENT MASS BALANCES BASED ON CHEMICAL ANALYSIS

	Fe	Ca	Mg	Al	Si	Na	K	Cl^-	$SO_4^=$
Analysis									
Avg. inlet (C_i), mass %	8.92	5.20	1.60	8.09	1.65	0.69	16.7	23.1	1.62
Avg. outlet (C_o), mass %	1.38	2.32	0.60	3.12	0.55	1.24	32.6	34.4	1.80
Avg. cyclone (C_c), mass %	13.0	7.73	2.20	11.4	2.4	0.40	9.3	12.9	2.33
C_i-C_o, %	7.54	2.88	1.00	4.97	1.10	-0.55	-15.9	-11.3	-0.185
C_c-C_o, %	11.62	5.41	1.60	8.28	1.85	-0.84	-23.3	-21.5	0.535
E_t*	0.649	0.532	0.625	0.600	0.595	0.655	0.682	0.526	-----
Component balance (based on E_t = 0.61 and average measured composition)									
Inlet mass, kg	8.92	5.20	1.60	8.09	1.65	0.69	16.7	23.1	-----
Outlet mass, kg	0.54	0.90	0.23	1.22	0.21	0.48	12.7	13.4	-----
Cyclone mass, kg	7.93	4.70	1.34	6.95	1.46	0.24	5.7	7.9	-----
Component closure, %	95	108	98	101	101	104	110	92	-----
Component efficiency, %	89	90	84	86	88	35	34	34	-----

* E_t = overall mass collection efficiency

4.5 MATHEMATICAL MODEL

The mathematical model was developed by Gooding, in conjunction with the laboratory pilot plant work, in order to better understand the effects of various design parameters. The final predictive equation for this model is:

$$E = 1 - \exp\left[- \frac{4FLY_c\rho}{\pi^2 S(1-F)^2}\right]$$

E = fractional collection efficiency, dimensionless;

F = filter packing density (actual volume of steel wires/volume occupied by filter), dimensionless;

L = filter depth, m;

S = wire radius, m;

Y_c = single wire collision radius, dimensionless;

ρ = probability of particle adhesion, dimensionless.

Y_c, the collision radius, is a dimensionless value derived from the solution of the trajectory model taking into account inertial, viscous, and magnetic forces. There are four parameters in the trajectory model -- A, G, K, and W -- which describe the particle behavior.

Parameter A accounts for the relative magnitudes of the applied magnetic field and the induced magnetic field in the ferromagnetic wire. A was assumed to be one since it can be shown that below the saturation values of stainless steel wire, $A \simeq 1$.

Parameter G accounts for the effect of gravity and was taken as zero since the calculated value was less than 2×10^{-5}.

Parameters W and K take into account the effects of the applied magnetic field and inertia on collection efficiency. More is given on parameters W and K in Section 8.3. Details of the model are given in the report by Gooding.[25]

4.6 SITE SELECTION FOR CURRENT FIELD TESTS

Since RTI had attained high collection efficiencies on at least two steel industry dusts, BOF and EAF, during the laboratory pilot plant work, it was decided to try to locate a more suitable site for the continuous HGMF pilot plant field tests. The higher iron content of BOF dust made it the first choice for process type. In November, 1980, a presentation was made to the

American Iron and Steel Institute and representatives of several steel corporations to obtain their assistance in locating a suitable site. The only site offer to result from the meeting was a scarfing operation.

Also at this time, there were negotiations with Dr. R. Hinson of Georgetown Steel Corporation about the possibility of performing the field tests at their electric arc furnace plant in Georgetown, South Carolina. Georgetown Steel Corporation had been contacted earlier and had expressed interest in performing the tests at their plant.

In December 1980 RTI performed particulate sampling tests at the Georgetown Steel plant and analyzed the dust samples for size distribution, chemical composition, and specific magnetization. The dust samples were taken isokinetically from the duct just ahead of the baghouse with MRI cascade impactors to obtain particle size distributions. Alundum thimbles were used to obtain large quantity samples for chemical and magnetic analysis. Dust samples were also obtained from the baghouse dust hoppers that Georgetown Steel Corporation is presently using for emissions control.

Figure 2 shows the size distribution of the dust samples taken and Figure 3 shows the averaged particle size distribution for Runs 2, 3, and 4. Due to the large differences between Run Number 1 and the others, it was felt that an error may have been made in the sampling or weighing procedure and therefore Run 1 was not included in the average particle size distribution. Table 4 shows the chemical composition of the samples while Figure 4 shows the magnetization values. Table 5 gives the chemical composition of samples taken from the Georgetown baghouse by Clemson University from February 25, 1980 through July 11, 1980. Based on the sample analysis, the mathematical model was then used to calculate the expected collection efficiency, by particle size, for two values of specific magnetization, and is presented in Figure 5. According to the model, a collection efficiency of at least 99 percent could be achieved for particle sizes of 0.9 microns and above. Below 0.9 microns, the efficiency falls off rapidly.

Figure 6 shows a comparison of the Georgetown Steel dust magnetization values with that of other electric arc furnace dusts. As can be seen from Figure 6, the three samples from Georgetown Steel, fall in the middle range of the specific magnetization values of the dust samples collected from three EAF's across the country.

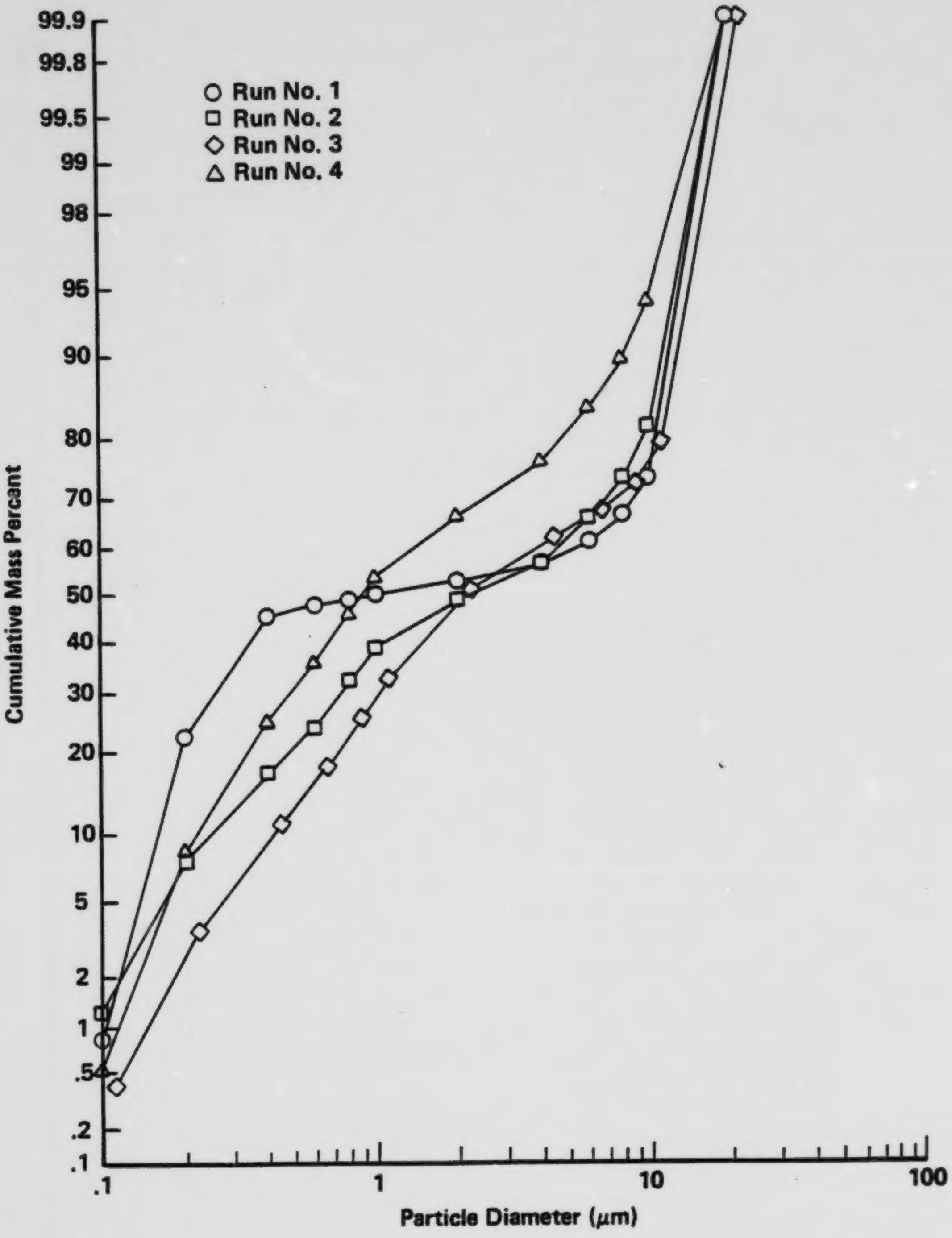

Figure 2. Particle size distribution, preliminary tests.

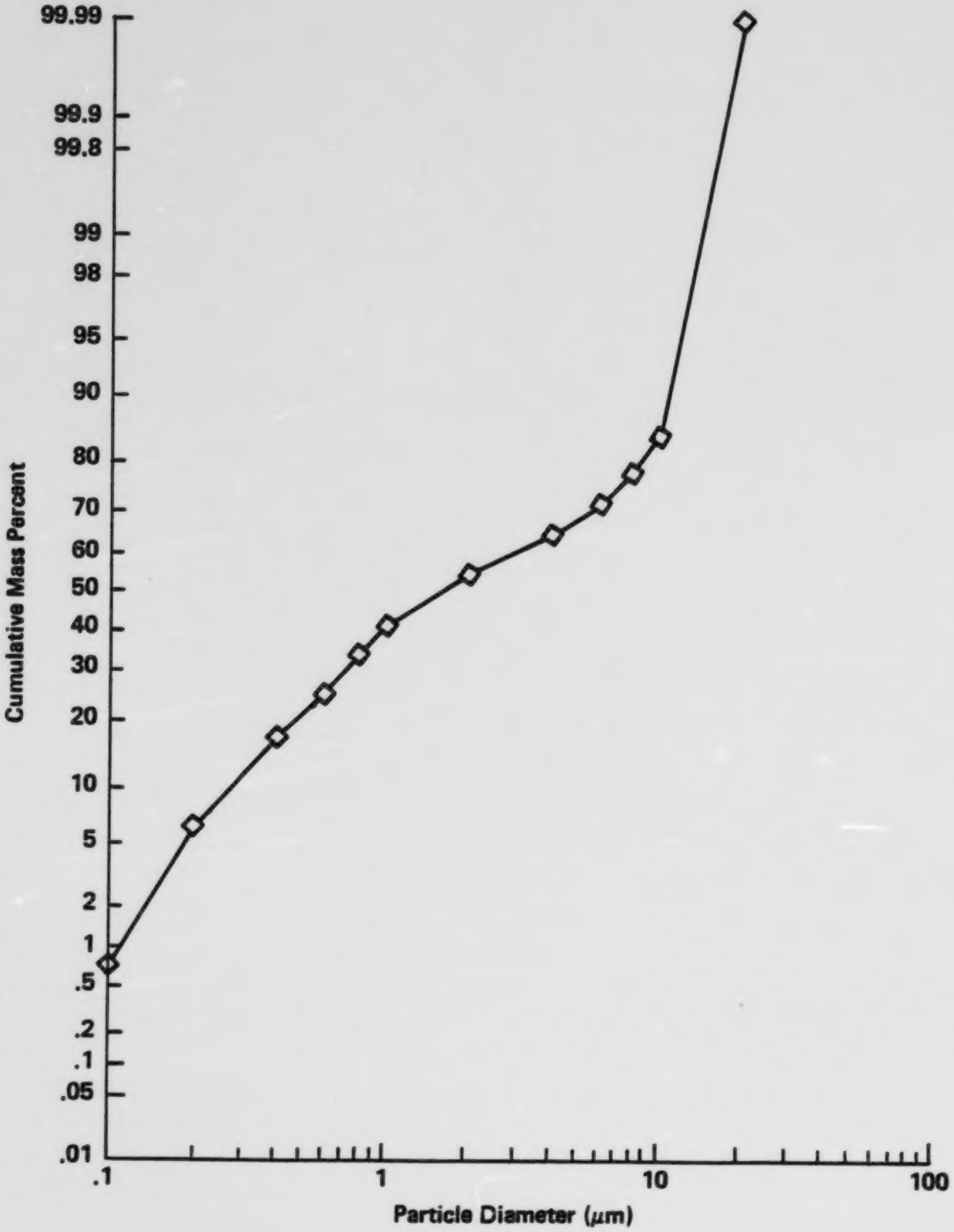

Figure 3. Particle size distribution, average of runs 2, 3 and 4.

TABLE 4. ELEMENTS PERCENT BY MASS (OBTAINED BY ATOMIC ABSORPTION)

Sample	Al	Si	Fe	Cr	Ca	Mg	K	Na	Mn	Pb	SO_4	$^{-}$Cl	Zn
Duct sample (12-17-80)	0.39	1.63	27.9	0.08	3.45	0.91	1.25	1.80	1.31	0.35	1.35	1.12	42.5
Baghouse sample (1-7-81)	0.32	1.8	34.4	0.08	8.83	2.89	1.14	1.46	2.78	1.13	2.21	0.56	10.0

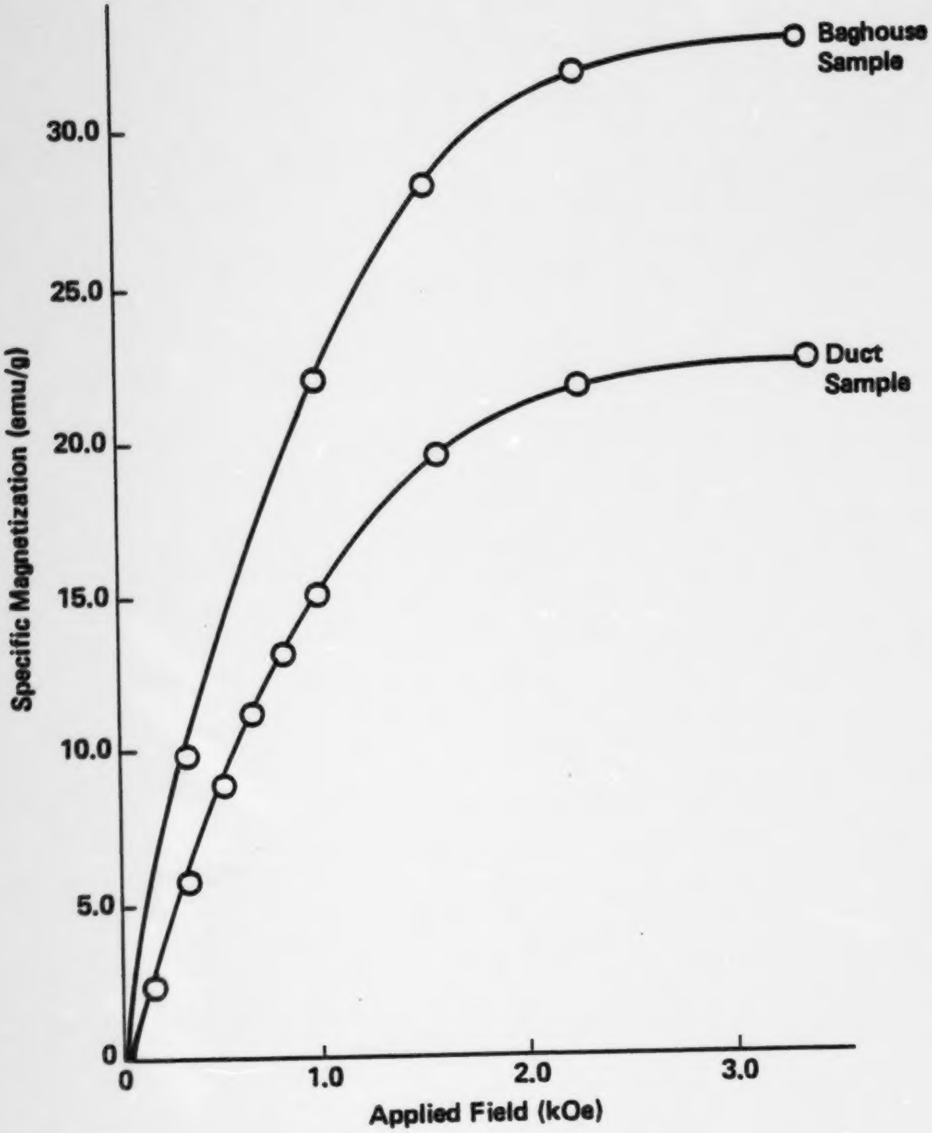

Figure 4. Georgetown Steel HGMF test—preliminary sampling program.

TABLE 5. BAGHOUSE DUST ANALYSIS

Below is a summary of the daily (Mon.-Fri.) Baghouse Dust Analysis from 2/25/80 through 7/11/80. The dust was sampled and then analyzed with atomic absorption spectroscopy techniques. (The statistical parameters are expressed as percentage composition.)

Fe, as Fe_2O_3

$\bar{x}$ = 46.19
s = 8.96
lo = 31.0
hi = 69.0
n = 78

Ca, as CaO

$\bar{x}$ = 5.23
s = 2.68
lo = 1.3
hi = 14.0
n = 79

Mg as MgO

$\bar{x}$ = 3.24
s = 1.11
lo = 1.30
hi = 7.60
n = 73

Mn, as MnO

$\bar{x}$ = 4.21
s = 1.47
lo = 1.69
hi = 7.5
n = 79

Zn, as ZnO

$\bar{x}$ = 18.36
s = 5.80
lo = 7.3
hi = 33.3
n = 79

Pb, as PbO_2

$\bar{x}$ = 3.06
s = .73
lo = 1.51
hi = 4.50
n = 79

Cu, as CuO

$\bar{x}$ = .21
s = .05
lo = .12
hi = .34
n = 79

K, as K_2O

$\bar{x}$ = 1.89
s = .63
lo = .66
hi = 3.52
n = 73

Cr

$\bar{x}$ = .09
s = .02
lo = .05
hi = .15
n = 79

x = arithmetic mean
s = standard deviation
n = number of determinations

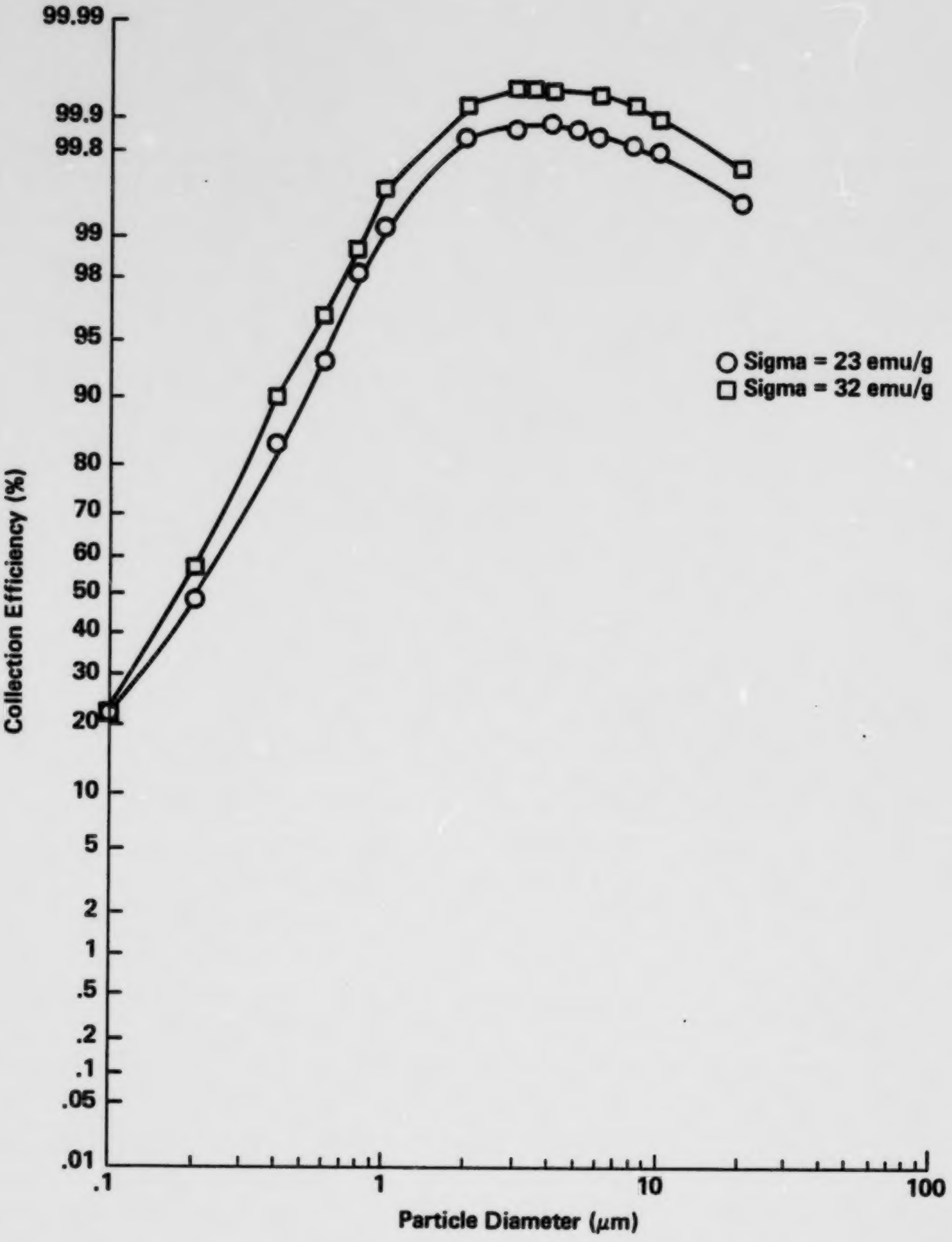

Figure 5. HGMF—Predicted collection efficiency vs. particle size.

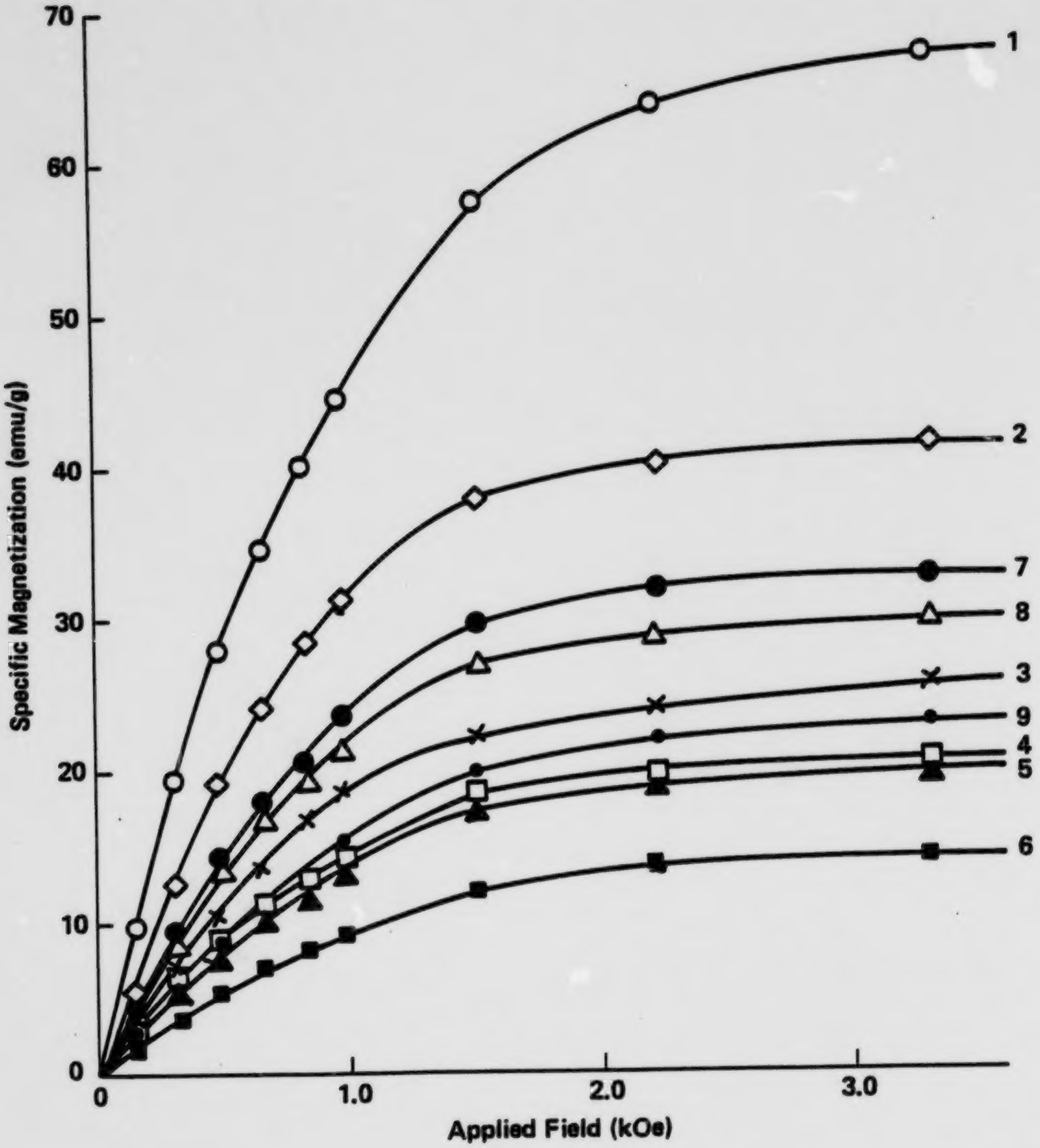

Figure 6. Magnetic analysis of EAF dust samples.

PERFORMANCE CHARACTERIZATION TESTS

Steel company	Specific Magnetization at 3.3 kOe (emu/g)	Curve No.
1. Armco Steel (Houston Works)	66.8	1
2. J&L Steel (Cleveland, Ohio)	41.5	2
3. Bethlehem Steel (Bethlehem Plant)	25.6	3
4. Lukins Steel (Coatesville, Pa)	20.5	4
5. Bethlehem Steel (Steelton Works)	19.3	5
6. Laclede Steel (Alton, Ill.)	13.6	6
7. Georgetown Steel Baghouse Sample (1/7/81)	32.3	7
8. Georgetown Steel Baghouse Sample (2/27/81)	29.6	8
9. Georgetown Steel Duct Sample (12/17/80)	22.5	9

Average specific magnetization for steel companies 1-6 = 31.2 emu/g

Average specific magnetization for Georgetown Steel = 28.1 emu/g

Due to the relatively high magnetization values and the representative composition of the Georgetown dust compared with other EAFs, it was decided to test the continuous HGMF mobile pilot plant at Georgetown Steel Corporation electric arc furnace in Georgetown, South Carolina.

5.0 DETAILED DESIGN AND CONSTRUCTION OF THE HGMF MOBILE PILOT PLANT

The mobile pilot plant is a continuous HGMF system housed in a 12.8 m (42 ft) freight van. The system is designed for a nominal flow capacity of 3,060 m^3/hr (1,800 cfm). Figure 7 is a flow schematic of the continuous HGMF system, while Figure 8 is a scale drawing of the HGMF mobile pilot plant.

The dirty gas enters the pilot plant through a 0.25 m ID stainless steel pipe (10" schedule 5). The gas passes by test ports through which samples can be drawn to determine inlet dust concentration, chemical composition, and size distribution and then is directed to the HGMF device. The magnetic filter is a Sala-HGMS® Carousel Model 120-05-00 (Sala Magnetics, Inc., Cambridge, Mass.) incorporating a magnet head and a cleaning station mounted 180° apart on a rotating carousel. The magnet coils are split into a saddle configuration to allow the carousel to be rotated through the magnetized zone by a variable speed drive. The carousel contains 48 removable cassettes which can be loaded with filter material to a depth of 0.15 m (5.8 in). The magnet head encloses an active face area of 0.085 m^2 (133 in^2) in the direction of fluid flow. The magnet head is designed to provide an applied field from 0.0 to 5.0 kG. The magnet head is energized by a dc modular power supply manufactured by Controlled Power Company (Troy, MI). In the range of gas velocities tested, 2 to 10 m/s, the gas residence time in the filter varied from 0.015 to 0.075 s.

After passing through the magnet, the gas then passes by another set of test ports and exists the pilot plant. Once leaving the pilot plant, the gas is directed through an orifice, for velocity (flow rate) determination, through an induced draft blower and then is exhausted to the atmosphere through an 8 m (26 ft) high stack.

After the filter material has passed through the magnetized zone and collected the dust particles, it then passes through the cleaning station. The filter is cleaned by backflushing with compressed air from a 0.095 m^3 tank mounted directly over the cleaning station. To clean the filter, the compressed air is released through a 0.10 m (4" nominal pipe size) Galigher Delta valve (Galigher Company, Salt Lake City, UT). The Galigher valve is a pneumatically actuated pinch valve consisting of a pair of identical elastomeric

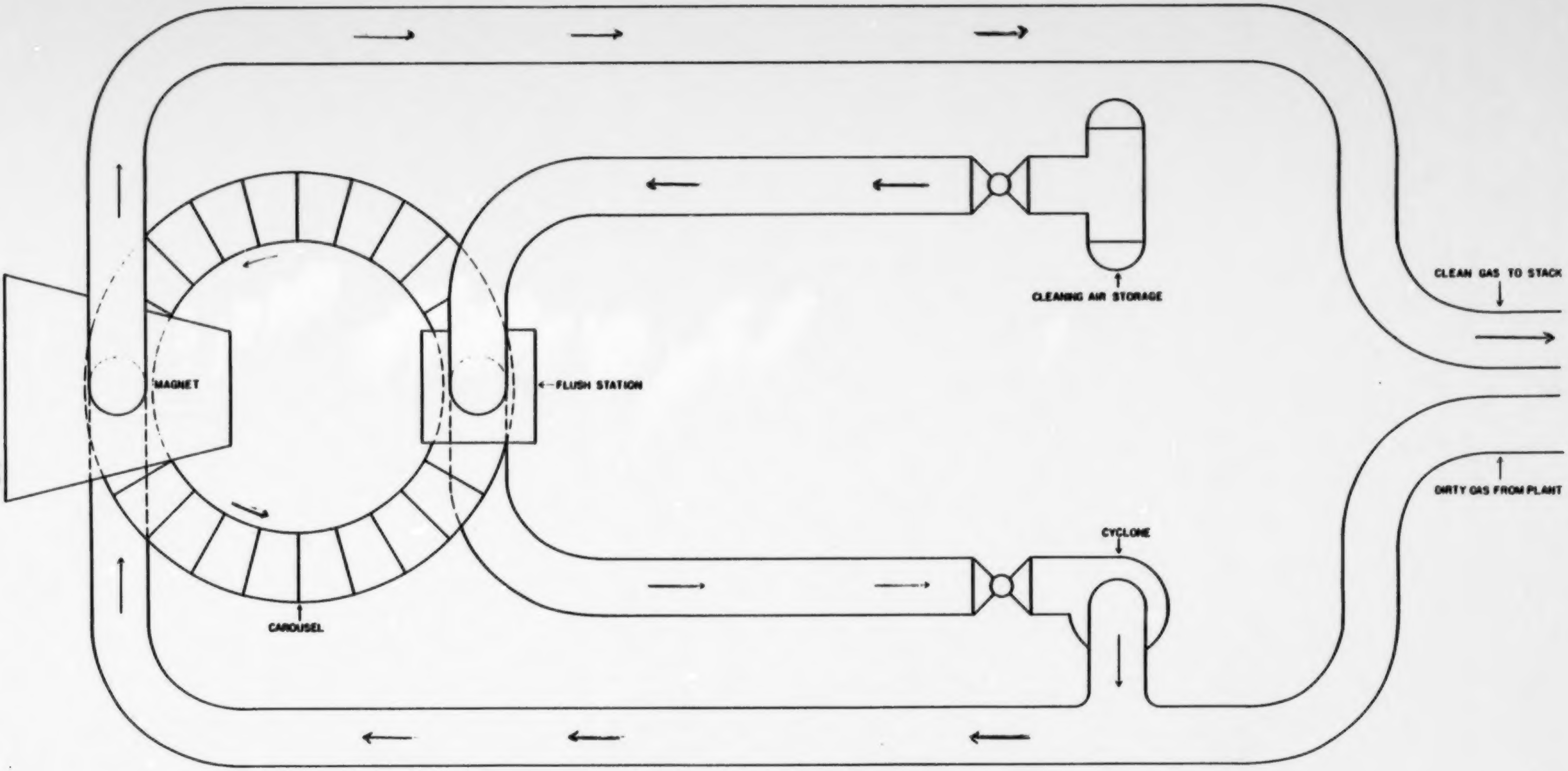
CLEAN GAS TO STACK
CLEANING AIR STORAGE
MAGNET
FLUSH STATION
DIRTY GAS FROM PLANT
CYCLONE
CAROUSEL

Figure 7. **FLOW SCHEMATIC OF CONTINUOUS H.G.M.F. SYSTEM**

Figure 8. **HGMF MOBILE PILOT PLANT**

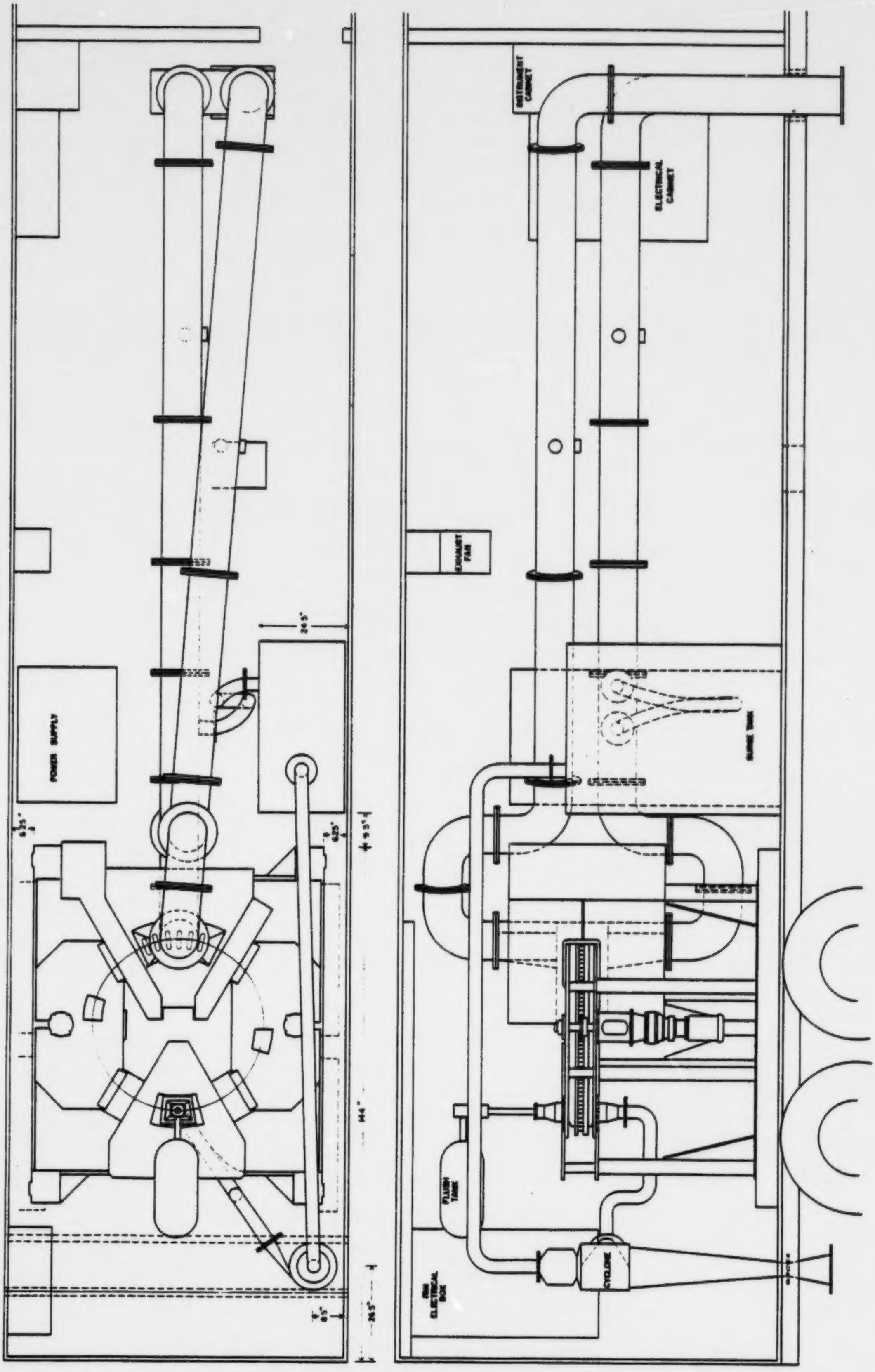
POWER SUPPLY
EXHAUST FAN
INSTRUMENT CABINET
ELECTRICAL CABINET
SURGE TANK
FLUSH TANK
CYCLONE
FAN ELECTRICAL BOX
24.5"
6.25"
6.25"
9.5"
144"
26.5"
8.5"

diaphragms contained within a cast aluminum split housing. The diaphragms are closed by introducing compressed actuator air into the chamber between the housing and the diaphragms. The valve can then be opened very rapidly by exhausting the actuator air through two large ports in the housing. The actuator air for the Galigher valve is controlled by a 0.38 m (15" nominal) Model 168S poppet valve manufactured by Kay Pneumatics (Commack, NY).

The agglomerated dust that is cleaned from the filter material with the cleaning air pulse is sent to a Kirk & Blum size 4, type C5 cyclone (Kirk & Blum Manufacturing Company, Cincinnati, OH). Exhaust from the top of the cyclone is then recycled into the dirty gas stream. Dust can be removed from the cyclone while the pilot plant is in operation through the double seal formed from two Norris butterfly valves (Dover Corporation/Norris Division, Tulsa, OK) mounted on the bottom of the cyclone hopper.

Figures 9 and 10 are photographs of the interior of the pilot plant taken during construction. Figure 9 was taken from the rear of the trailer and shows the Sala Magnetics Carousel and the cleaning station in the foreground. The large black magnet head is visible behind the cleaning station. Figure 10 was taken from the front of the trailer and shows the inlet and outlet pipes connected to the magnet head. The magnet power supply and the surge tank leading from the cyclone can also be seen.

The induced draft blower which moves the gas through the pilot plant is a modified Centrifan Model RB50-2 (Centrifan Company, Greenville, SC). The blower was modified so that it would exhaust 3,060 m^3/hr at a suction pressure of -13.7 kPa (-55 inches H_2O) and a temperature of 150° C. The entire system is designed to allow continuous operation at temperatures of up to 200° C. All interior and exterior pipe is insulated with jacketed fiberglass.

The front section of the trailer contains an enclosed air-conditioned laboratory and control room. All of the gauges and controls are mounted on a single control panel facing the operator in order to simplify operation of the pilot plant.

A Robertshaw DCM-1000 Controller (Robertshaw Controls Company, Anahiem, CA), is used to maintain a constant gas flow through the plant. The controller receives its signal from a Robertshaw Model 117 differential pressure transmitter which measures the pressure difference across an orifice located in the clean gas pipe. The controller then sends a signal to adjust the butterfly control valve located on the blower exhaust. The orifice pressure drop and

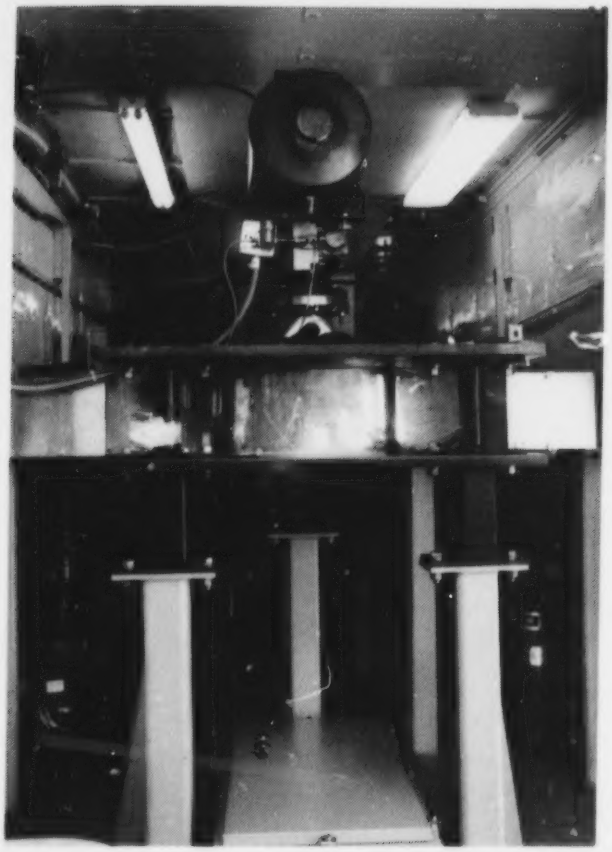

Figure 9. HGMF pilot plant under construction.

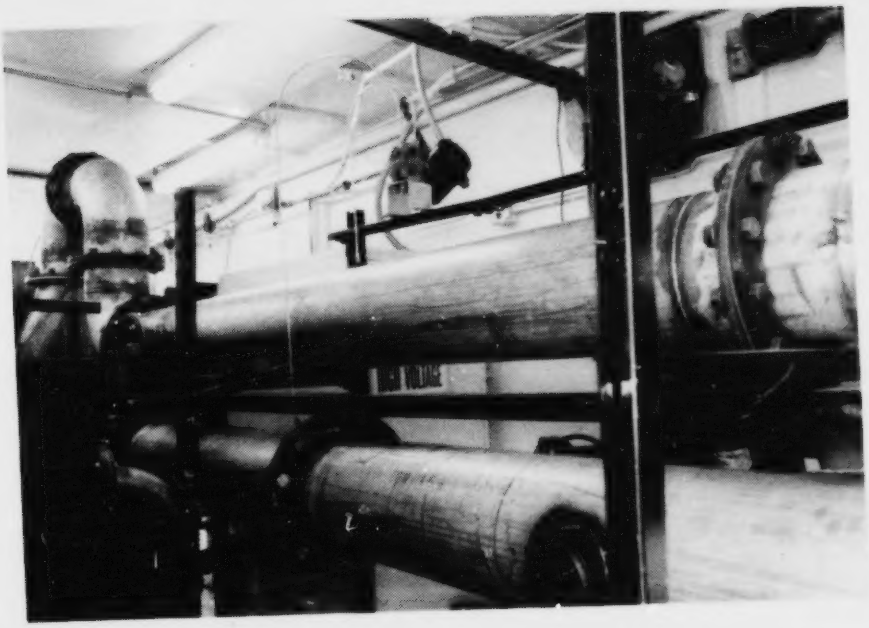

Figure 10. HGMF pilot plant under construction.

the filter pressure drop are displayed and recorded on two Robertshaw Model 225 strip chart recorders located in the control panel. A Xanadu Model UPT 100-10-10 solid state programable timer (Xanadu Controls, Springfield, NJ) is used to sequence the firing of the flush tank with the rotation of the filter matrix. An Omega Model 199 KC digital temperature indicator (Omega Engineering, Inc., Stamford, CT) is also mounted on the control panel and receives its signal from the chromel/alumel thermocouples located in the inlet and outlet piping of the pilot plant. A Flow Technology, Inc. portable turbine flow meter with a digital readout of gas velocity is used to monitor the gas flow in the plant and as a safety check against the orifice pressure differential system.

The laboratory control room also contains a workbench, a wet sink, desk space, a lab oven, a solvent sink and a lab hood. MRI Model 1502 cascade impactors (Meteorology Research, Inc., Altadena, CA) are used to determine particle size distribution and concentration. A Perkin-Elmer Model AD-2Z microbalance (Perkin-Elmer Corporation, Norwalk, CT) is used to weigh the filters and impactor substrates.

The utility requirements of the pilot plant are electricity and water. The main power panel is breakered for 400 amperes of 440 ac volt input. The total connected load is 300 amperes. Power consumption at 300 amperes would be 0.043 kW/m^3. The major equipment operates off 440 vac and a transformer is provided to step down to 240 vac and 120 vac. Water consumption is approximately 2.3 m^3/hr (10 gpm) for magnet cooling, compressor aftercooler, and occasional use of the lab sink.

6.0 FIELD OPERATIONS

6.1 DESCRIPTION OF THE ELECTRIC ARC FURNACE AT GEORGETOWN, SOUTH CAROLINA

The dust source is an EAF shop utilizing three arc furnaces operating continuously in a staggered batch operation. The Georgetown Steel raw steel production facilities are composed of three 68 Mg (75-ton) per cycle DeMag electric arc furnaces. The charge to the furnaces consists of scrap and prereduced iron pellets. The scrap charged is obtained primarily from external sources; about 5 to 10 percent is reclaim scrap. Prereduced pellets are produced on-site from South American iron ores. Other materials added to the furnaces during the course of the production cycle include limestone, coke, ferromanganese, and ferrosilicon.

The air pollution control system serving the electric furnaces includes direct shell evacuation combined with a canopy hood above each furnace to capture fugitive emissions. Figure 11 shows a diagram of the typical EAF with this type of control system. Gas cleaning is provided by a positive pressure baghouse supplied by American Air Filter. The gas flow rate through the system is about 17,800 m^3/min (630,000 acfm) at an average temperature of 71° C (160° F). Approximately 18,200 kg (40,000 pounds) of dust are collected daily by the baghouse. The average dust concentration in the gas stream is 0.71 g/m^3 (0.31 gr/acf). Composition of the gas stream is essentially that of air because of the large fraction of air drawn in by the canopy hood.

The test location is shown roughly in Figure 12. A slipstream of gas was taken from the duct at the approximate point marked "test site." The pilot plant was located underneath the elevated duct at that point. The gas stream conditions at the extraction point are listed below:

Pressure	-1.7kPa (-7 inches H_2O)
Temperature	71° C (160° F)
Velocity	17 m/s (55.65 ft/s)
Reynolds Number	4.1×10^6

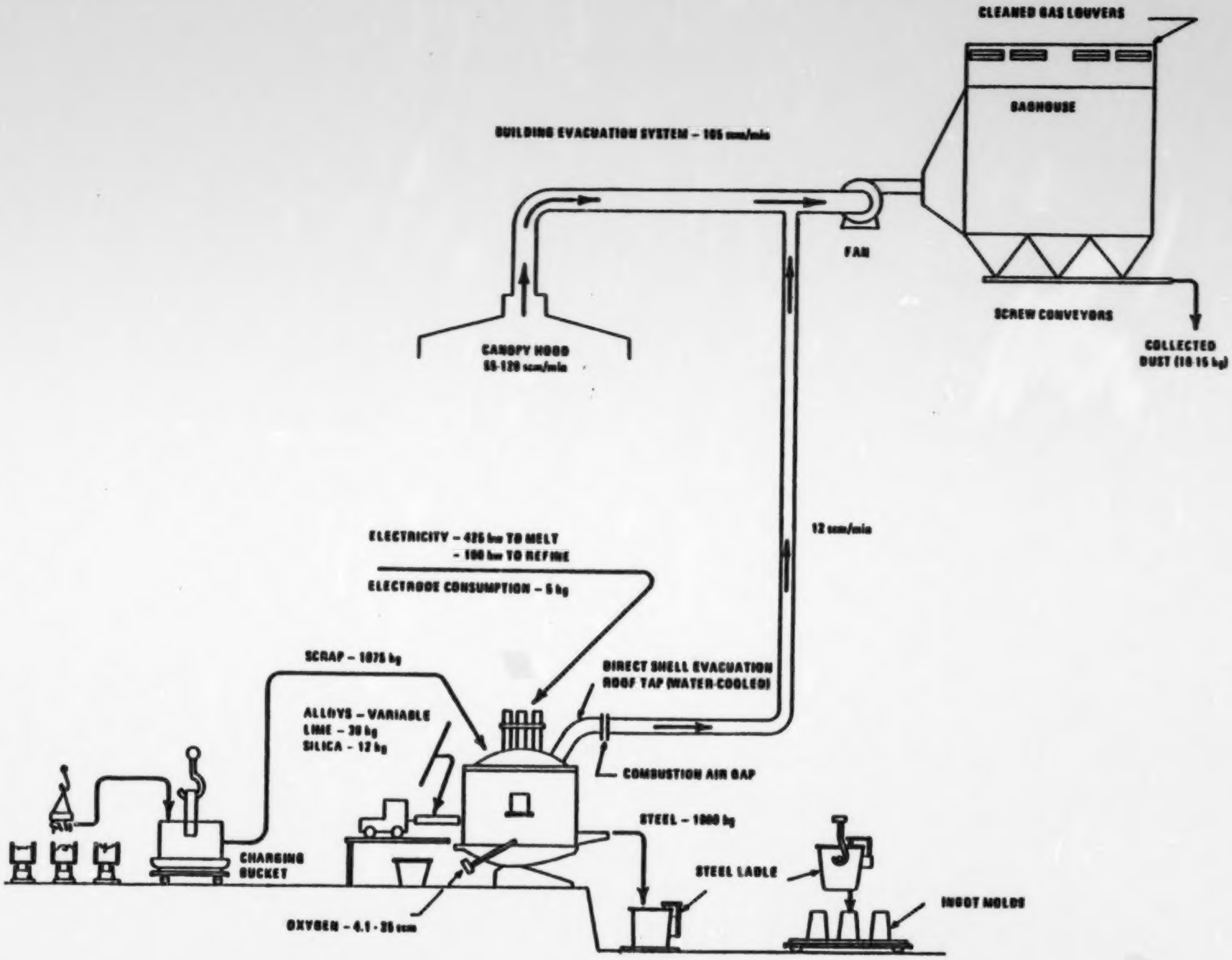
CLEANED GAS LOUVERS
BAGHOUSE
BUILDING EVACUATION SYSTEM – 105 scm/min
FAN
SCREW CONVEYORS
COLLECTED DUST (10-15 kg)
CANOPY HOOD 55-120 scm/min
12 scm/min
ELECTRICITY – 425 kw TO MELT
– 100 kw TO REFINE
ELECTRODE CONSUMPTION – 5 kg
SCRAP – 1075 kg
DIRECT SHELL EVACUATION ROOF TAP (WATER-COOLED)
ALLOYS – VARIABLE
LIME – 30 kg
SILICA – 12 kg
COMBUSTION AIR GAP
STEEL – 1000 kg
CHARGING BUCKET
STEEL LADLE
INGOT MOLDS
OXYGEN – 4.1 - 25 scm

Figure 11. Material balance of electric arc furnace based on 1,000 kg of steel produced.

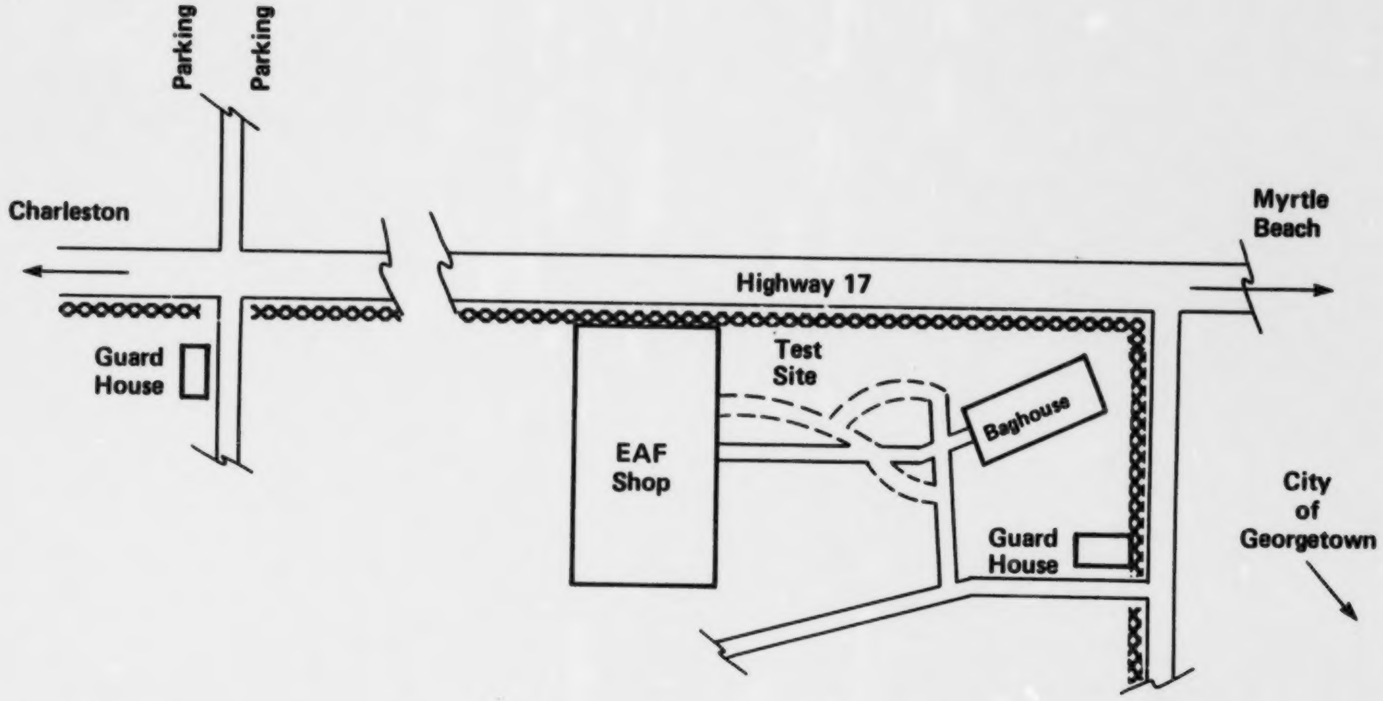
Parking
Parking
Charleston
Guard House
Highway 17
Myrtle Beach
Test Site
EAF Shop
Baghouse
Guard House
City of Georgetown

Figure 12. Rough site map.

6.2 INSTALLATION AND STARTUP OF THE PILOT PLANT

The HGMF mobile pilot plant arrived at the Georgetown Steel plant on June 17, 1981, and the installation and utility hook up began. Approximately 30 m of 0.25 m ID (10" schedule 5) stainless steel pipe was used to connect the pilot plant to the steel mill exhaust. A 0.21 m nozzle was placed in the center of the 4.88 m diameter plant exhaust duct. The nozzle was facing into the plant duct flow and was sized to give isokinetic flow at the average plant and pilot plant flow conditions. The average temperature and pressure in the plant exhaust duct was 71° C and -1.7 kPa (-7 inches H_2O) gauge.

The blower and stack were installed, piping insulated and electrical and water connections made. The startup and debugging of the system was then begun.

6.2.1 Temperature Control

A Universal Model 3500 FA forced-air construction heater (National Riverside Co., Rancho Cucamonga, CA) was used for pilot plant cold startups. The heater burns propane gas to heat 2,400 m^3/hr of air to a maximum of 115° C. A tee and appropriate valving were used so that the heater could preheat the pipe coming from the steel plant duct and the pilot plant interior piping. The preheat procedure usually required about 20 minutes to raise the piping to approximately 60° C. The steady state temperature drop from the inlet to the outlet of the pilot plant usually averaged about 10° C.

6.2.2 Filter Cleaning

The preliminary tests with the initial filter cleaning system seemed to indicate that this system would work. The initial system used a 0.038 m (1.5" nominal) Model 168S poppet valve to release the compressed air from the cleaning tank. The first tests indicated that a tank pressure of 272 kPa gauge (40 psig) and a carousel rotation speed of 0.000424 rev/s for every m/s of gas velocity through the filter would achieve a steady state pressure drop across the filter for each gas velocity. However, with each successive shutdown and startup of the pilot plant, the pressure drop across the filter was slowly increasing for each gas velocity. Neither the increase in cleaning tank pressure to 340 kPa gauge (50 psig) nor the increase in carousel rotation speed seemed to help.

It was then decided to install a 0.10 m (4" nominal pipe size) Galigher Delta valve to exhaust the cleaning tank instead of the 0.038 m poppet valve.

The Galigher valve exhausted the tank almost instantaneously achieving the steady state pressure drop across the filter with a cleaning tank pressure of 272 kPa gauge (40 psig) and a carousel rotation speed of 0.000424 rev/s for every m/s of gas velocity through the filter. This did, however, increase the force of the pulse through the recycle line and into the inlet pipe just ahead of the filter.

6.2.3 Magnet Operation

Several problems were experienced with the magnet operation initially. The magnet cooling water outlet temperature was reaching approximately 55° C (130° F) above the inlet temperature indicating insufficient cooling waterflow. A small pump was installed to increase the cooling water flow through the coils.

Initially the magnet power supply was only reaching a maximum of 400 amperes before the dc breakers tripped and shut the system down. This was much less than the 500 amperes needed to give a maximum applied field of 5.0 kgauss. With the help of Controlled Power Company, the manufacturers of the power supply unit, the voltages between several points in the power supply were checked and found to be normal. All electrical connections between the power supply and magnet were rechecked. The dc breakers were checked and found to be satisfactory. The dc ampere output was then checked and the gauge was found to be faulty. A new current gauge was installed and no further problems with the power supply were experienced.

After a few hours of operation, the magnet carousel stopped rotating. After checking the dc motor controllers the problem was found to be two defective resistors. The resistors were replaced and no further problems occurred.

6.2.4 Flow Measurement and Control

The flow measurement and control in the pilot plant utilizes the measurement of the pressure difference across the orifice. A pitot tube traverse was performed on several occasions to check the gas flow with that indicated by the orifice pressure differential. The gas velocity indicated by the orifice was within 10 percent of that indicated by the pitot tube traverse.

The approximate values for the proportional gain and integration constant of the Robertshaw DCM-1000 Controller were obtained by adjusting these parameters while the pilot plant was in operation. Once these values were set, the controller maintained a contant gas flow in the pilot plant with no problems.

Due to an earlier problem with the output of one of the Robertshaw 117 differential pressure transmitters, magnehelic gauges were installed beside the control panel as a safety check on the pressure drop readings.

6.2.5 Final Site Setup

Figures 13 and 14 are pictures of the HGMF Mobile Pilot Plant installed at the Georgetown plant site.

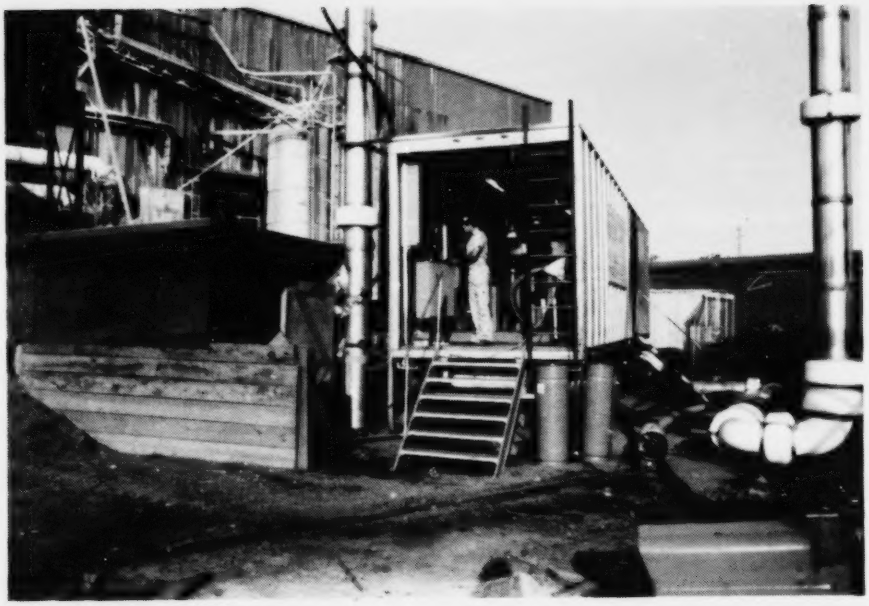

Figure 13. HGMF pilot plant at Georgetown Steel.

Reproduced from best available copy.

Figure 14. HGMF pilot plant at Georgetown Steel.

7.0 PERFORMANCE CHARACTERIZATION

7.1 TEST PLAN

The test program was designed to test the effects of four parameters on collection efficiency, and the reliability of the equipment during long term operation. The four parameters to be varied were applied field, gas velocity, filter type, and filter packing density. The long term testing was to be a 500 hour continuous operation. The 500 hour long term test was cancelled however in favor of added performance characterization tests. As explained in Section 7.4.2 the long term performance test was felt to be less important than determining the reason for performance poorer than that achievable by other particulate control devices.

7.1.1 Performance Characterization and Optimization

The selection of an optimum set of operating conditions was the goal of this phase of the testing. The selection of optimum conditions was to be based on statistical analysis of the performance data obtained under varied operating conditions. Performance under each set of conditions was to be measured by sampling the HGMF inlet and outlet particulate concentrations. Overall efficiency would be determined on a mass basis and fractional efficiency would be determined by measuring inlet and outlet particle size distribution. Periodically during the characterization, bulk samples of the particulate were to be obtained from the inlet, the outlet, and the cyclone catch in order to obtain the chemical composition and its effect on performance and vice versa.

7.1.2 Performance Data for Principal Variables

Following selection of the cleaning cycle parameters the test program examination of principal variables on filter performance was to begin. The priorities established for this group of measurements were as follows:

1) vary magnetic field strength and gas velocity through the filter,
2) vary the filter media, and
3) vary the packing density of the media.

The variation of the filter packing density and filter type were lower on the priority list due to the difficulty of changing these. Both require shutdown of the unit and dismantling of the carousel, a time consuming process.

The program was to be started with a steel wool matrix at a packing density of 0.015 (volume fraction occupied by steel wool), for which the effect of magnetic field strength and velocity on performance would be investigated. The second major step would be to switch from a steel wool matrix to an expanded metal matrix for tests varying the magnetic field strength and velocity. Superior performance for either filter type would lead to further tests on that type for different packing densities, as time and budget allowed.

Within the initial tests on steel wool at a packing density of 0.015, a statistical experimental design was selected for controlling the value of the variables, field strength and velocity, as well as the number and pattern of repetition of performance measurements. The purpose of the statistical design was to examine the changes in performance over the range of variables and provide for repetition of certain experimental points in order to better estimate experimental error. In addition to error caused by measurement inaccuracies, there would be error introduced by random process variations (electric arc furnace operations). The repetitions would, however, allow us to gauge both the measurement inaccuracy and furnace operation variation.

The statistical design selected was a central composite, second order response surface design containing nine test points with repetitions as noted in Figure 15. With the center point and extreme values of both variables defined, the intermediate test points are given by the statistical design. The pattern variable values permits ready computation of variance components and estimation of coefficients for first and second order effects caused by each variable. The order of the tests would be selected at random.

Following the initial test series the filter media was to be changed to expanded metal and the tests repeated. Since no prior experimental work had been done with expanded metal, performance difference was a principal question. It was hoped that equivalent performance might be achieved at signficantly lower pressure drops as compared to the steel wool, which would lead to lower operating costs on a full scale system.

With respect to the fourth variable, packing density, there was expected to be a tradeoff between performance and pressure drop. Better performance could be achieved at higher packing densities, but with correspondingly higher pressure drops.

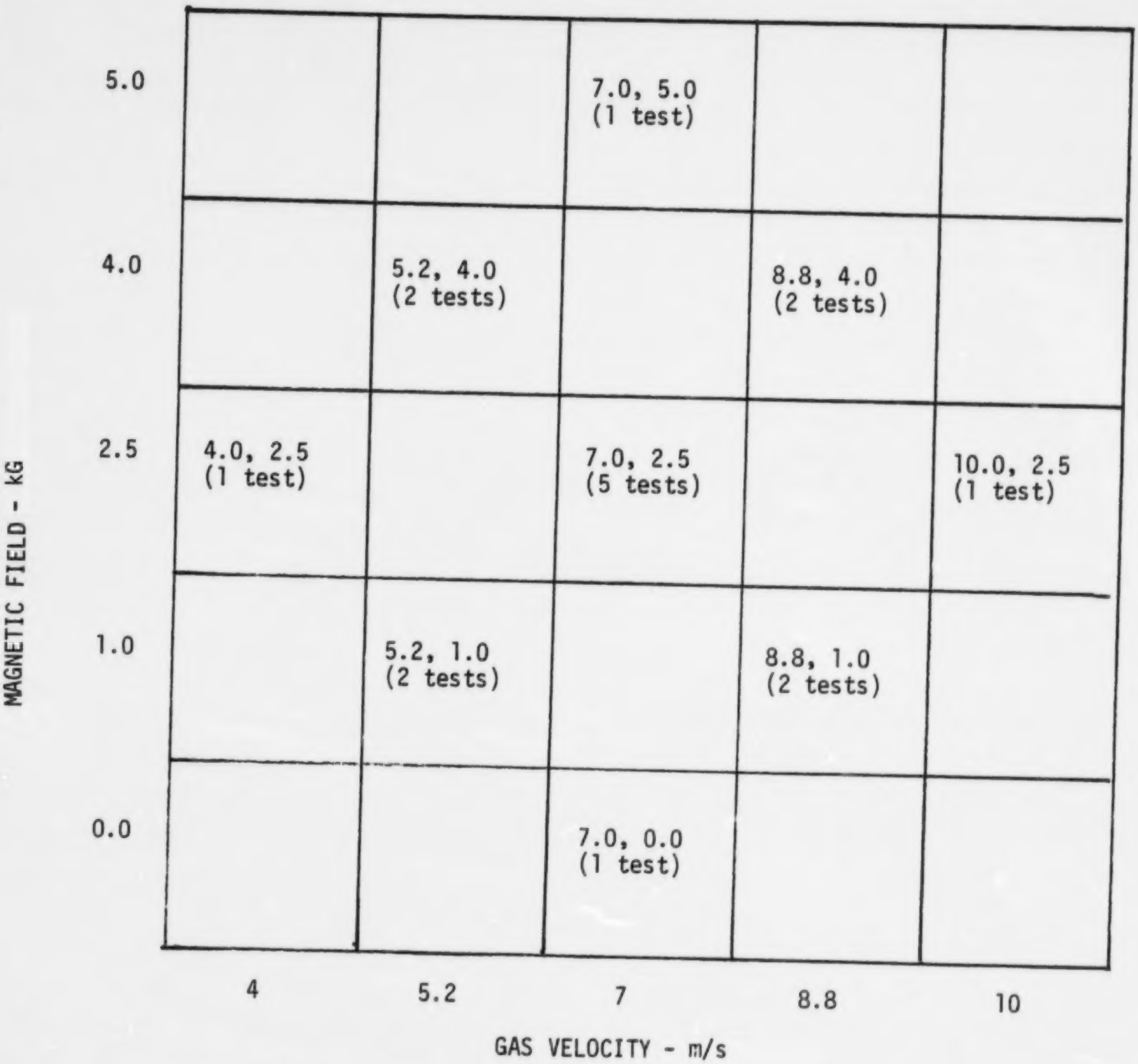

MAGNETIC FIELD - kG	4	5.2	7	8.8	10
5.0			7.0, 5.0 (1 test)		
4.0		5.2, 4.0 (2 tests)		8.8, 4.0 (2 tests)	
2.5	4.0, 2.5 (1 test)		7.0, 2.5 (5 tests)		10.0, 2.5 (1 test)
1.0		5.2, 1.0 (2 tests)		8.8, 1.0 (2 tests)	
0.0			7.0, 0.0 (1 test)		

Figure 15. HGMF TEST POINTS.

Using the optimum conditions defined by the above tests, the continuous 500 hour test was to be conducted.

7.2 TEST PROCEDURES

7.2.1 Sampling Procedures

Particle size distribution measurements were made at the inlet and outlet sampling locations with MRI Model 1502 cascade impactors. The particulate sampling procedure utilized in these tests was adopted from EPA guidelines for the use of cascade impactors (Harris, 1977). The majority of the impactor substrates were precoated with Apiezon L grease and baked at 150° C for 4 hours. Several impactor runs were performed with Kapton substrates to allow trace element analysis by particle size.

The nozzle sizes and sample rates were selected to obtain a velocity isokinetic with the gas velocity in the pipe. The temperature of the impactors was controlled to within ± 20° C of the stack gas temperature which ranged from 30° C to 70° C. Several impactor blanks were also run as a control measure to determine the weight gains attributed to reactions of the stack gas with the substrate.

Since the impactors were used external to the pipes, the probes were washed with acetone to recover any material that did not reach the impactor. The probe wash mass was included in the total mass calculations but not in the fractional efficiency calculations since no attempt was made to assign a size to it.

The sampling nozzles used with the cascade impactors were 90° bend type. Preparation of the particle size distributions graphs for this report assumed no significant loss of impactor-sizeable particles to the nozzle wall. In fact, such nozzle wall losses do occur. Calculations for the nozzle sizes used in this sampling work show nozzle cut sizes in the range of 3 to 5 μm. For this reason, data for impactor stages with cut points above 3 to 5 μm probably incorrectly portray the weight distribution. The practical effect of this data limitation is loss of resolution in the size distribution curve above the nozzle cut point i.e., one is forced to begin extrapolation of the curve at 3 to 5 μm rather than 8 to 10 μm.

A sampling train as shown in Figure 16 was used for the impactor sampling and for the particulate concentration sampling.

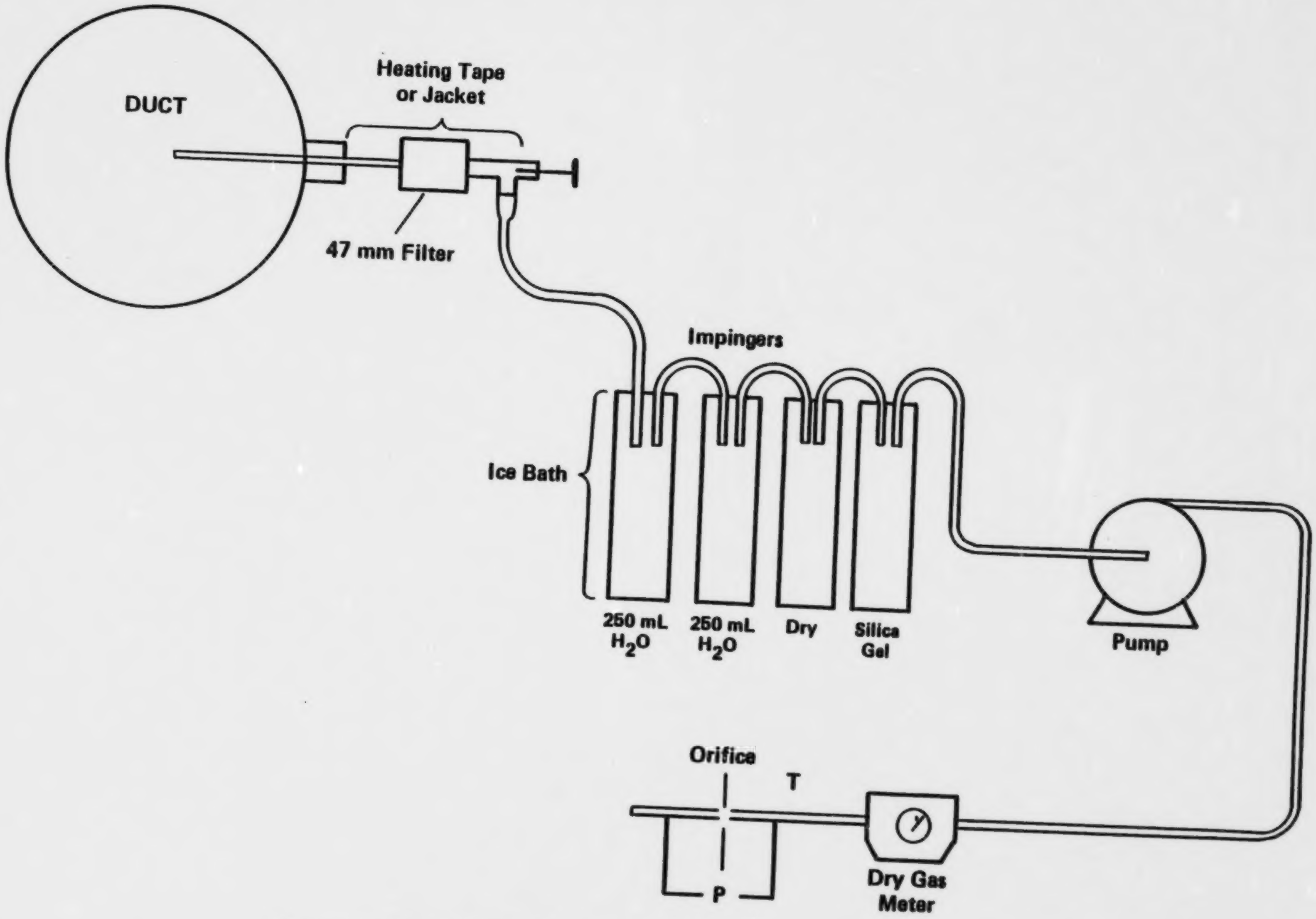
DUCT
Heating Tape or Jacket
47 mm Filter
Impingers
Ice Bath
250 mL H_2O
250 mL H_2O
Dry
Silica Gel
Pump
Orifice
T
P
Dry Gas Meter

Figure 16. Filter train for determination of mass efficiency.

The particulate concentration sampling utilized a 47 mm diameter fiberglass pad in a heated filter holder located outside the duct. The procedure to measure the gas velocity and control the sampling flow was similar to that described for the cascade impactor.

The weighing of the impactor substrates and the filters is a critical operation in the successful execution of the test program. The balance, a Perkin-Elmer Model AD-2Z microbalance, is calibrated with a class M weight which is NBS traceable. Because a weighing-by-substition method is used, a reference control disc is frequently weighed to verify the accuracy of the balance.

7.2.2 Filter Operating Procedures

As stated in Section 6.0 of this report, the optimum carousel speed and cleaning system firing cycle was determined by operation of the pilot plant. The criterion was the optimum combination of filter dust loading and cleaning pulse force and timing in order to achieve a steady state pressure drop across the filter. The optimum dust loading was achieved with a carousel speed of 0.000424 rev/s for every m/s of gas velocity through the filter. The optimum cleaning pulse pressure was 272 kPa gauge (40 psig) with the cleaning system firing through each cassette once for each revolution of the carousel. Whenever the gas velocity through the filter was changed, there had to be a corresponding change in the carousel rotation speed and the cleaning tank cycle in order to obtain the same filter dust loading.

The applied magnetic field in the filter was controlled by the current output of the dc power supply operating the magnet. The dc current versus applied field calibration curve was prepared and check by Sala Magnetics, Inc. Whenever the applied magnetic field was to be changed, then the d.c. current output of the power supply was set to the appropriate value according to the calibration curve.

7.3 COARSE GRADE STAINLESS STEEL WOOL MATRIX

The initial filter medium was American Iron and Steel Institute Type 430 medium grade stainless steel wool packed to a density of 0.015 (1.5 percent by volume) and came packed in the carousel from Sala Magnetics. The average fiber diameter of this material is 120 μm.

Table 6 is a summary of the results obtained from the steel wool matrix performance characterization tests. Measured overall efficiencies ranged from

TABLE 6. GEORGETOWN STEEL HGMF TESTS (STEEL WOOL MATRIX--PACKING DENSITY 0.015)

Field strength kilogauss	Velocity m/s	Pressure drop** cm H_2O	Concentration grams/scm Inlet	Concentration grams/scm Outlet	Efficiency percent
0*	7.0	38.1-58.0	0.458	0.197	57.2
1.0	5.2	25.4-35.6	0.226	0.041	82.4
1.0	5.2	25.4-35.6	0.773	0.082	89.3
1.0	8.8	61.0-76.2	0.844	0.265	68.7
1.0	8.8	61.0-76.2	0.730	0.108	85.3
2.5	4.0	15.2-22.9	0.270	0.048	82.4
2.5	4.0	15.2-22.9	0.291	0.046	84.4
2.5	7.0	38.1-50.8	0.862	0.096	88.9
2.5	7.0	38.1-50.8	0.153	0.025	84.1
2.5	7.0	38.1-50.8	1.048	0.059	94.4
2.5	7.0	38.1-50.8	0.435	0.053	88.2
2.5	7.0	38.1-50.8	0.611	0.078	87.4
2.5	10.0	76.2-91.4	0.657	0.085	87.3
4.0	5.2	25.4-35.6	0.270	0.050	81.4
4.0	5.2	25.4-35.6	0.602	0.053	91.1
4.0	5.2	25.4-35.6	0.178	0.053	71.0
4.0	5.2	25.4-35.6	0.201	0.043	79.0
4.0	8.8	61.0-76.2	0.430	0.046	89.3
4.0	8.8	61.0-76.2	1.025	0.108	89.5
5.0	7.0	38.1-50.8	0.693	0.066	90.6

* The applied magnetic field was zero, however, a remnant field of about 100 gauss is present under this condition.

**The low value of ΔP corresponds to the free flow of gas through the slotted entry of the carousel; the high value occurs when two of the slots are covered by the gas seal as the carousel turns.

a low value of 57.2 percent with no applied magnetic field to a high value of 94.4 percent. The bulk of the measured efficiencies at magnetic field strengths at and above 2.5 kilogauss were in the range of 80 to 90 percent. Figures 17 through 22 present the particle size distribution calculated from the experimental data. The curves drawn through the data points are produced from a computerized data reduction scheme which calculates the stage cut points and then transforms the cumulative distribution versus stage cut points to log-normal space. It then fits a natural cubic spline to the transformed data and differentiates the cumulative curve to obtain the differential distribution. The differential distributions of corresponding inlet and outlet data are then multiplied by the total mass concentrations (excluding probe washes) and ratioed to obtain the fractional efficiency or penetration curve. The mass mean particle diameter measured at the filter inlet ranged from 2 to 7 μm. The mass mean diameters measured at the filter outlet ranged from 0.9 to 2.5 μm. Fractional efficiencies by particle size are present in Section 8.1.2. As discussed in Section 7.2.1, caution should be used in drawing conclusions about particle size data above 5 μm.

The data did show a general trend of increasing efficiency with an increase in field strength, but there seemed to be very little correlation of either collection efficiency or outlet concentration with gas velocity. Part of the difficult in assessing the effects of operating variables is attributable to the large variation in inlet concentrations. Statistical analyses of the test data discussed in Section 8.0 more clearly demonstrates the effects of these variables.

As is evident the pressure drop through the filter increased with increasing gas velocity. A low value of 15.2 cm H_2O occurred at a velocity of 4 m/s and a high value of 76.2 cm H_2O occurred at 10 m/s. The low value in the range of pressure drops accompanying each test run is the value considered to be the potential steady state pressure drop. The upper value of the ranges occurred when slots in the revolving carousel were partially covered by the gas seals. In a full scale system design the impact of gas seals on pressure drop could be minimized by changing the slot design.

The performance characterization tests for the steel wool matrix with a packing density of 0.015 could not remove a sufficient percentage of the dust while operating under practical conditions. It was then decided to change to an expanded metal matrix for more performance characterization tests.

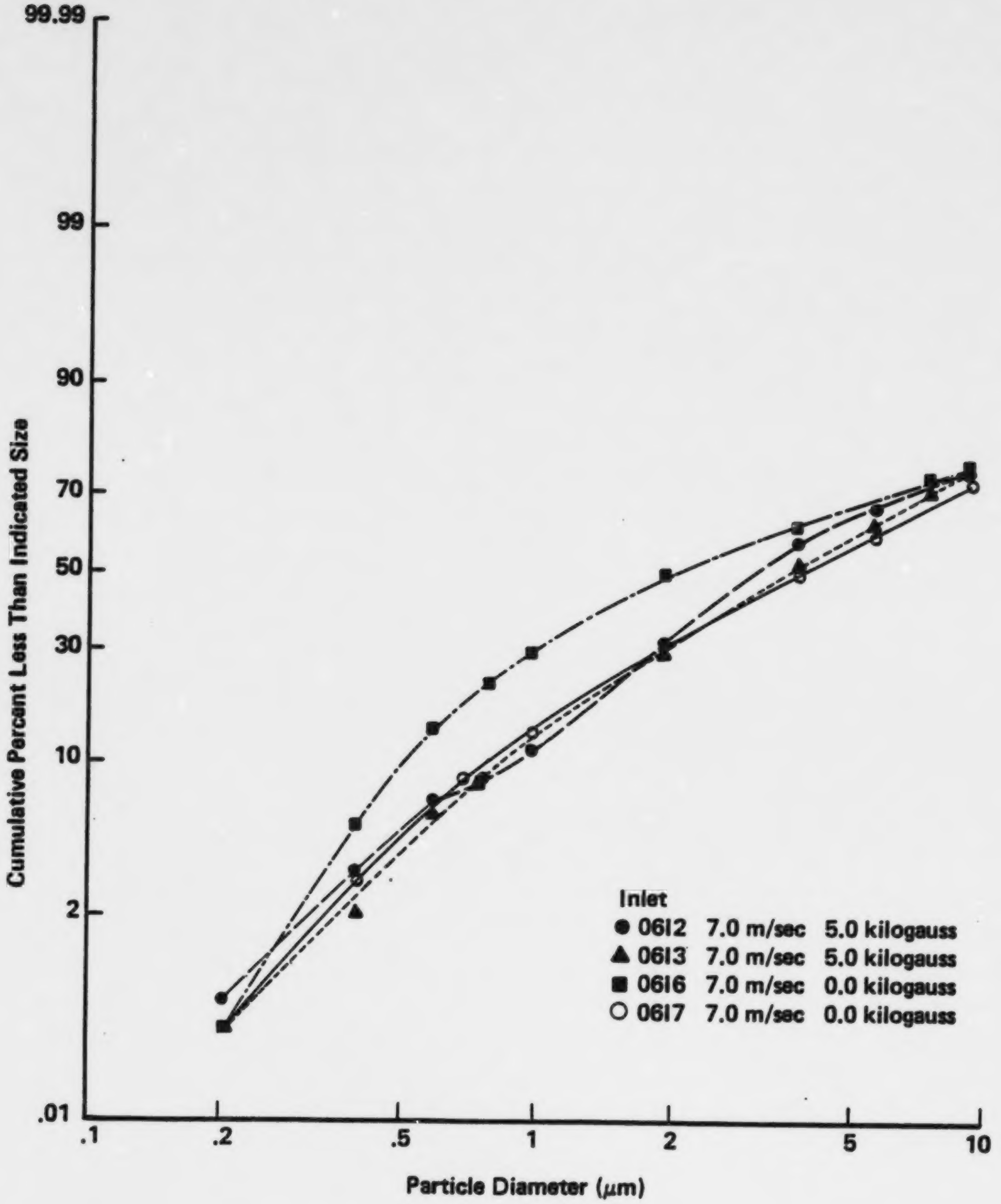

Figure 17. Georgetown Steel HGMF test—steel wool matrix (packing density 0.015).

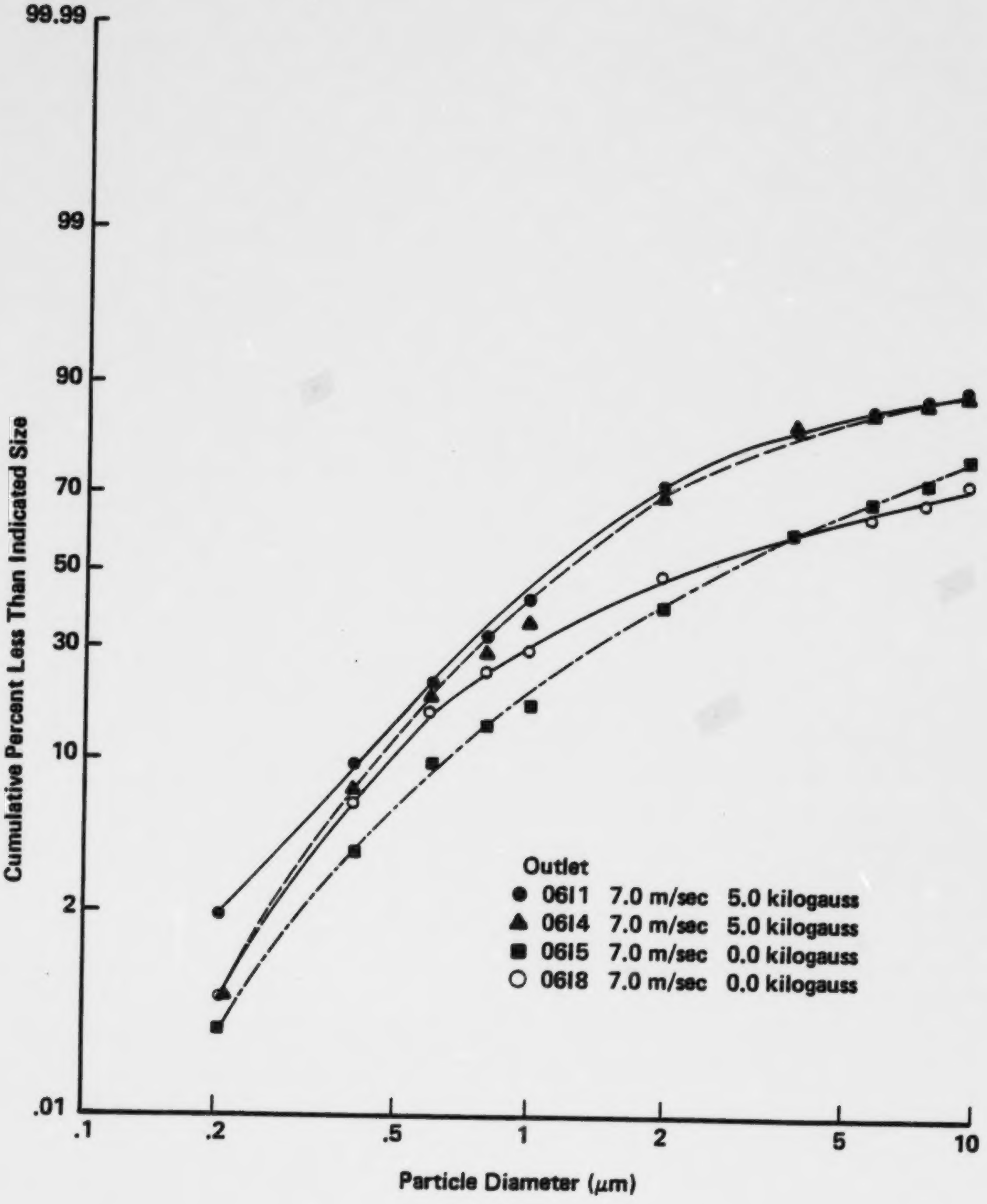

Figure 18. Georgetown Steel HGMF test—steel wool matrix (packing density 0.015).

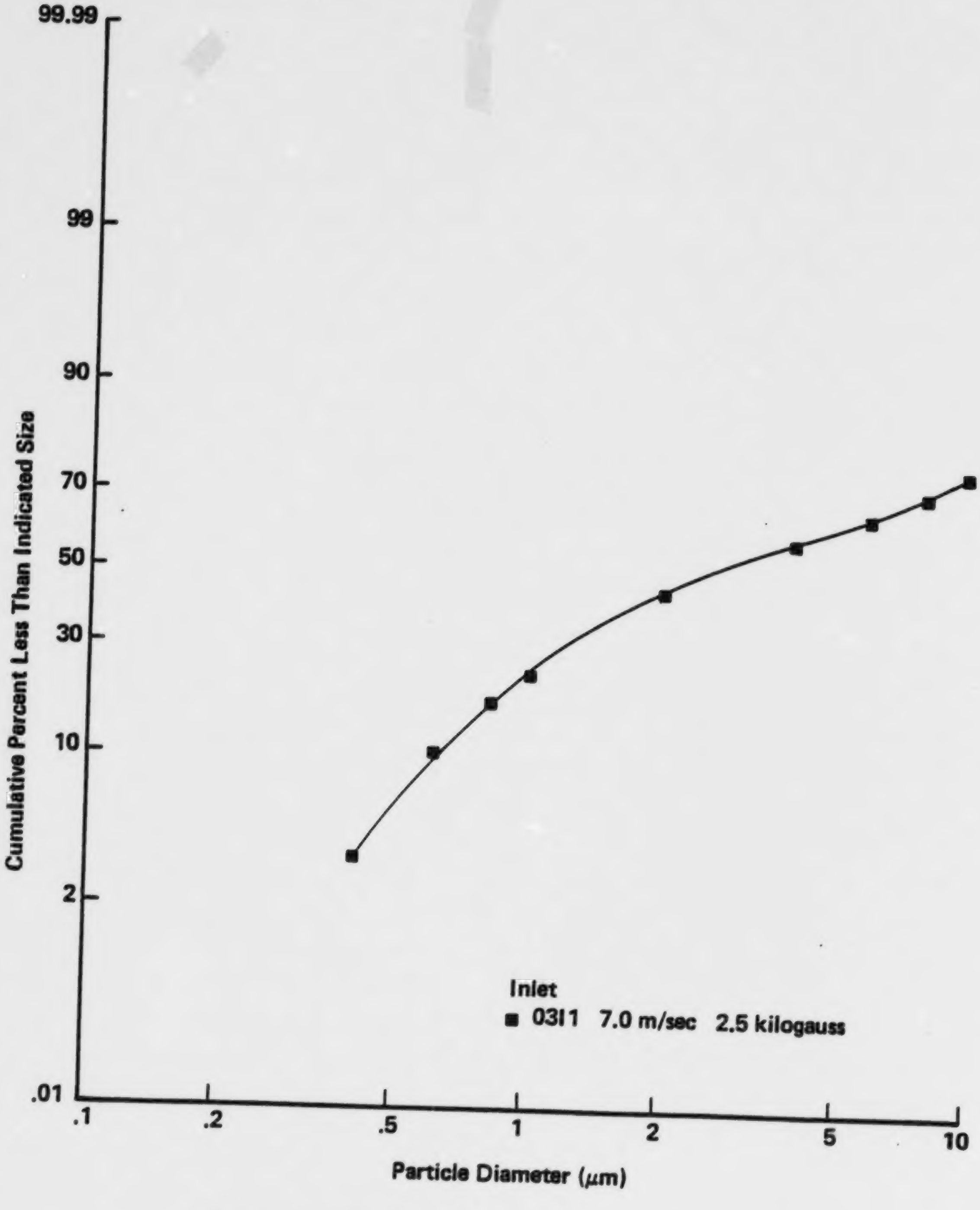

Figure 19. Georgetown Steel HGMF test—steel wool matrix (packing density 0.015).

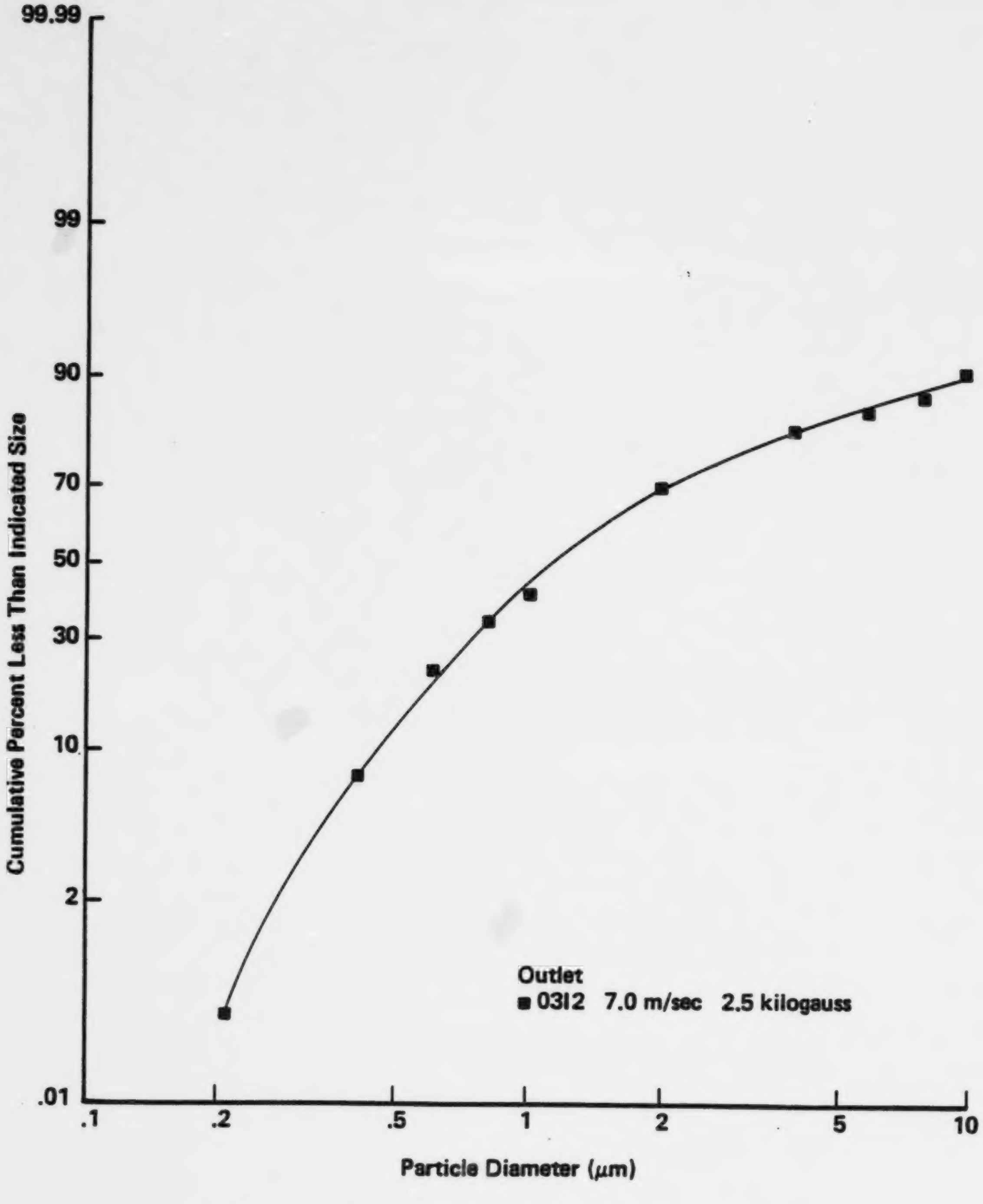

Figure 20. Georgetown Steel HGMF test—steel wool matrix (packing density 0.015).

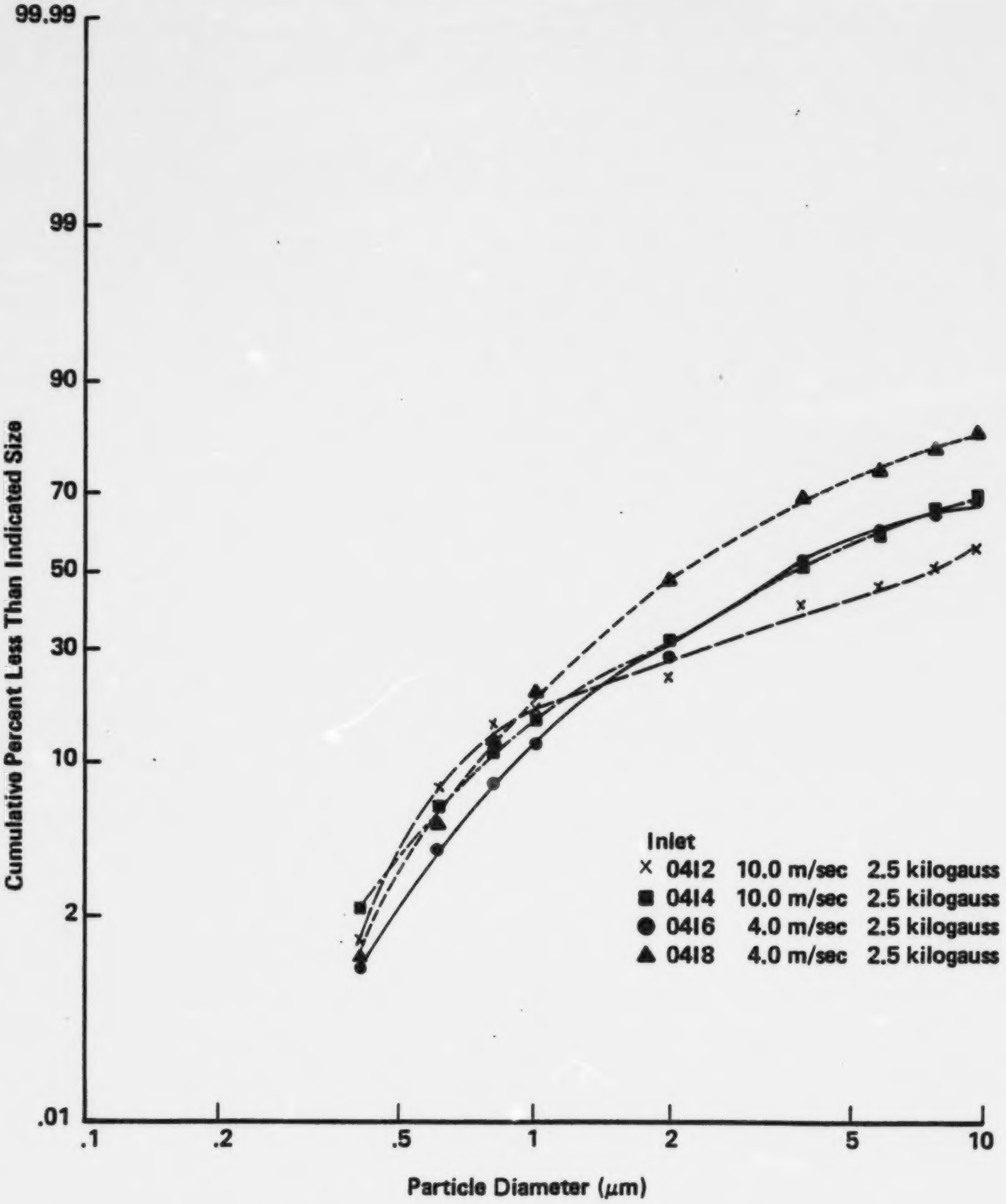

Figure 21. Georgetown Steel HGMF test—steel wool matrix (packing density 0.015).

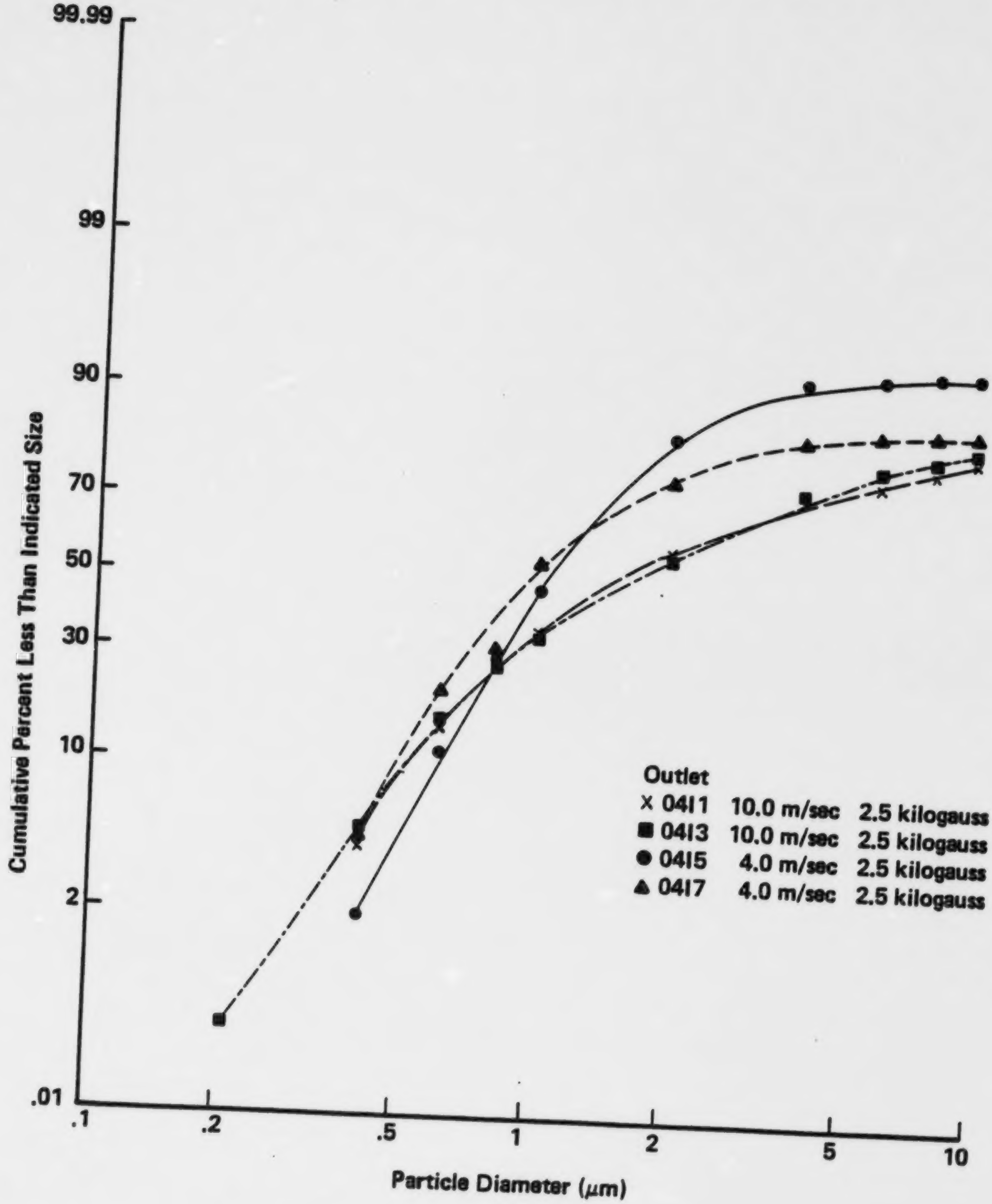

Figure 22. Georgetown Steel HGMF test—steel wool matrix (packing density 0.015).

7.4 EXPANDED METAL MATRIX

The expanded metal matrix (layers of wide mesh screen) can be packed with all of the fibers perpendicular to the magnetic field and in the optimum position for particle capture. It was hoped this would allow us to obtain a higher collection efficiency for the same pressure drop as was attained with a stainless steel wool matrix.

7.4.1 Packing Density of 3.5 Percent by Volume

The average fiber diameter of the expanded metal matrix is 300 μm as compared to the steel wool fiber diameter of 120 μm. The approximate packing density of the expanded metal matrix with the same fiber to fiber distance was calculated to be 0.035. This matrix was then packed into the carousel and a series of performance characterization tests were run.

Table 7 is a summary of the results obtained from the series of performance characterization tests run with the expanded metal matrix packed to a density of 0.035.

Measured efficiencies ranged from a low value of 72.9 percent with no applied magnetic field to a high value of 94.2 percent. As in the case of the steel wool data, the bulk of the measured efficiencies at field strengths at and above 2.5 kilogauss were in the range of 80 to 90 percent.

It is difficult to see a clear trend of efficiency changes with field strength changes due mainly to the widely varying inlet concentrations. Statistical analyses of test data discussed in Section 8.0 more clearly demonstrate the effects of variable changes on efficiency. Pressure drops through the filter matrix varied from a low value to 12.7 cm H_2O at a velocity of 5.2 m/s to a high value of 53.3 cm H_2O at velocity of 10 m/s. These values are lower than the corresponding values for steel wool. More thorough pressure drop comparisons are presented in Section 8.1.2.

Figure 23 through 28 show the calculated particle size distributions. The mass mean particle diameter measured at the filter inlet ranged from 0.8 to 3 μm during these tests. At the filter outlet the mass mean diameters ranged from 0.7 to 2.6 μm. The highest outlet mass mean diameter, 2.6 μm, was measured with no applied field. Excluding the no applied field cases the highest outlet mass mean particle diameter was 1 μm. Fractional efficiencies by particle size are presented in Section 8. As discussed in Section 7.2.1 caution should be used in drawing conclusions about particle size data above 5 μm.

TABLE 7. GEORGETOWN STEEL HGMF TESTS (EXPANDED METAL MATRIX--PACKING DENSITY 0.035)

Field strength kilogauss	Velocity m/s	Pressure drop** cm H_2O	Concentration grams/scm Inlet	Concentration grams/scm Outlet	Efficiency percent
0*	7.0	38.1-50.8	0.524	0.142	72.9
1.0	5.2	12.7-20.3	0.517	0.101	80.6
1.0	5.2	12.7-20.3	0.327	0.085	73.9
1.0	8.8	38.1-50.8	0.496	0.133	73.2
1.0	8.8	38.1-50.8	0.679	0.160	76.4
2.5	4.0	---	0.915	0.124	86.5
2.5	7.0	25.4-38.1	1.174	0.069	94.2
2.5	7.0	25.4-38.1	0.936	0.094	90.0
2.5	7.0	25.4-38.1	0.446	0.066	85.2
2.5	7.0	25.4-38.1	0.469	0.114	75.6
2.5	7.0	25.4-38.1	1.288	0.194	84.9
2.5	10.0	53.3-66.0	0.577	0.062	89.1
4.0	5.2	12.7-20.3	1.235	0.146	88.1
4.0	5.2	12.7-20.3	0.355	0.073	79.6
4.0	8.8	38.1-50.8	0.501	0.082	83.6
4.0	8.8	38.1-50.8	1.039	0.153	85.3
4.95	7.0	25.4-38.1	0.844	0.169	80.1

* The applied magnetic field was zero, however, a remnant field of about 100 gauss is present under this condition.

**The low value of ΔP corresponds to the free flow of gas through the slotted entry of the carousel; the high value occurs when two of the slots are covered by the gas seal as the carousel turns.

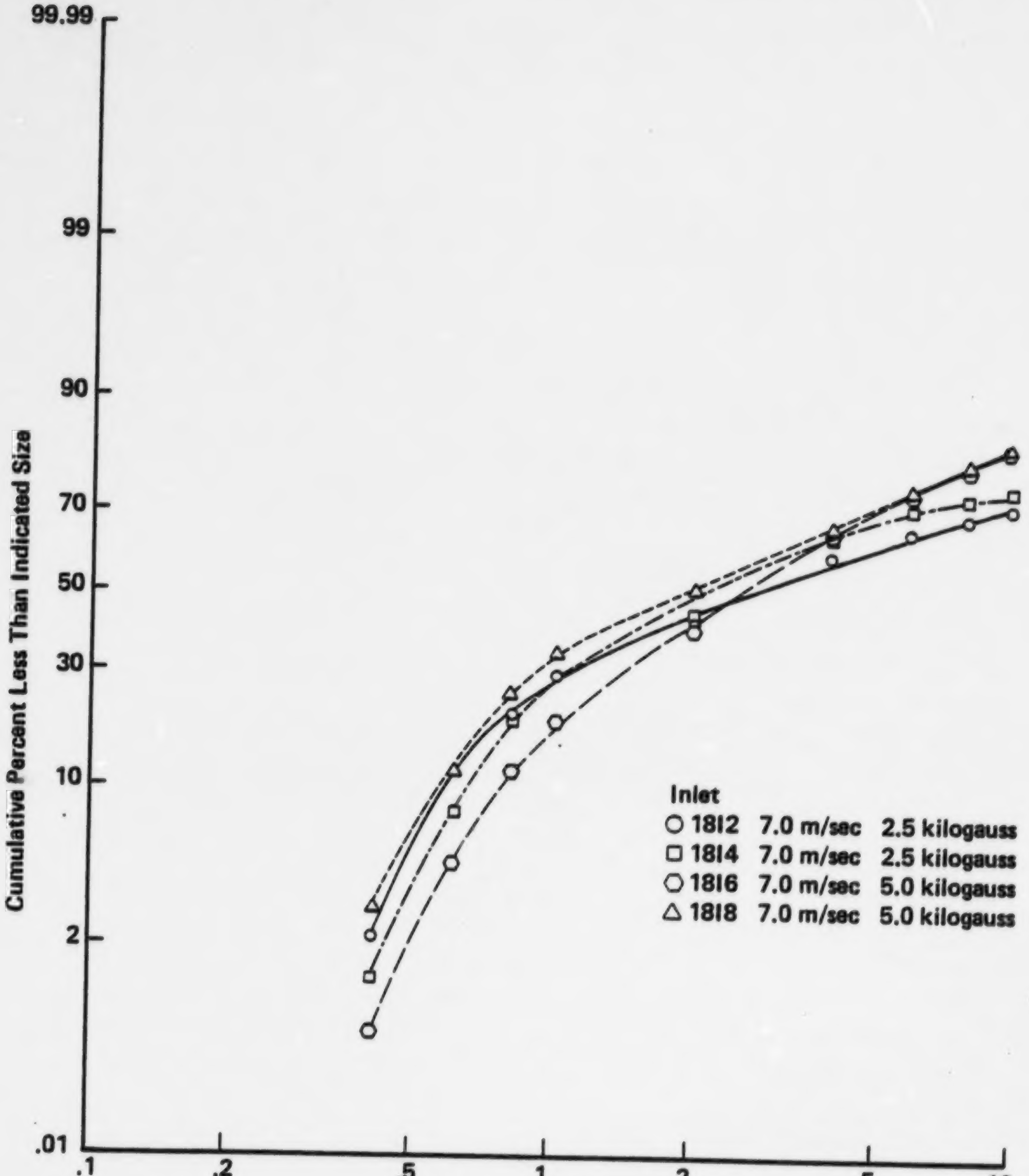

Figure 23. Georgetown Steel HGMF test—expanded metal matrix (packing density 0.035).

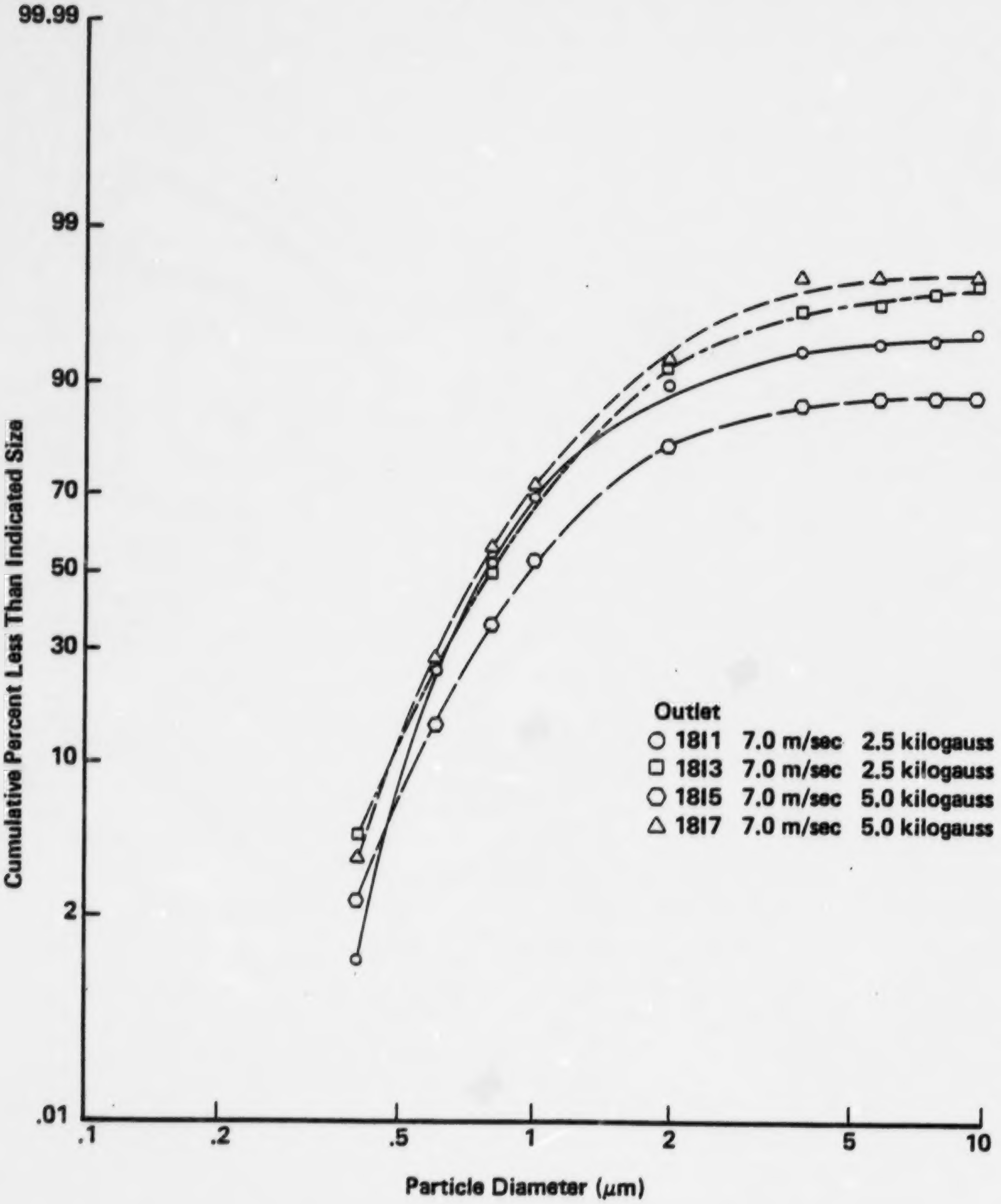

Figure 24. Georgetown Steel HGMF test—expanded metal matrix (packing density 0.035).

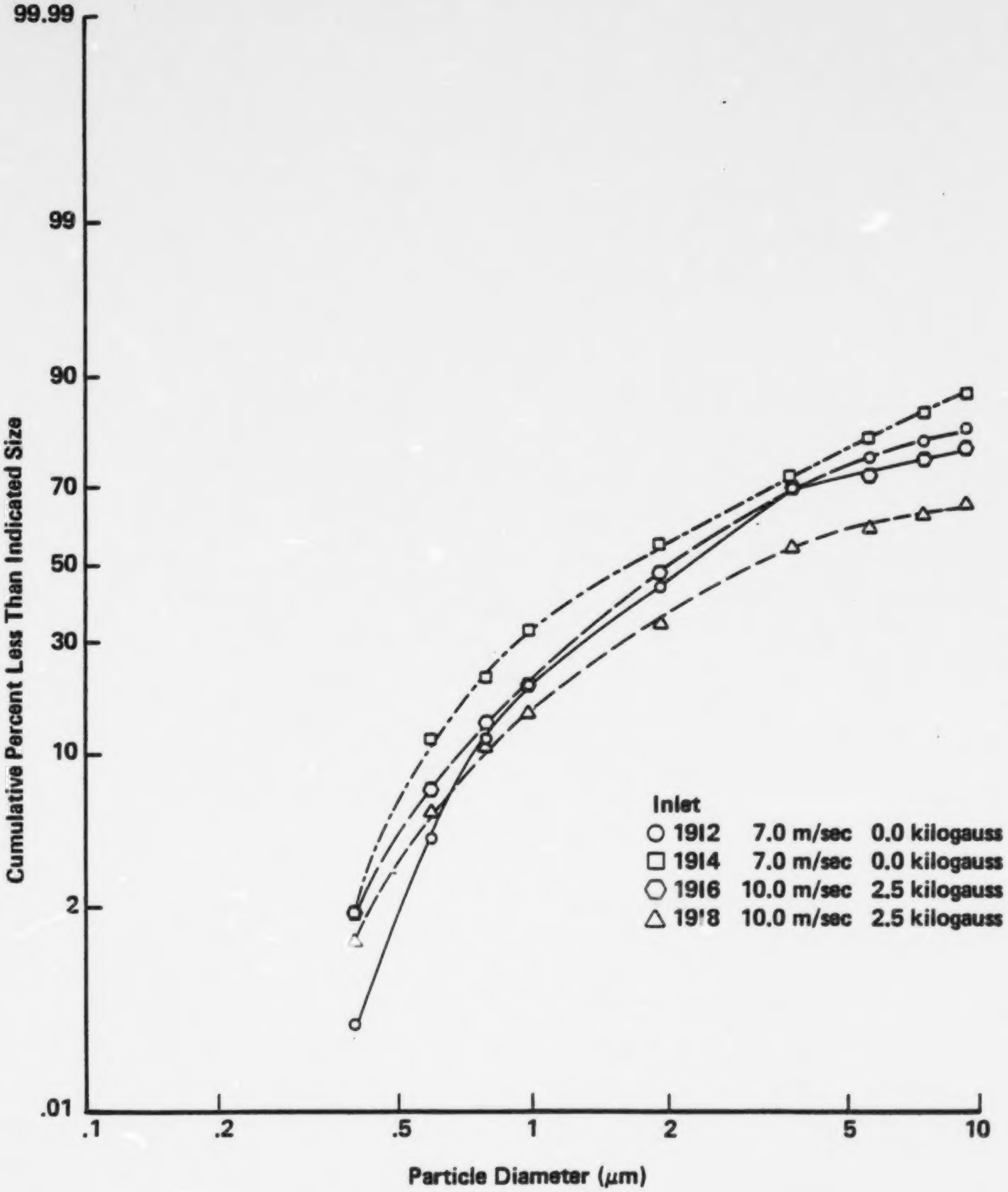

Figure 25. Georgetown Steel HGMF test—expanded metal matrix (packing density 0.035).

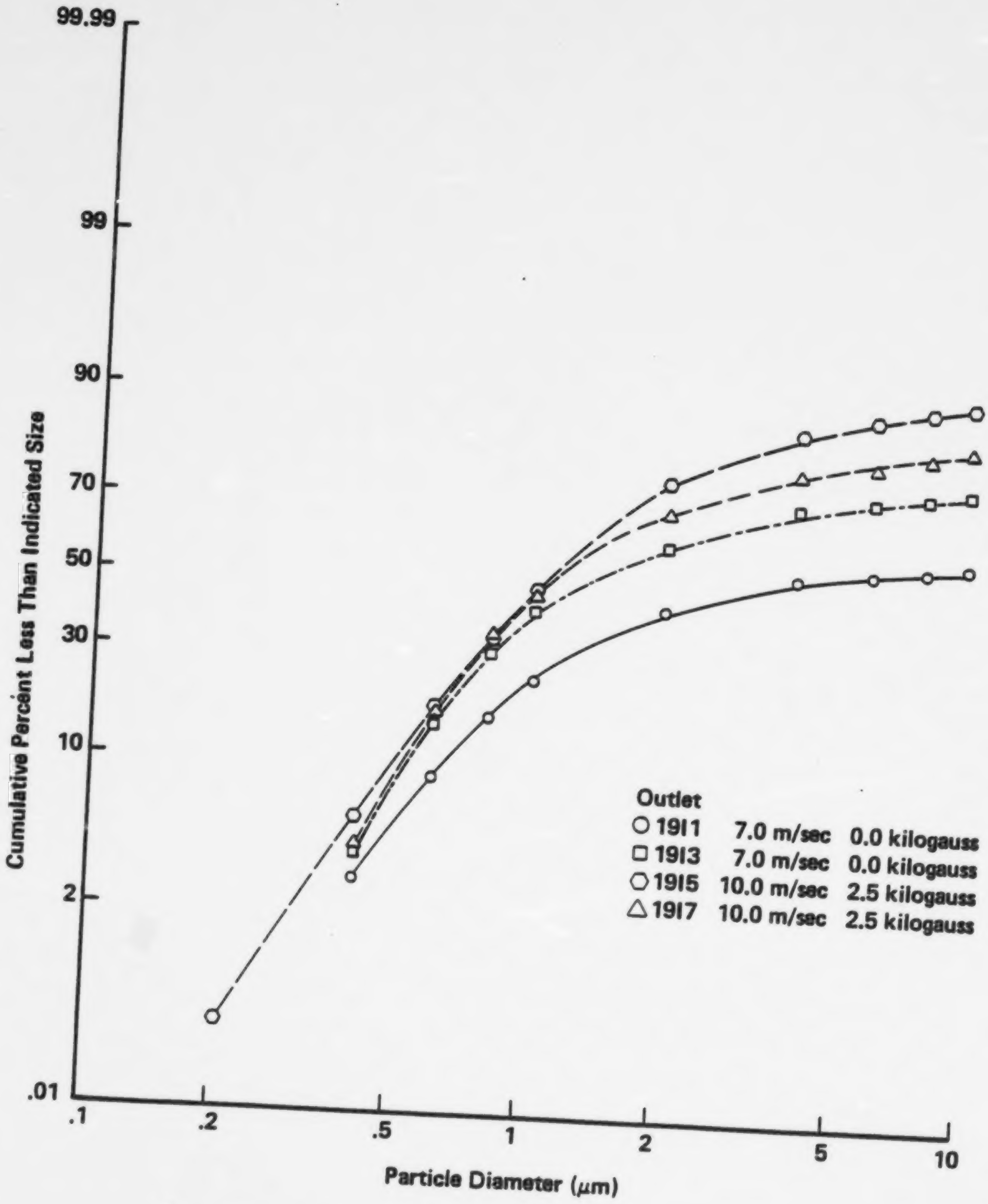

Figure 26. Georgetown Steel HGMF test—expanded metal matrix (packing density 0.035).

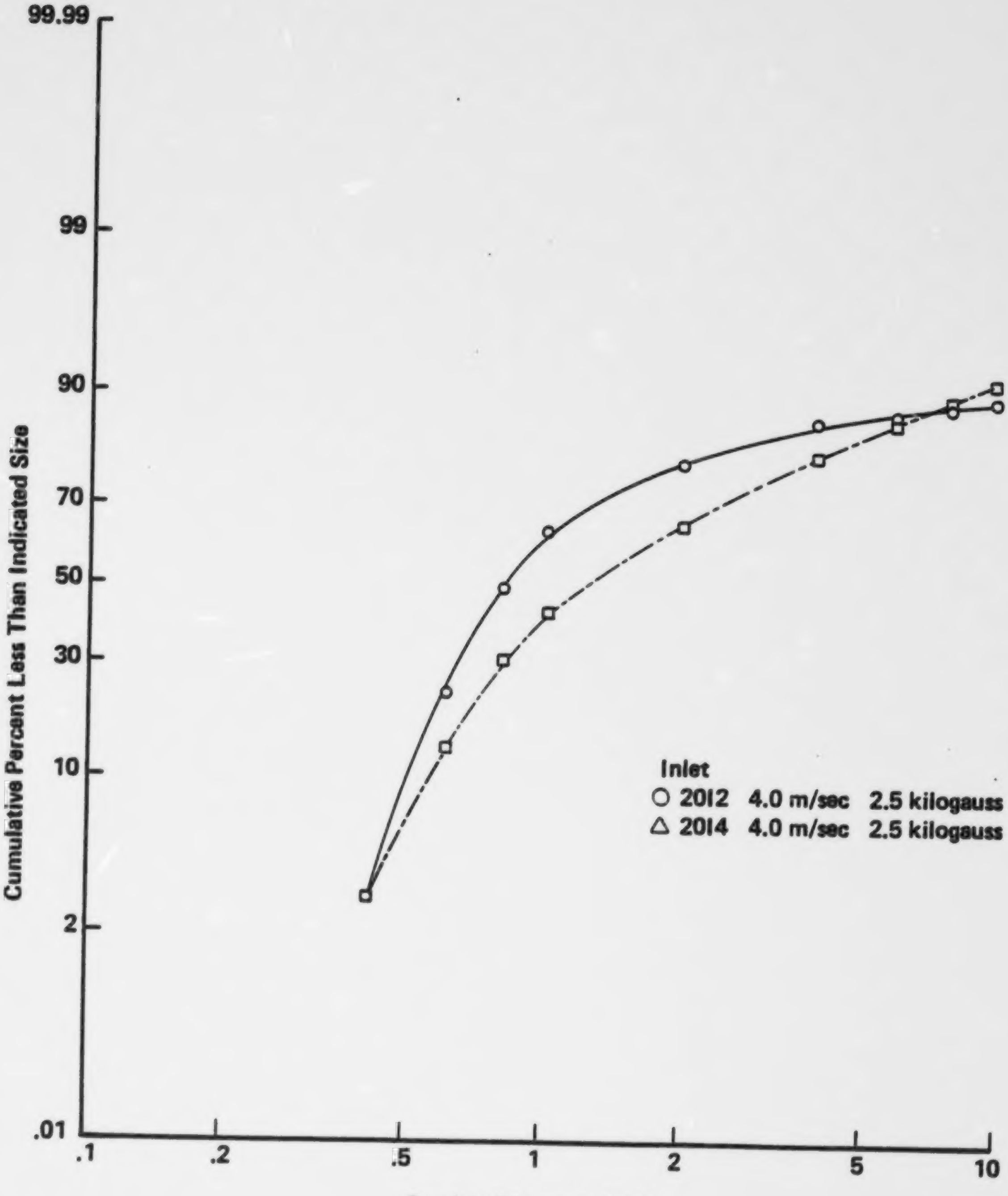

Figure 27. Georgetown Steel HGMF test—expanded metal matrix (packing density 0.035).

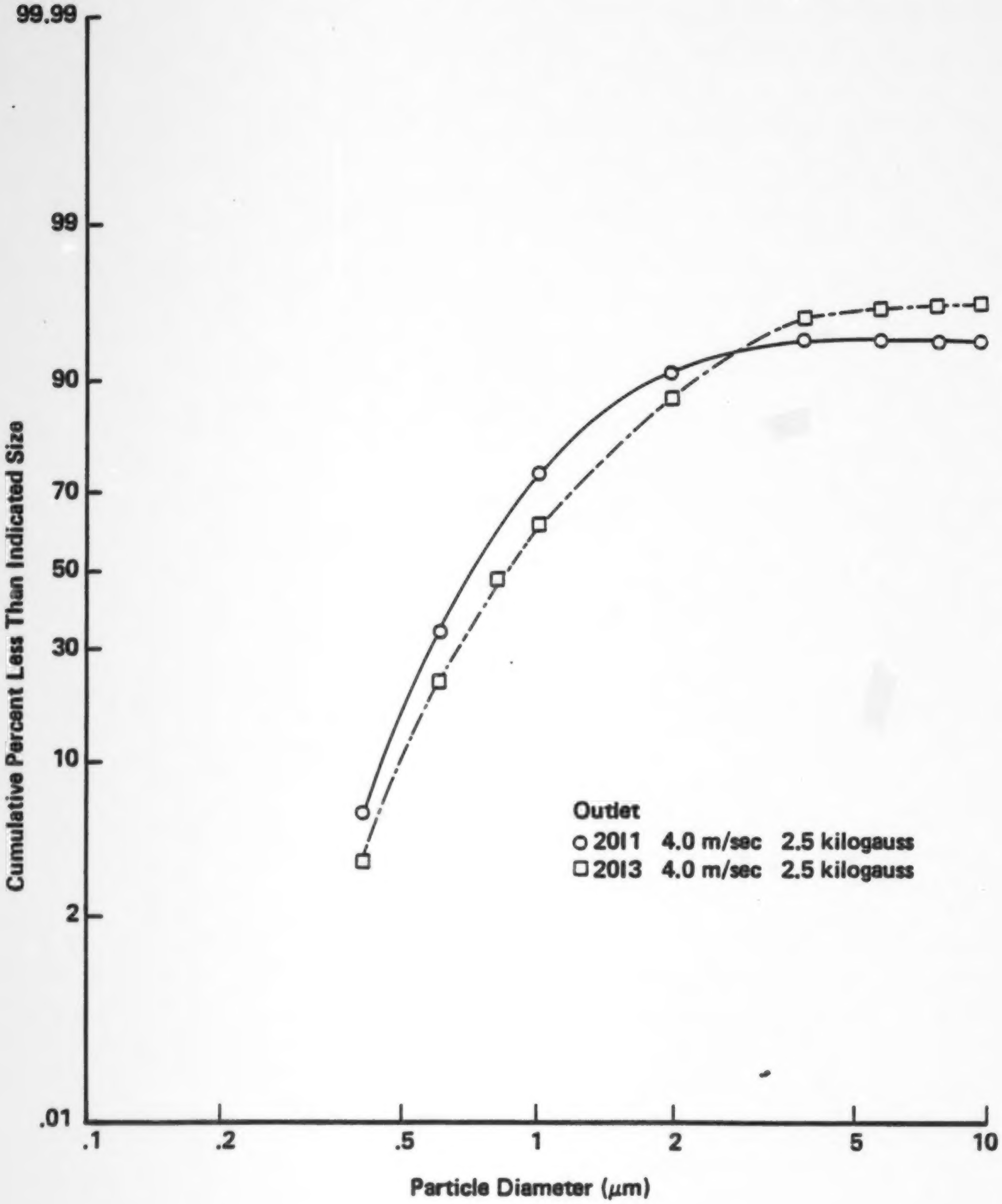

Figure 28. Georgetown Steel HGMF test—expanded metal matrix (packing density 0.035).

While the pressure drop values were improved for the same gas velocities, however, there was no improvement in the collection efficiency or in the outlet concentration values. For this reason it was then decided to increase the packing density of the expanded metal matrix and perform additional characterization tests.

7.4.2 Packing Density of 6.0 Percent by Volume

The pilot plant was shutdown and the carousel dismantled in order to repack the cassettes to a packing density of approximately 0.06. The unpacking and repacking process was relatively time consuming, requiring about three man-weeks to complete. The equipment was then reassembled and the testing begun.

Because of concerns about remaining project funds, it was decided that a complete set of 17 characterization test runs would not be performed. Initially test runs were made varying field strength from 0.1 to 5 kilogauss and velocity from 5.2 to 8.0 m/s. When relatively high pressure drops were encountered, an additional group of 3 test runs was made at a velocity of 2 m/s for field strengths of 0.1, 2.5, and 5 kilogauss.

Table 8 shows the results from the tests with the expanded metal matrix at this higher packing density. Measured overall efficiencies ranged from a low value of 79.4 percent with no applied field (excluding an apparently anomalous result of 68.5 percent at 2.5 kilogauss) to a high value of 96.4 percent. The measured efficiencies at field strengths of 2.5 kilogauss and above are in the range of 89 to 96 percent, clearly higher than those efficiencies measured for the previous two test series. As in the case of the steel wool tests there is a trend of higher efficiency with increasing field strength. Statistical analyses in Section 8 more clearly demonstrate the effect of operating conditions on measured efficiencies.

Pressure drops ranged from a low value of 1.3 cm H_2O at a velocity of 2m/s to a high value of 55.9 cm H_2O at a velocity of 8.8 m/s. Since no tests were run at 2 m/s with the steel wool matrix or expanded metal matrix at 3.5 percent packing density, low end comparisons have to be made at 5.2 m/s. At this velocity the pressure drops were 25.4 cm, 12.7 cm, and 22.9 cm H_2O for steel wool, expanded metal at 3.5 percent density, and expanded metal of 6 percent density, respectively.

TABLE 8. GEORGETOWN STEEL HGMF TESTS (EXPANDED METAL MATRIX--PACKING DENSITY 0.06)

Field strength kilogauss	Velocity m/s	Pressure drop** cm H_2O	Concentration grams/scm		Efficiency percent
			Inlet	Outlet	
0.0*	2.0	1.3-5.8	0.259	0.046	82.4
0.0*	7.0	30.5-48.3	0.504	0.104	79.4
2.5	2.0	1.3-3.8	0.240	0.009	96.4
2.5	7.0	30.5-48.3	0.612	0.066	89.2
2.5	7.0	30.5-48.3	0.229	0.072	68.5
2.5	7.0	30.5-48.3	0.598	0.053	91.1
4.0	5.2	22.9-27.9	1.037	0.063	93.9
4.0	8.8	55.9-68.6	1.474	0.054	96.3
5.0	2.0	1.3-3.8	0.383	0.018	95.3
5.0	7.0	30.5-48.3	0.269	0.022	91.7
5.0	7.0	30.5-48.3	0.936	0.052	94.4

* The applied magnetic field was zero, however, a remnant field of about 100 gauss is present under this condition.

**The low value of ΔP corresponds to the free flow of gas through the slotted entry of the carousel; the high value occurs when two of the slots are covered by the gas seal as the carousel turns.

Figures 29 and 30 show the particle size distributions for this test series. The mass mean particle diameters measured at filter inlet were 2.1 and 2.9 μm, respectively. The filter outlet measured mass mean particle diameters were 0.84 and 0.89 μm, respectively. Fractional efficiencies by particle size are presented and discussed in Section 8.1.2. As discussed in Section 7.2.1 caution should be used in drawing conclusions about particle size data above 5 μm.

During the above particle measurements runs the impactors were loaded with Kapton substrates to permit chemical analysis of the particles on a particle size basis. Results of these analyses are presented in Section 8.2.2.

Although the overall efficiencies for this test series were significantly improved over those of the previous two test series, a problem with the technology was still apparent in that measured efficiencies were not in a range competitive with proven high efficiency technology i.e., scrubbers, precipitators, and fabric filters. At this point field experimental work was interrupted to analyze and review all the data obtained to date. The intent was to determine the cause for residual mass penetration at the 5 to 10 percent level and to consider whether changes could be made to the system to improve its performance. With the HGMF not yet being competitive with other collecting devices in performance there would be little justification for a 500-hour long term test to examine reliability.

Results of the data review and analysis are contained in Section 8, as well as a discussion of the bases for conclusions. Without further details in this section, a decision was made to forego the 500-hour test and use the limited remaining funds on additional performance characterization with the expanded metal matrix at 6 percent packing density.

7.4.3. Additional Testing

Since the initial cleaning system consisting of a 0.045 m^3 (12 gallon) air tank and a 1½ inch poppet valve had to be changed to a 0.095 m^3 (25 gallon) tank with a 4 inch Galigher valve, the surge tank was inadequate to dampen the pulse from the cleaning system. This resulted in a considerable surge of gas entering the inlet pipe just ahead of the filter each time the cleaning system fired. A visible puff of smoke could be seen coming from the stack each time the cleaning system was pulsed. It was thought that this surge of air just ahead of the filter might be reentraining particles already removed from the

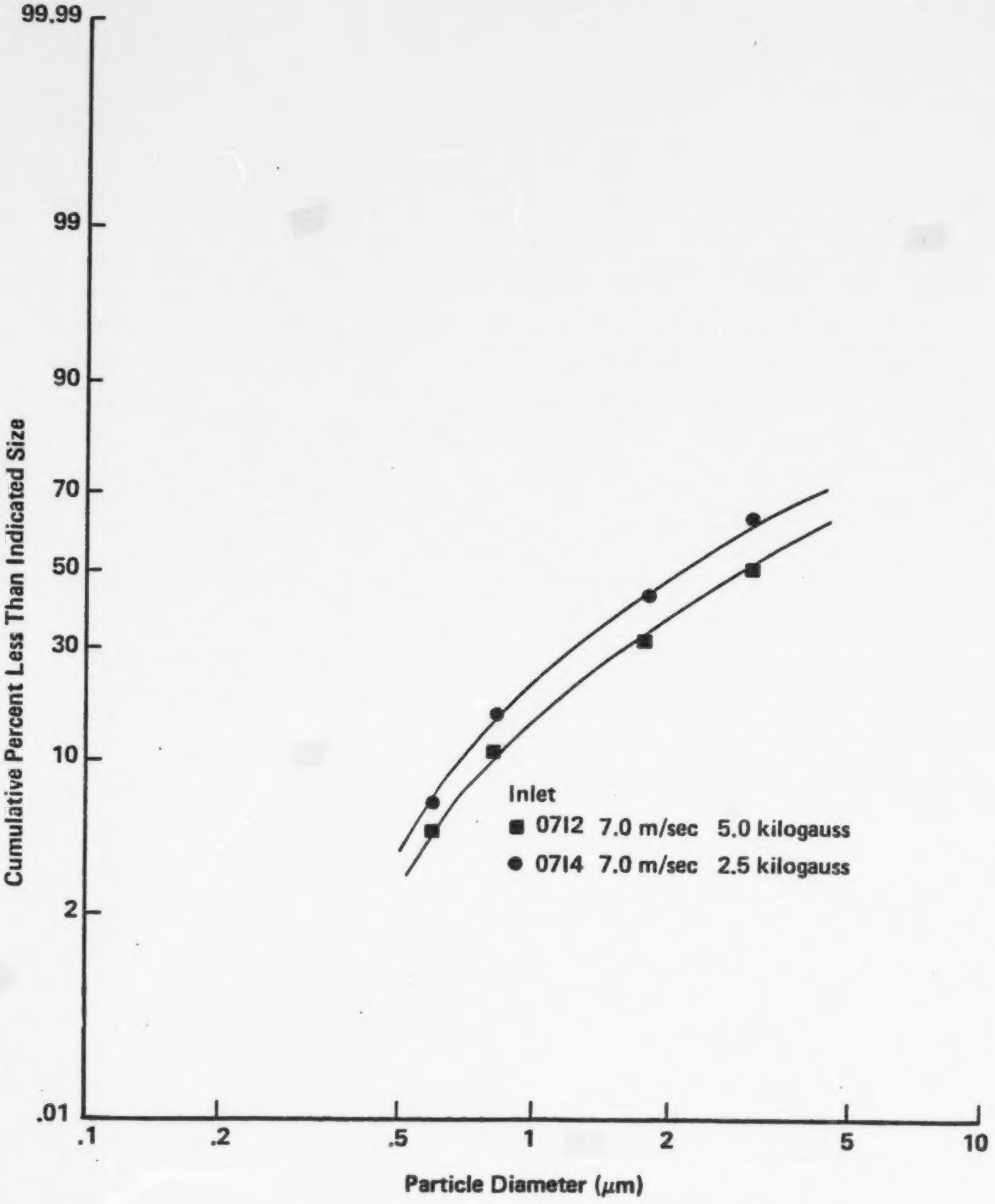

Figure 29. Georgetown Steel HGMF tests expanded metal matrix (packing density 0.06).

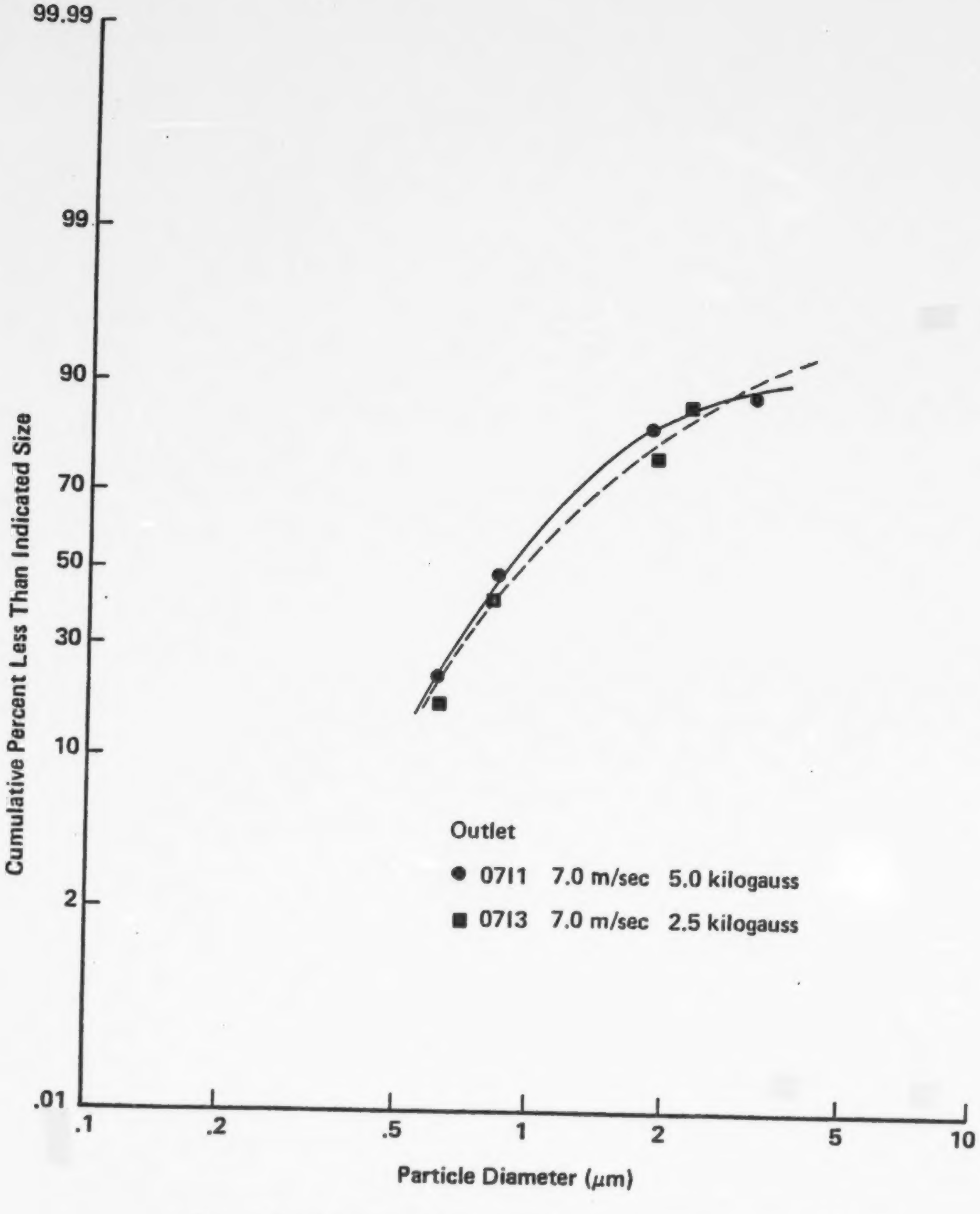

Figure 30. Georgetown Steel HGMF test expanded metal matrix (packing density 0.06).

gas stream by the magnetic filter and consequently reducing collection efficiency. For this reason it was decided to carry out additional performance characterization tests with the recycle line disconnected. The velocity selected for these tests was chosen to give a pressure drop somewhat similar to that for a fabric filter system.

Table 9 shows the results obtained from these performance characterization tests. Measured efficiencies ranged from a low value of 85.1 percent to a high value of 93.5 percent. These performances were obviously not better than those measured with the recycle line connected. Comparisons of the two data sets for expanded metal at 6 percent packing density are presented in Section 8.

Pressure drops averaged 31.8 cm H_2O for these six test runs. Figures 31 and 32 show the particle size distributions calculated from the test data. The mass mean particle diameters of the filter inlet ranged from 1.6 to 4.0 μm. At the filter outlet the mass mean particle diameter ranged from 0.8 to 1.1 μm. Section 7.2.1 discusses caution to be used in drawing conclusions about particle size data above 5 μm.

TABLE 9. GEORGETOWN STEEL HGMF TESTS (EXPANDED METAL MATRIX--PACKING DENSITY 0.06, NO RECYCLE)

Field strength kilogauss	Velocity m/s	Pressure drop* cm H_2O	Concentration grams/scm Inlet	Concentration grams/scm Outlet	Efficiency percent
2.5	5.2	22.9-33.0	0.551	0.070	87.2
2.5	5.2	21.6-30.5	0.355	0.024	93.3
2.5	5.2	22.9-33.0	0.769	0.074	90.3
5.0	5.2	21.6-27.9	0.412	0.041	90.1
5.0	5.2	19.1-27.9	0.369	0.055	85.1
5.0	5.2	22.9-30.5	0.805	0.052	93.5

---

*The low value of ΔP corresponds to the free flow of gas through the slotted entry of the carousel; the high value occurs when two of the slots are covered by the gas seal as the carousel turns.

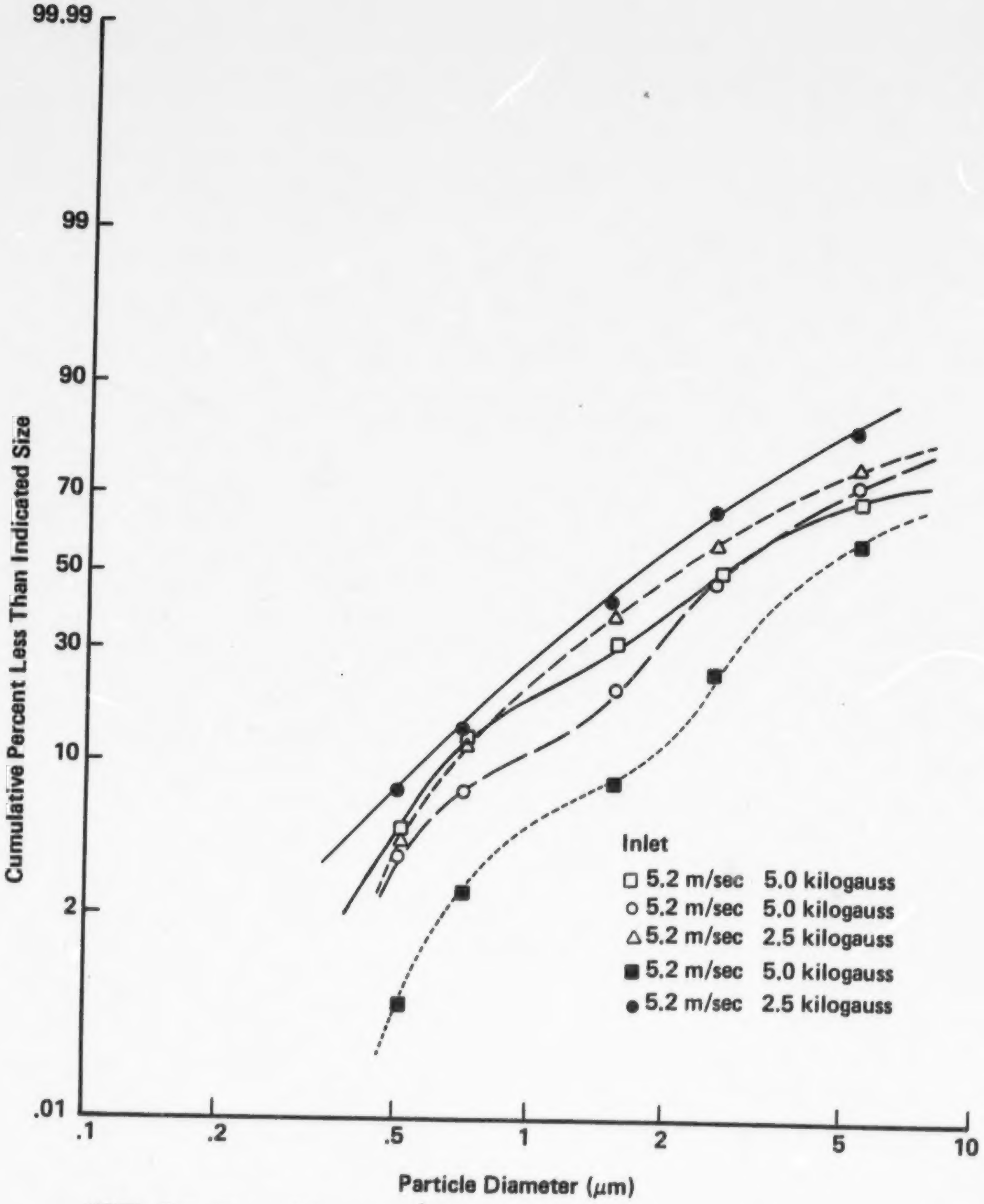

NOTE: Test with recycled gas stream disconnected.

Figure 31. Georgetown Steel HGMF test—expanded metal matrix (packing density 0.06).

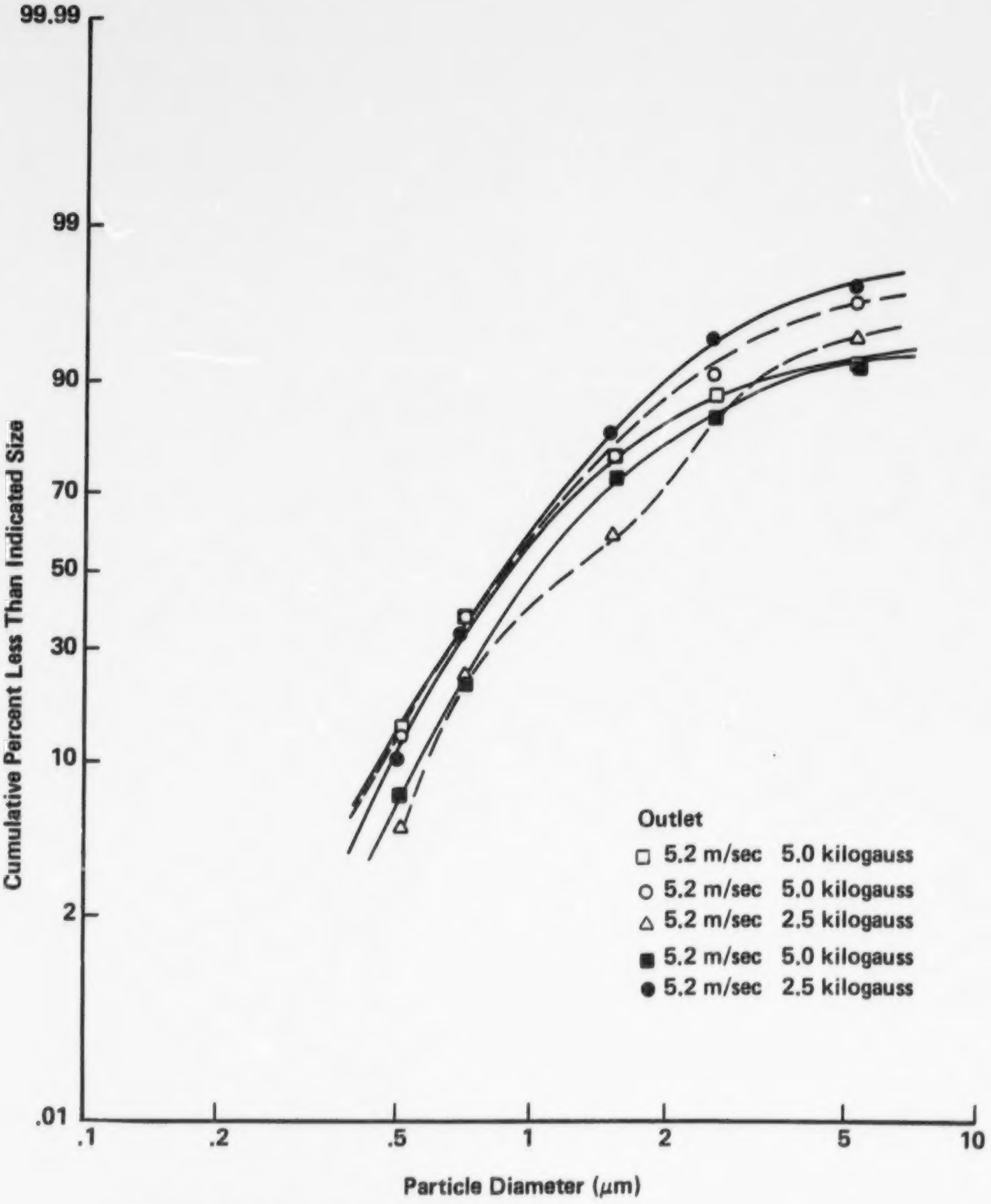

NOTE: Test with recycled gas stream disconnected.

Figure 32. Georgetown Steel HGMF test—expanded metal matrix (packing density 0.06).

8.0 DATA ANALYSIS

8.1 PERFORMANCE DATA

Analyses of HGMF system performance were made by examining overall inlet and outlet mass measurements, and by examination of fractional particle size efficiency (penetration) as affected by the controlled variables of magnetic field strength, gas velocity through the filter, packing density, and packing type. The statistical experimental design provided data over a range of independent variable values facilitating statistical analysis of overall performance and assisting graphical interpretation of effects on fractional size efficiency.

8.1.1 Overall Performance

Multiple linear regression techniques were used to analyze the data. The groups of data for each matrix type and packing density were obtained in sequence, rather than randomly, owing to the difficulty of changing the carousel cassettes. Also because of this factor, statistical analyses were performed on the data grouped by packing type and packing density. At the end of the data gathering period when data from all the tests were available the data were lumped together and multiple linear regression was used to examine relationships for the aggregated data. The ready availability of computer facilities made an exhaustive approach to regression analyses on the data possible.

Prior to beginning the statistical analysis there was no notion as to whether penetration (1-efficiency) or outlet mass (or concentration) would be a better choice for the dependent performance variable, therefore both cases were studied. Another factor to remember as the statistical analyses are discussed is that identification of effects of pilot plant operating variables may have been easier had the inlet dust concentration been maintained at some fixed value. Unfortunately, random process variations (three nearly independently operated furnaces) produced about a 6:1 range of variations in inlet concentrations, not to mention important variations in dust chemical composition.

8.1.1.1 Steel Wool-Packing Density 1.5 Percent. There were twenty test runs performed with this matrix and packing density. The test data were previously listed in Table 6. Table 10 is a partial tabular display of the regression forms examined. Multiple correlation coefficients are listed as well as the significance of the regression (F-statistic).

While the statistical design was chosen to promote evaluation of first and second order effects of the principle independent variables (field strength and velocity), the regression model that gave the best fit was an exponential model. As shown in Table 10, the model in column 1 with second order effects:

$$\text{Outlet concentration} = 0.0135 - 0.0067\ \text{FS} + 0.001\ (\text{FS})^2 + 0.0052\ \text{Vel} + 0.001\ (\text{Vel})^2 - 0.0042\ (\text{FS})(\text{Vel}) + 0.066\ (\text{In Conc}),$$

had a correlation coefficient of 0.856 and F-statistic of 5.92. The exponential model listed in column 6:

$$\ln\ (\text{Outlet mass}) = -1.23 - 0.319\ \ln(\text{FS}) + 0.690\ \ln\ (\text{Inlet mass})$$

$$\text{Outlet mass} = \frac{0.292\ (\text{Inlet mass})^{0.690}}{\text{FS}^{0.319}}$$

had a correlation coefficient of 0.893 and F-statistic of 33.64.

Comparison of columns 4 and 6 show that a better correlation was achieved using outlet mass (velocity x outlet concentration) as the dependent variable than with penetration (1-efficiency) as the dependent variable.

One premise with which the experimental program began, namely that velocity was a significant independent variable, was not clearly demonstrated in the statistical analysis. In every case where velocity was treated as an independent variable, the addition of velocity to the regression model did not significantly improve the correlation coefficient or F-statistic. Stepwise regressions, when adding velocity to a given model, gave insignificant t-statistics for the velocity coefficient. In spite of this fact, velocity does appear in the best fit regression equation since both inlet and outlet mass rates are computed using the velocity. The benefit of using mass rate instead of concentration is demonstrated by comparing columns 2 and 6. Both

TABLE 10. HGMF OVERALL PERFORMANCE REGRESSION COEFFICIENTS, STEEL WOOL MATRIX

Independent Variables*	Dependent Variables 1 Outlet Concentration	 2 ln (Outlet Conc.)	 3 Penetration	 4 ln (Penetration)	 5 Outlet Mass (Vel x Outlet Conc.)	 6 ln (Outlet Mass)
FS	-0.0067	-----	-0.149	-----	-0.227	-----
(FS)^2	0.0010	-----	0.024	-----	-----	-----
ln(FS)	-----	-0.315	-----	-0.319	-----	-0.319
Vel	0.0052	-----	-0.053	-----	-----	-----
(Vel)^2	0.0010	-----	0.003	-----	-----	-----
ln(Vel)	-----	0.283	-----	-----	-----	-----
FS x Vel	-0.0042	-----	-----	-----	-----	-----
In Conc	0.066	-----	-----	-----	-----	-----
ln (In Conc)	-----	0.482	-----	-----	-----	-----
Inlet Mass (Vel x In Conc)	-----	-----	-----	-----	0.120	0.690
ln (Inlet Mass)	-----	-----	-----	-0.310	-----	-----
Intercept	0.0135	-3.37	0.554	-1.23	0.772	-1.23
R (Correlation Coefficient)	0.856	0.846	0.629	0.734	0.747	0.893
F-statistic	5.92	13.42	2.45	9.95	10.73	33.64

*FS = Magnetic field strength. Vel = Velocity. In Conc = inlet concentration.

the correlation coefficient and F-statistic are better for the column 6 model using mass rates.

8.1.1.2 Expanded Metal-Packing Density 3.5 Percent. There were 17 test runs performed with this matrix at this packing density. The test data were previously listed in Table 7. Table 11 is a partial tabular display of the regression forms examined. As in Table 10 multiple correlation coefficients and F-statistics are also listed.

Table 11 only displays the logarithmic forms (which algebraicly convert to an exponential model) of variables because the best fits of the data were obtained in that form. As in the case of the steel wool matrix tests, the best regression fit was provided by the exponential model listed in column 3. The equation of best fit was:

$$\text{Outlet mass} = \frac{0.372\ (\text{Inlet mass})^{0.617}}{FS^{0.152}}$$

However, the fit for this data is not as good as for the steel wool data. On examination of residuals (actual outlet mass rate minus predicted outlet mass rate) one data set stands out as a possible outlier. At the time of the initial sampling results, the measured filter performance seemed unusually high for the seventh test listed in Table 7. The sample weights and calculations were rechecked, but no error was discovered. Nevertheless, the residual for this test run is about 7 times the standard error for the estimate regression and, therefore, subject to suspicion. If that set of test data is deleted, the numbers in parentheses in column 3 are the revised regression coefficients, correlation coefficient, and F-statistic. As expected, there is a considerable improvement in the degree of fit. As with the steel wool data, gas velocity by itself did not prove to be a significant correlating variable in the expanded metal tests.

8.1.1.3 Expanded Metal - Packing Density 6.0 Percent. Initially there were 11 test runs performed at this packing density. Subsequent to the preliminary data review an additional 6 test runs were made with the system as described in Section 7.4.3. Table 12 is a partial tabular display of the regression forms examined for the initial 11 test runs. Multiple correlation coefficients, F-statistics, and regression coefficients are presented.

TABLE 11. HGMF OVERALL PERFORMANCE REGRESSION COEFFICIENTS EXPANDED METAL MATRIX, 3.5 PERCENT

		Dependent Variables	
Independent Variables	1 ln (Outlet Conc.)	2 ln (Penetration)	3 ln (Outlet Mass)
ln(FS)	-0.130	-0.152	-0.152 (-0.155)*
ln(Vel)	-0.020	-----	----- -----
ln(Inlet Conc)	0.485	-----	----- -----
ln(Inlet Mass)	-----	-0.383	0.617 (0.748)*
Intercept	-2.319	-0.989	-0.989 (-1.18)*
R (Correlation Coefficient)	0.574	0.651	0.699 (0.829)*
F-statistic	2.13	5.14	6.67 (14.35)*

* Parenthetical values apply to regression without the seventh test in Table 7, an apparent outlier.

TABLE 12. HGMF OVERALL PERFORMANCE REGRESSION COEFFICIENTS EXPANDED METAL MATRIX, 6 PERCENT

Independent Variables	Dependent Variables 1 ln (Outlet Conc.)	 2 ln (Penetration)	 3 ln (Outlet Mass)	
ln(FS)	-0.284	-0.302	-0.302	(-0.284)*
ln(Vel)	-0.803	-----	-----	(1.499)*
ln(Inlet Conc)	0.304	-----	-----	-----
ln(Inlet Mass)	-----	0.0176	1.018	(0.304)*
Intercept	-4.635	-2.291	-2.291	(-5.589)*
R (Correlation Coefficient)	0.876	0.609	0.881	(0.957)*
F-statistic	7.68	2.36	13.90	(25.42)*

* Parenthetical values apply to regression including ln(Vel) as an independent variable.

As in the case of the steel wool data and expanded metal at 3.5 percent packing density, the best fit was the exponential model listed in column 3. The equation matching the earlier two test series was:

$$\text{Outlet mass} = \frac{0.101\ (\text{Inlet mass})^{1.018}}{\text{FS}^{0.302}}$$

For this test series the velocity through the matrix was found to be an important correlating variable, whereas it was not for either of the previous two data sets. The parenthetical entry in column 3 lists the appropriate values. Both the correlation coefficient and F-statistic are significantly improved by addition of velocity to the model. The equation including velocity is:

$$\text{Outlet mass} = \frac{0.0037\ (\text{Inlet mass})^{0.304} (\text{Vel})^{1.499}}{\text{FS}^{0.284}}$$

That velocity should be an important correlating variable is not surprising. By reference to the above equation, an increase in velocity would produce an increase in outlet mass, if all other variables are held constant. A potential explanation could be that higher velocity is indicative of increased reentrainment losses. As to why velocity proved to be an important correlating variable for expanded metal at packing density of 6 percent when it was not for either the steel wool or less densely packed expanded metal, it may be argued that the lower penetration levels observed for 6 percent packing were predominantly reentrainment losses and, therefore, more sensitive to velocity changes. While the data tend to support this argument, the experimental program was not sufficiently rigorous to state it with certainty.

As explained in Section 7.4.3 an additional six test runs were made with the filter cleaning system recycle line disconnected. The intent of these measurements was to examine performance without the influence of recycled fines and the periodic surge of the cleaning system recycled gas stream. These performance data were added to the previous eleven test runs and regression analyses performed for the same models given in column 3 of Table 12. Comparison of the regression coefficients, correlation coefficients, and F-statistics is presented in Table 13. The addition of the last six test runs

TABLE 13. COMPARISON OF REGRESSION STATISTICS
EXPANDED METAL MATRIX - 6 PERCENT

	Regression Coefficients				
Test runs	ln (FS)	ln (Inlet mass)	ln (Vel)	R	F
1-11	-0.302	1.018	-----	0.88	13.90
(1-11)*	-0.284	0.304	1.499	0.957	25.42
1-17	-0.233	0.987	-----	0.848	17.97
(1-17)*	-0.227	0.364	1.391	0.922	24.45

*Parentheses indicate model including velocity as an independent variable.

to the 6 percent packing density expanded metal data base produced a small decrease in the multiple correlation coefficient and F-statistic.

The hypothesis that disconnection of gas cleaning system recycle line would improve overall magnet performance was examined graphically as shown in Figure 33. The regression line shown is based on all 17 test runs. The performance data from the last 6 test runs are clearly not better than the data from the first 11 test runs. In fact the last six test runs, in general, show poorer performance for given values of the regression function. Disconnection of the recycle gas line did not produce an improvement in system performance.

8.1.1.4 Performance Summary--All Matrices, All Packing Densities. The comparative performance of the filter system for both matrices and packing densities can be seen in Figure 34. The performance data are plotted as penetration versus regression function. The line through each data set is the regression curve for that data set. The regression coefficients a, b, and c for each set of data are given in Table 14. To compare the performance one must examine the penetration at low values of the regression function for each data set. Looking at the functional relation of each variable in the regression function it is expected that best performance would be measured for low regression function values, i.e., low inlet mass, low velocity, and high field strength. Differing absolute values of the regression function occur between sets because of the different regression coefficients for each data set. At low values of the regression function, poorest performance was measured for expanded metal at 3.5 percent packing density, with clearly best performance from expanded metal at 6 percent packing density.

Table 15 provides a comparison of predicted penetration for both matrices and packing densities at fixed system operating conditions. Predicted penetrations are lower for expanded metal at 6 percent packing density and the observed pressure drop was also lower for this matrix than for steel wool. Pressure drop was significantly lower for expanded metal at 3.5 percent packing density, but its predicted penetration is about twice as high as that for 6 percent packing density at the higher field strengths. Based on Table 15, expanded metal at 6 percent packing density would be the preferred matrix.

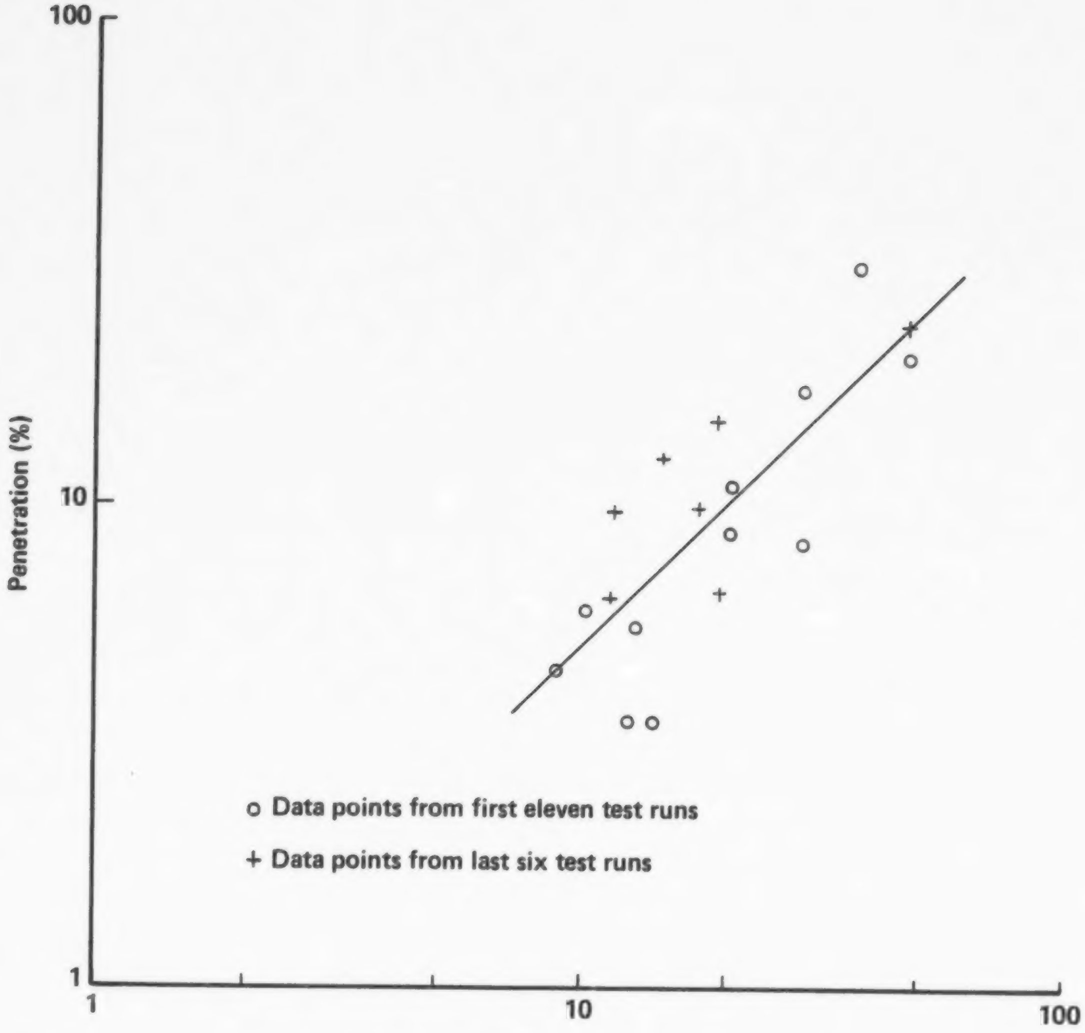

$$\frac{\text{Regression Function}}{\text{Inlet Mass}} = \frac{(\text{Inlet Mass})^{0.364}\ (\text{Velocity})^{1.39}}{(\text{Field Strength})^{0.227}\ (\text{Inlet Mass})}$$

Figure 33. Georgetown Steel HGMF test—expanded metal matrix (packing density 0.06).

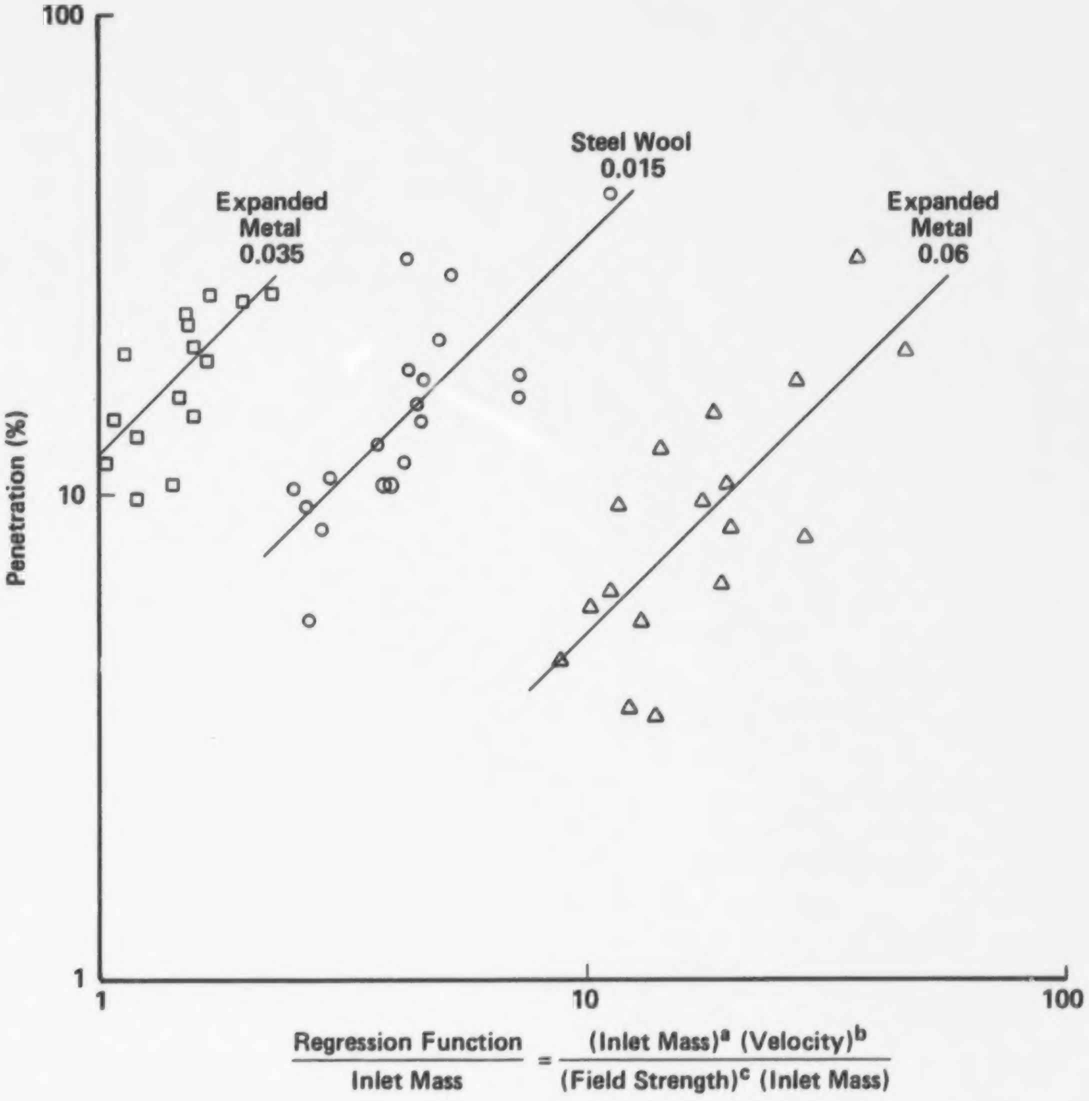

Figure 34. Georgetown Steel HGMF test—penetration vs. regression function (all matrices and packing densities).

TABLE 14. REGRESSION COEFFICIENTS FOR EACH FILTER MATRIX AND PACKING DENSITY

Model: $\text{Outlet mass} = \text{Intercept} \times \frac{(\text{Inlet mass})^a(\text{Velocity})^b}{(\text{Field Strength})^c}$

Matrix and packing density	Intercept	Regression Coefficients a	b	c	R	F
Steel wool, 0.015	0.034	0.482	0.801	0.315	0.913	26.76
Expanded metal, 0.035	0.123	0.647	0.351	0.139	0.847	10.17
Expanded metal, 0.06	0.005	0.364	1.39	0.227	0.922	24.45

TABLE 15. PREDICTED FILTER PERFORMANCE FOR EACH FILTER MATRIX AND PACKING DENSITY

Model: $\text{Outlet mass} = \text{Intercept} \times \frac{(\text{Inlet mass})^a(\text{Velocity})^b}{(\text{Field Strength})^c}$

	Matrix and Packing Density					
Operating conditions*	Steel wool 0.015 Penetration %	ΔP**	Expanded metal 0.035 Penetration %	ΔP**	Expanded metal 0.06 Penetration %	ΔP**
0.1 kilogauss 7m/s	26.2	38.1	22.5	25.4	15.2	30.5
2.5 kilogauss 7m/s	9.5	38.1	14.4	25.4	7.3	30.5
5.0 kilogauss 7m/s	7.6	38.1	13.1	25.4	6.2	30.5

* Inlet concentration = 1.0 gram/m^3.
**Actual pilot plant ΔP, cm H_2O.

8.1.2 Performance By Particle Size

The MRI cascade impactor size data were used to generate particle size fractional efficiency (penetration) curves. Simultaneously obtained inlet and outlet distribution curves were used, and in some cases data taken under duplicate conditions have been combined to provide composite fractional efficiency curves. The solid portion of the curves represents the range of particle sizes over which data were obtained, as opposed to the broken line segments representing extrapolated portions. The curves were generated assuming no nozzle wall losses. Discussion in Section 7.2.1 explains that such wall losses do occur and, therefore, all particle size distribution curves above 5 μm may not correctly portray the size distribution.

Figures 35-38 display the effects of increasing magnetic field strength at constant velocity for steel wool, expanded metal 3.5 percent packing density, and expanded metal 6 percent density, respectively. The curves show the predominant effect of increasing field strength to occur on particle sizes in the range of 1 to 10 μm. The reduction in penetration occurring from the 2.5 kilogauss to 5.0 kilogauss change is much lower than that from the no applied field (0.1 kilogauss remnant field) to 2.5 kilogauss change.

Figures 39 and 40 show the effect on penetration from changing filter velocity keeping constant field strength, for velocities of 4, 7, 10 m/s. As in the case of varying field strength, the predominant effect seems to be on particle sizes greater than 1 μm. In Figure 39 penetration decreases as velocity decreases. Potential explanations for this apparent effect are improved performance with increasing residence time, and increased reentrainment, thus, poorer performance with increasing velocity. The trend is not consistently present in Figure 40. The 7 m/s and 10 m/s curves follow the trend, but the 4 m/s curve does not. Looking at all the curves, Figures 35-40, it is evident that the filter is relatively inefficient for particle sizes below 1 μm in diameter. This leads to the question of whether the inefficiency in the smaller particle size range is inherent to the design and magnet operating conditions chosen for these tests, or attributable to variation in size related particle characteristics. The next section discusses the chemical and magnetic characterization of the electric arc furnace dust.

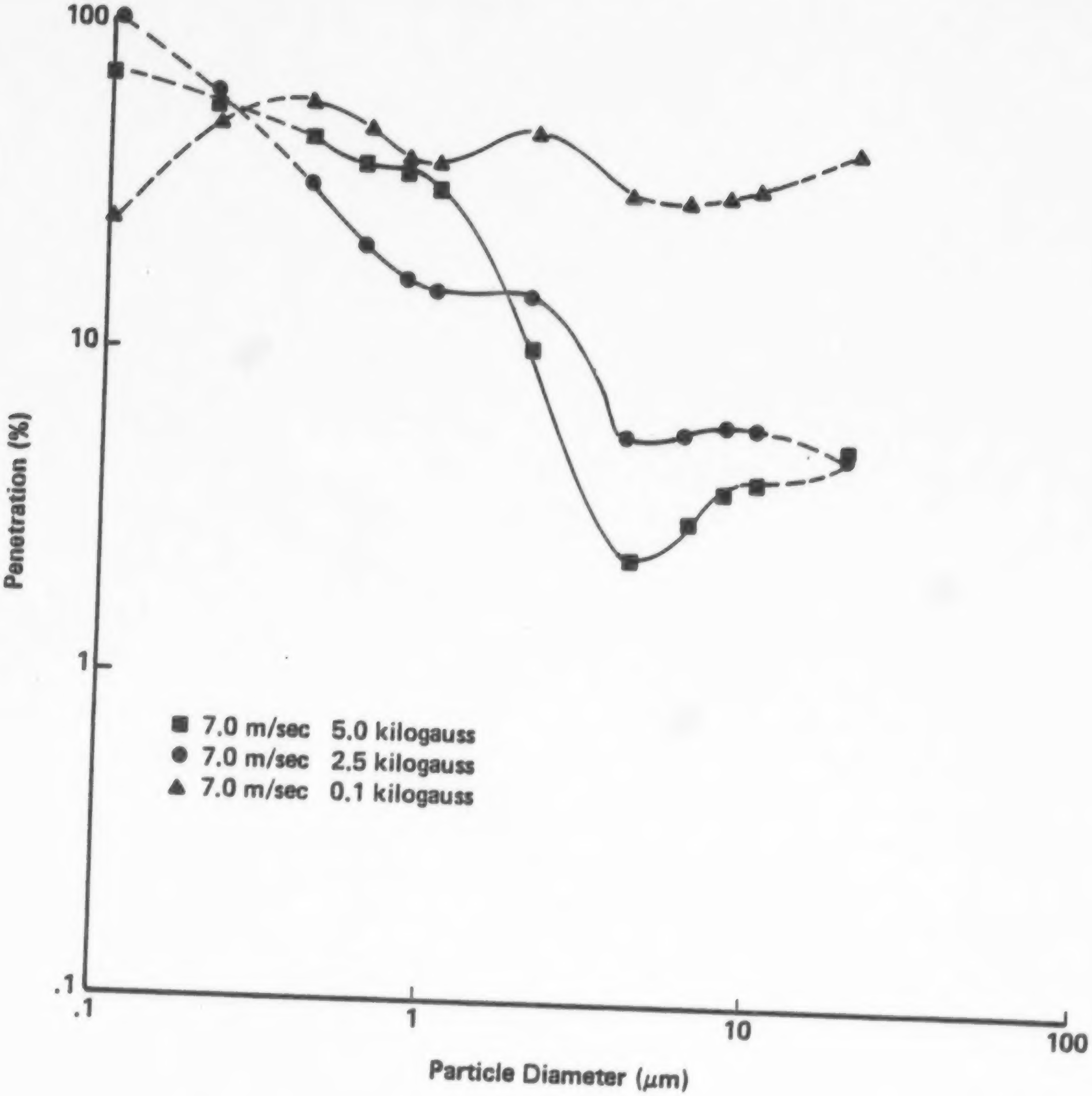

Figure 35. Georgetown Steel HGMF test—penetration vs. particle size (steel wool matrix 0.015).

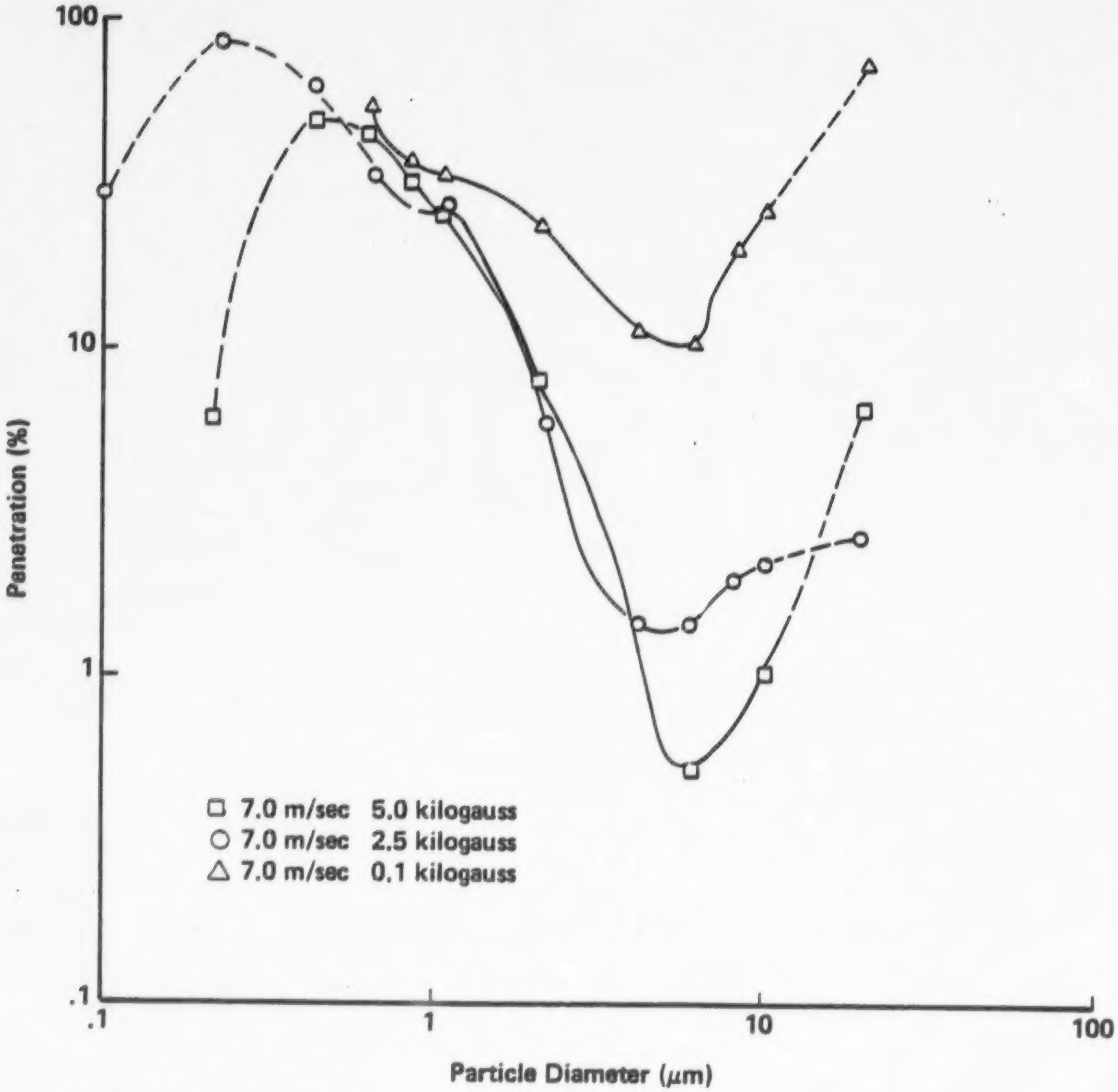

Figure 36. Georgetown Steel HGMF test—penetration vs. particle size (expanded metal matrix 0.035).

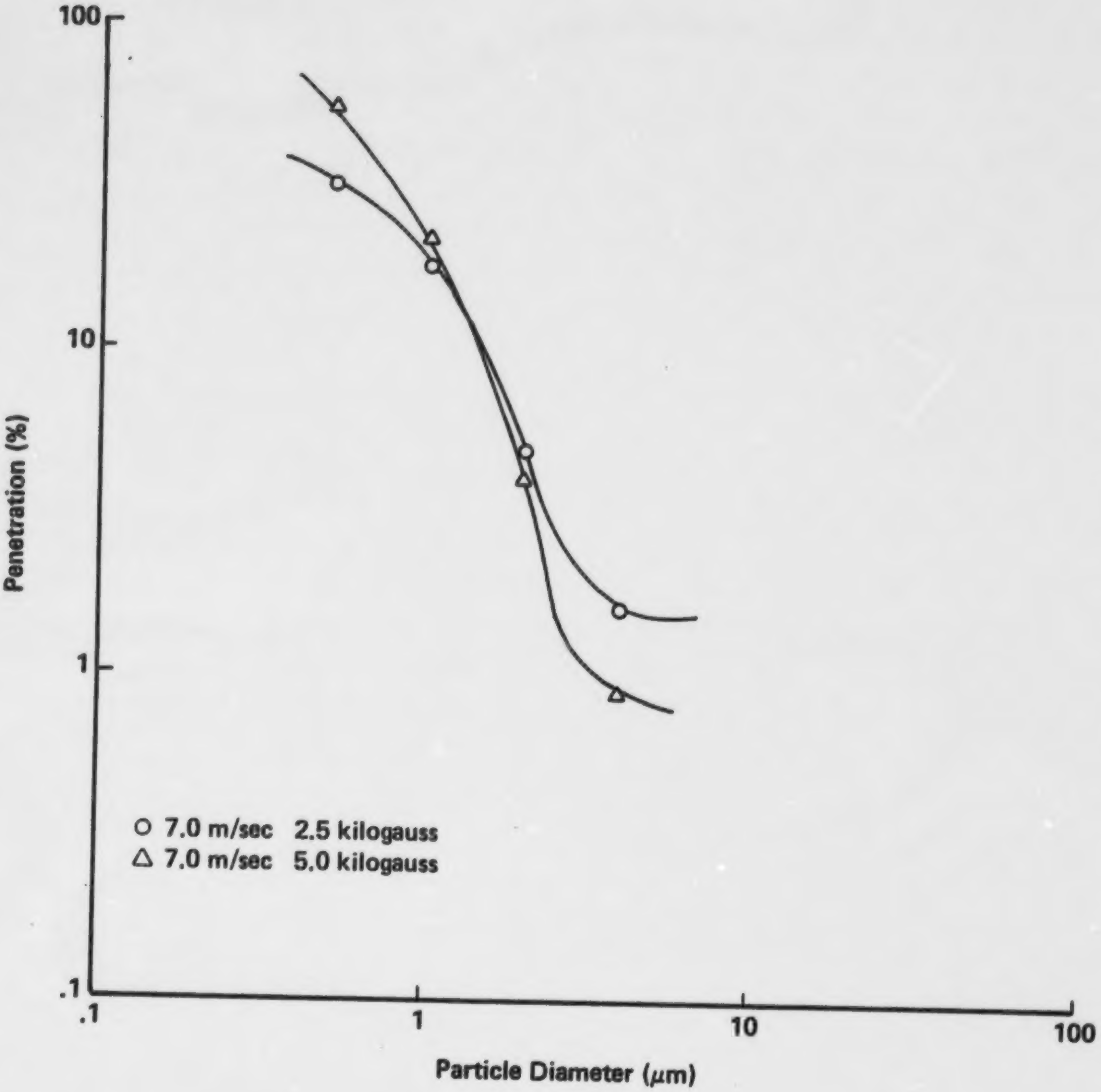

Figure 37. Georgetown Steel HGMF test—penetration vs. particle size (expanded metal matrix 0.06).

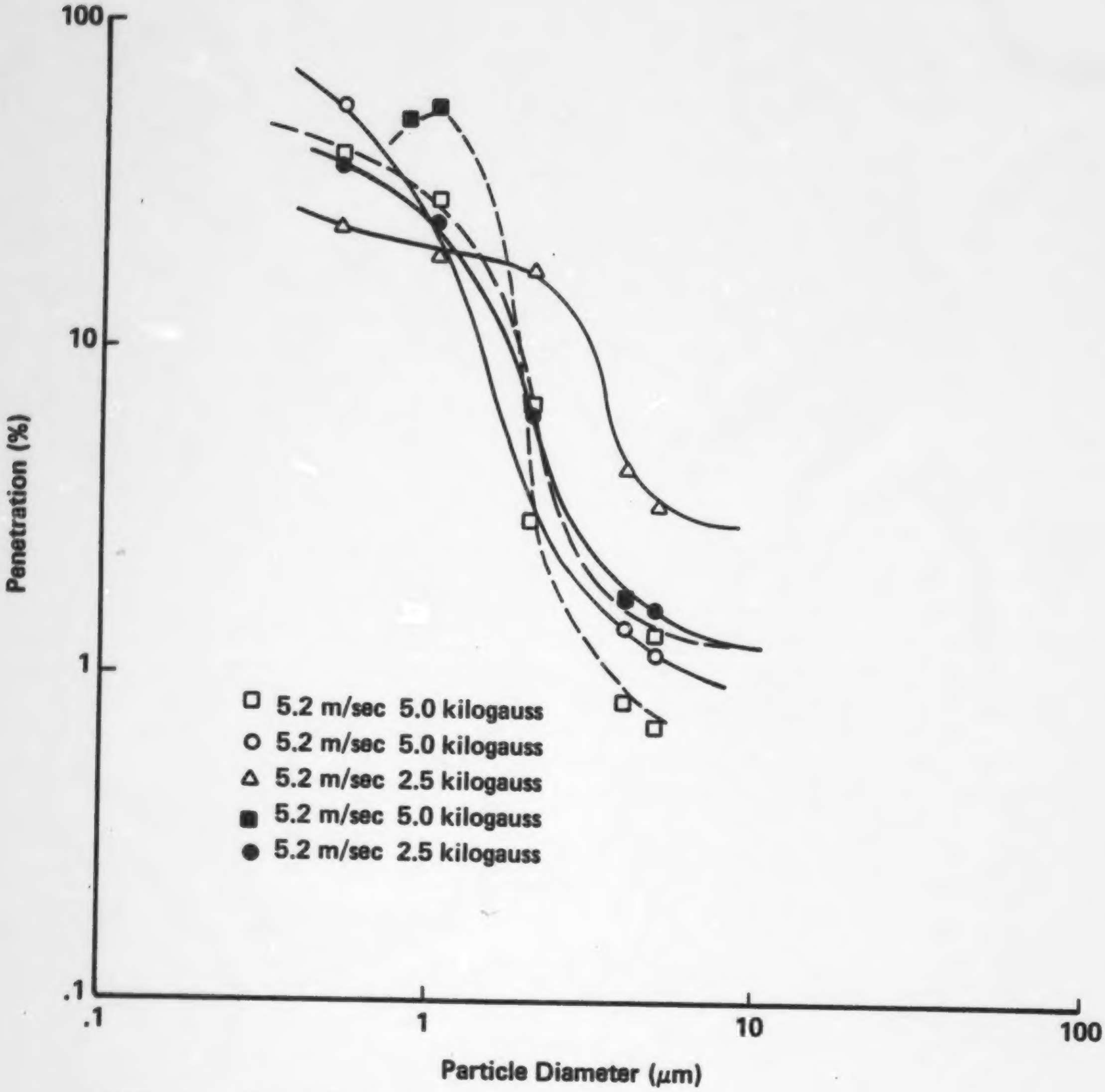

NOTE: Test with recycled gas stream disconnected.

Figure 38. Georgetown Steel HGMF test—penetration vs. particle size (expanded metal matrix 0.06).

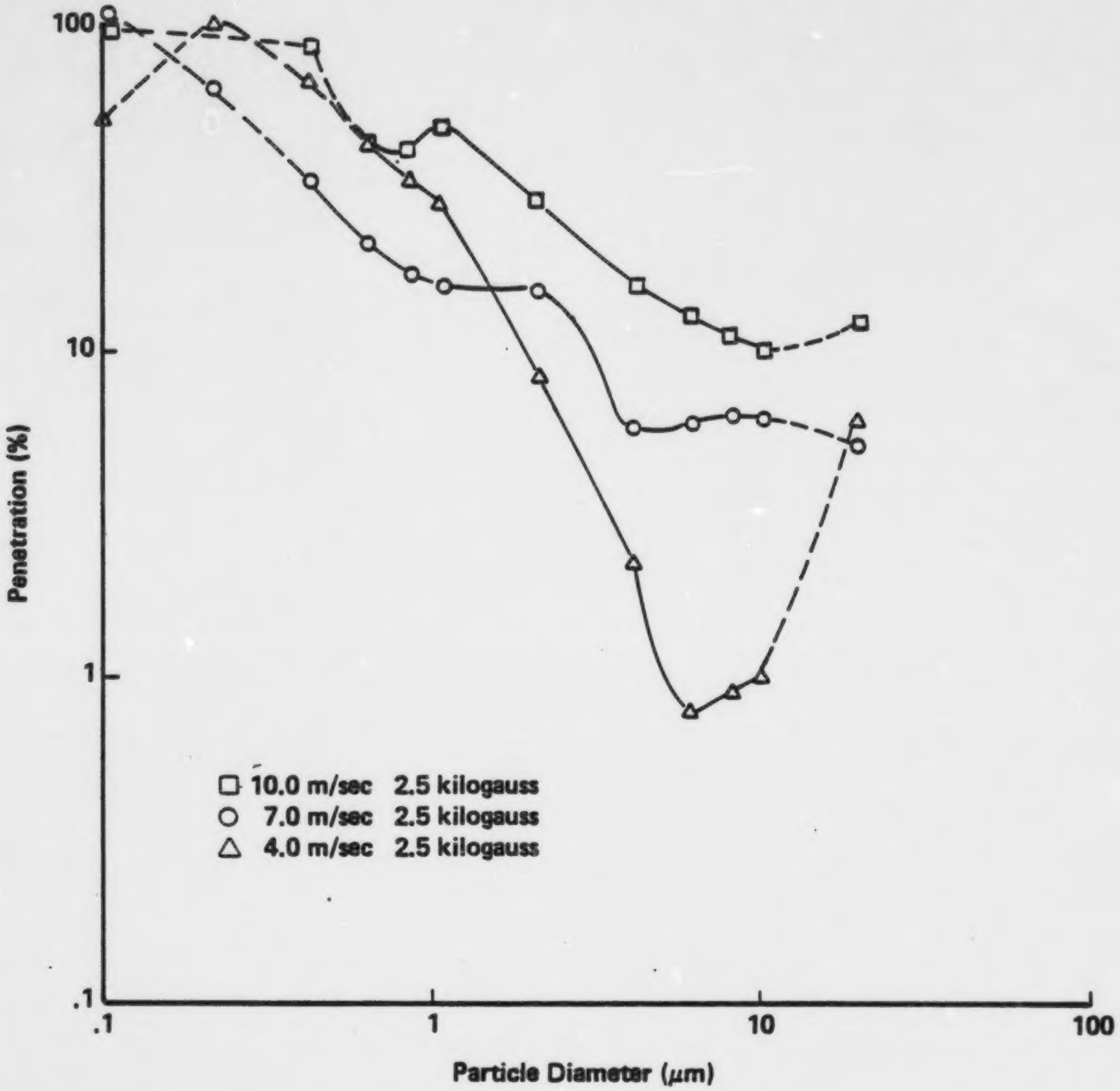

Figure 39. Georgetown Steel HGMF test—penetration vs. particle size (steel wool matrix 0.015).

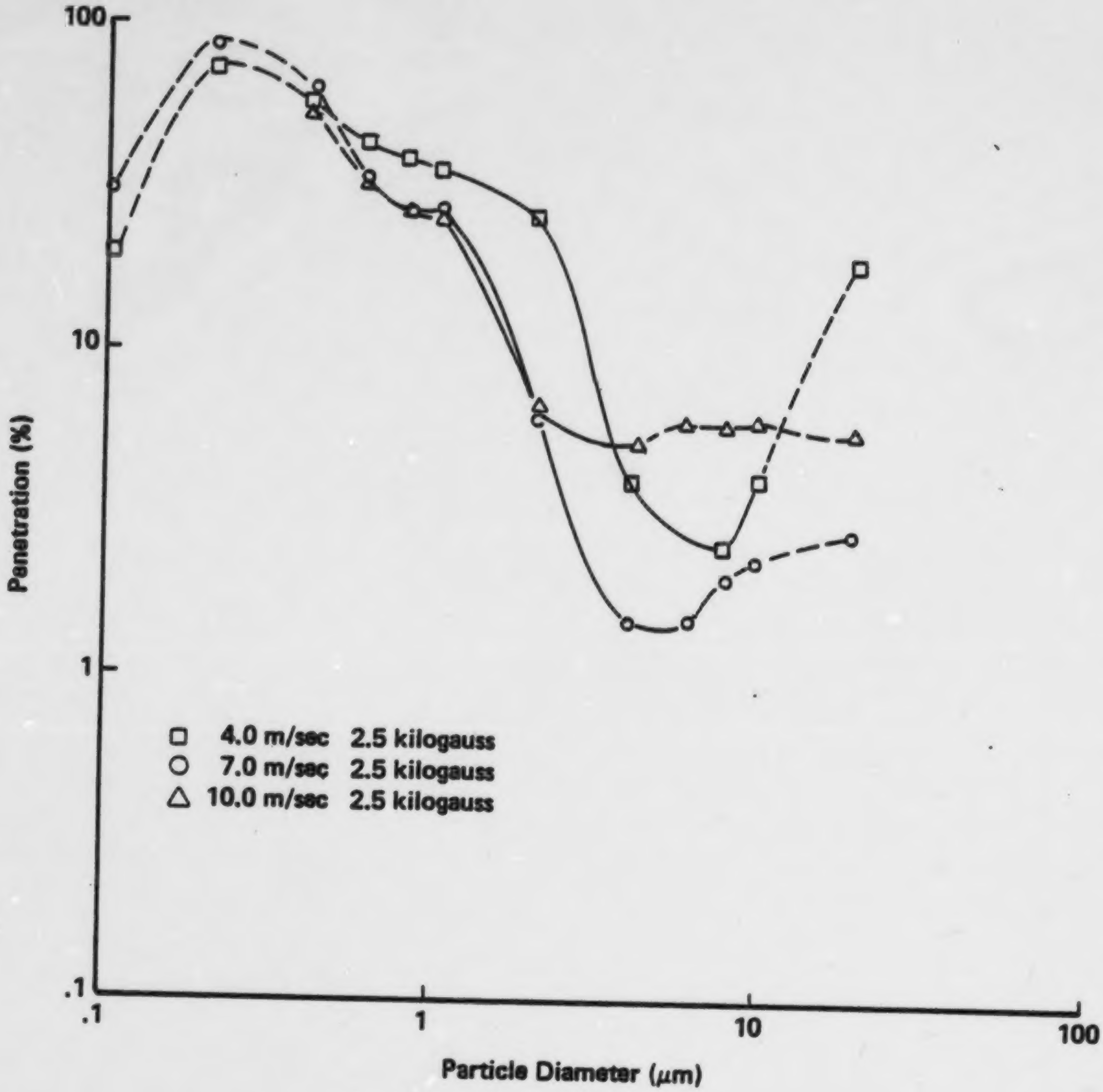

Figure 40. Georgetown Steel HGMF test—penetration vs. particle size (expanded metal matrix 0.035).

8.2 CHEMICAL AND MAGNETIC CHARACTERISTICS OF ELECTRIC ARC FURNACE DUST

Chemical and magnetic characteristics of the dust were determined for two classes of samples. One class of samples was obtained by extracting dust from the inlet and outlet ducts simultaneously over a period of 12 to 16 hours. Due to the large quantities of dust expected, alundum thimbles were used as the filtering media with sampling performed isokinetically to assure size representativeness in the sample. During the sampling period dust samples were also removed from the cyclone in the continuous matrix cleaning system.

The other class of samples used to determine chemical and magnetic characteristics were obtained from the cascade impactors. For several particle size test runs, the particulate captured on each impactor stage was recovered and subjected to analyses. The quantity of sample obtained from the impactors was minute in comparison with the thimble samples. Therefore, the kind of analyses that could be performed was limited.

8.2.1 Magnetic Analyses

Measurement of specific magnetization was used as one indicator of the range of particle characteristics encountered during the pilot plant tests. The specific magnetization tests were performed by Dr. Herbert Hacker at Duke University. The specific magnetization was obtained with a Faraday Balance which consists of a Cahn Model RG electronic balance and a Varian 4005 electromagnet. The balance is capable of measuring the susceptibility and magnetization of a wide range of materials as a function of temperature and magnetic field intensity. Basically, the instrument measures the force on a small magnetic sample when it is suspended in an inhomogeneous magnetic field supplied by an electromagnet. The force is expressed as

$$Fx = \sigma_g m \, dH/dx$$

where σ_g is the magnetization per unit mass, m is the mass of the sample, and dH/dx is the field gradient in the vertical direction. The pole faces of the electromagnet are machined so as to produce a constant value if dH/dx over the volume of space containing the sample. The force is measured with a Cahn Model RG electrobalance capable of determining forces in the 0.1 mg range.

In performing the measurements, the ferromagnetic effluent powders are first demagnetized by simultaneously reversing and reducing the magnetic field from 3.3 kilo-oersteds (kOe) down to zero field. Then the force is measured as a function of magnetic field as it is increased monotonically from zero up to 3.3 kOe. Using this technique, the data yields the virgin magnetization curve, i.e., data independent of remnant and hysteresis effects.

The calibration of the Faraday Balance depends on knowledge of the field gradient (dH/dx) in the region in which the sample hangs. Measurements of dH/dx have been carried out using a Rawson Rotating Coil Gaussmeter which yields accuracies of 1 to 2 percent. In addition, measurements on high purity samples of "standard" materials, whose magnetic properties are well known, were used to determine values of dH/dx. Through these techniques confidence is established that the magnetization is accurate to within 2 percent.

In calculating the magnetization, the mass of the sample must be accurately known. Typical values of sample mass are in the range of 0.2 to 0.5 mg for effluent dust of the type used in this study. To accurately determine these small masses, a separate Cahn Model RTL electrobalance with digital readout is used with special precautions taken to eliminate small, stray electrostatic forces of submilligram magnitude.

Table 16 lists the specific magnetizations of all thimble dust samples and the cyclone dust samples at 3.3 kOe applied field. The overall variation in specific magnetization was from 22.1 to 34.4 electromagnetic units/gram (emu/g) which corresponds well with the values of 23 and 32 emu/gram found in the preliminary test data.

Closer examination of the data in Table 16 reveals that the outlet dust samples apparently contain a relatively significant amount of magnetic material. For the low field case (0.1 kilogauss) the outlet dust specific magnetization is about 80 percent of the inlet dust value. For the 2.5 kilogauss field cases, the outlet dust specific magnetization is about 65 percent of the inlet values. In the high field case (5.0 kilogauss), the outlet value is about 50 percent of the inlet value.

To look at the magnetic properties as a function of particle size, one set of simultaneously collected inlet and outlet cascade impactor plate samples was analyzed. The impactor stages were labelled A through G in order of descending particle size. Figure 41 shows specific magnetization at the saturation field value of 3.3 kOe for each impactor stage. Unfortunately there was not sufficient recovered dust on stages A and B of the outlet impactor for this measurement to be made. The data tend to show that specific

TABLE 16. SPECIFIC MAGNETIZATION OF BULK DUST SAMPLES*

Operating conditions	Inlet	Outlet	Cyclone
Steel wool, packing density - 0.015			
2.5 kilogauss, 7 m/s	22.1	14.7	27.3
0.1 kilogauss, 7m/s	27.7	22.5	33.3
Expanded metal, packing density - 0.035			
2.5 kilogauss, 7 m/s	31.6	20.0	39.2
Expanded metal, packing density - 0.06			
5.0 kilogauss, 7 m/s	34.4	17.6	37.8
2.5 kilogauss, 7 m/s	26.8	17.7	38.0

*Electromagnetic units/gram at an applied field of 3.3 kOe.

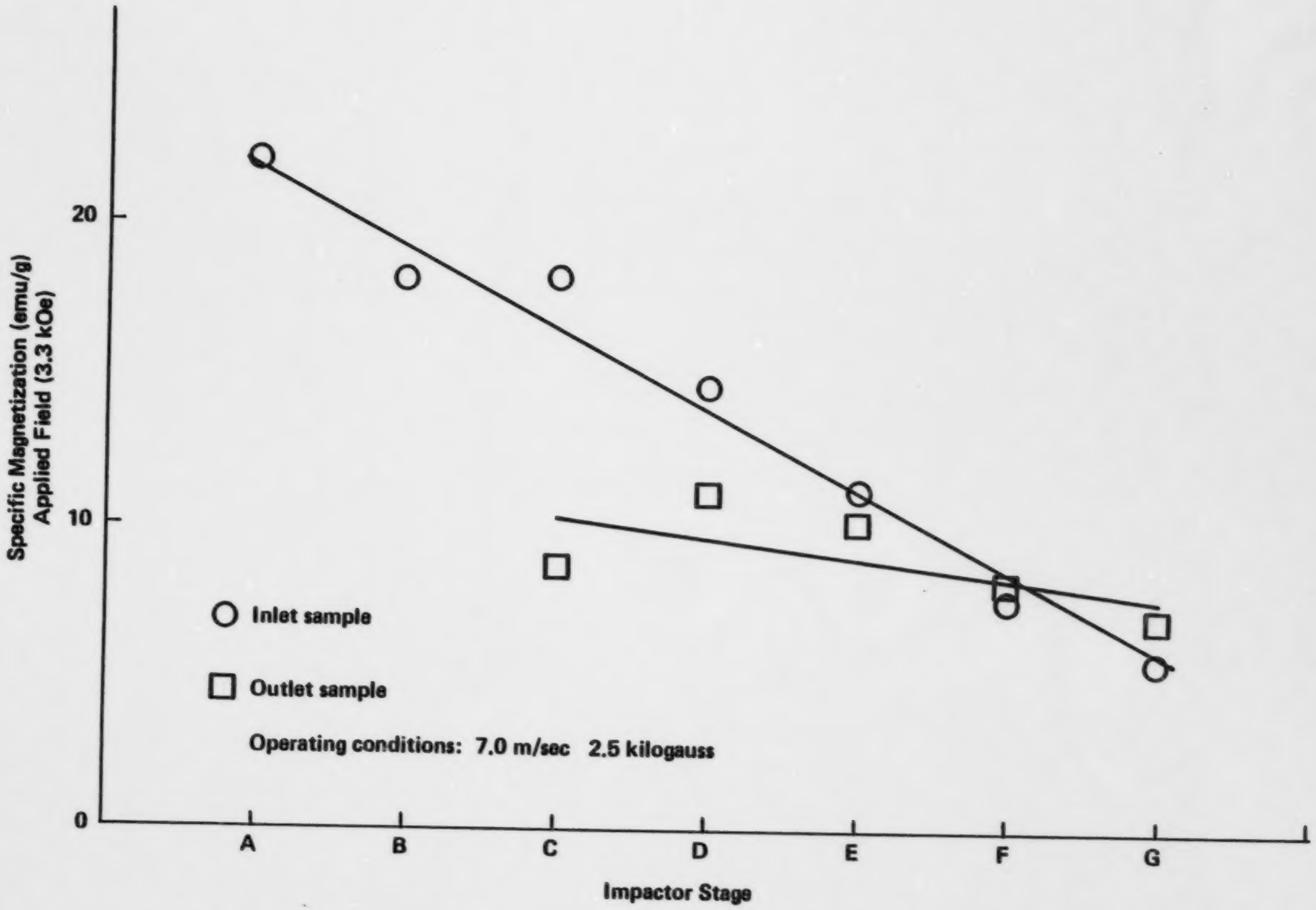

Figure 41. Georgetown Steel HGMF test—specific magnetization vs. particle size, steel wool matrix (packing density 0.015).

magnetization decreases with decreasing particle size, except that stage C seems to run counter to this trend on both inlet and outlet samples. The magnetization data also tend to support the fractional-penetration-by-particle-size data that show preferential removal of larger particle size material. For impactor stages C, D, and E the specific magnetization is lower for the outlet than for the inlet, suggesting the larger magnetic particles are being preferentially removed. Because the data are limited to one set of samples, however, the above is a suggestion rather than a conclusion.

8.2.2 Chemical Analyses

The bulk samples collected with alundum thimbles from the inlet and outlet ducts were analyzed by atomic absorption to determine the amount of certain metals present. For aluminum and silicon, samples and varying amounts of a known standard were digested as follows. Approximately 20-50 mg of sample or standard were mixed with 0.2 g of $LiBo_2$ and 0.05 g of KI in a platinum crucible. The crucible was heated over an air-methane flame until the mixture was a molten bead. Heating was continued for 5 minutes and the bead was then dissolved in 10 percent HNO_3 and diluted to 50 mL with 10 percent HNO_3. Measurements were then made by flame atomic absorption (N_2O - acetylene flame). For all other elements from 0.25 - 0.5 g of sample were digested with 3 mL of concentrated HNO_3 and then brought to dryness. The residue was taken up in 3 mL Aqua Regia (1 part HNO_3 - 3 parts HCl), diluted to 100 mL, and filtered. Any subsequent dilutions were performed with the same acid media. Standards were prepared with the same acid media and a blank was run as well. Measurements were made via flame atomic absorption (air - acetylene and N_2O - acetylene flame). The results of these analyses are listed in Table 17.

The inlet concentrations of iron varied between 29.2 percent and 35.7 percent. In every case the percentage of iron in the outlet sample was lower than the inlet sample, showing preferential removal of iron compounds.

With one exception, the no applied field case (0.1 kilogauss remnant field), the alkaline metals sodium and potassium increased in weight percent from inlet to outlet. Zinc content increased in weight percent from the inlet to outlet in four of the five cases with a small decrease occurring in the fifth case.

Table 18 lists the elemental penetrations calculated from the alundum thimble sample analyses. Variations in penetration can be seen with varied

TABLE 17. CHEMICAL ANALYSES OF BULK DUST SAMPLES - WEIGHT PERCENT

	Steel wool						Expanded metal						
	Packing density - 0.015						Packing density - 0.035			Packing density - 0.06			
	2.5 kG, 7 m/s			0.1 kG, 7 m/s			2.5 kG, 7 m/s			5 kG, 7 m/s		2.5 kG, 7 m/s	
Element	In	Out	Cyclone	In	Out	Cyclone	In	Out	Cyclone	In	Out	In	Out
Na	4.46	7.63	2.27	3.89	3.41	2.56	2.84	4.58	1.40	1.53	3.46	1.08	3.18
K	2.64	5.17	1.13	1.92	2.14	1.07	2.14	4.90	0.82	1.93	4.58	2.20	4.55
Ca	4.56	3.53	6.83	3.65	3.71	5.05	5.57	4.12	6.51	7.25	4.63	5.59	4.29
Mg	5.79	3.40	5.04	3.45	3.05	4.30	5.18	3.41	4.48	4.13	2.63	5.33	3.34
Fe	29.2	24.2	32.4	33.4	30.9	35.6	31.9	28.0	33.8	35.7	23.0	32.0	26.2
Zn	8.77	7.83	4.96	10.8	14.7	7.38	7.95	11.8	4.33	5.79	9.6	8.65	12.2
Al	0.40	0.31	0.38	0.32	0.38	0.55	0.39	2.50	0.63	0.70	2.22	0.46	1.09
Si	1.93	1.01	2.49	2.35	1.76	2.30	2.66	13.0	2.43	3.22	2.61	2.46	2.24
Pb	1.98	1.96	0.95	1.87	3.09	1.13	0.56	0.88	0.29	0.92	2.59	1.16	1.99
Cr	0.09	0.13	0.11	0.13	0.14	0.09	0.07	0.95	0.08	0.08	0.11	0.09	0.10
Mn	23.9	17.5	18.6	17.5	15.8	18.1	20.6	15.6	14.4	31.5	18.3	36.5	30.8

TABLE 18. ELEMENTAL PENETRATION PERCENT - BULK SAMPLES

Filter operating condition	Na	K	Ca	Mg	Fe	Zn	Al	Si	Pb	Cr	Mn	Overall penetration
7/30/81 Steel wool - 0.015 2.5 kG, 7 m/s	21.8	25.0	9.9	7.5	10.6	11.4	9.9	6.7	12.6	18.4	9.3	12.8
7/31/81 Steel wool - 0.015 0.1 kG, 7 m/s	28.9	36.8	33.6	29.2	30.6	44.9	39.2	24.7	54.6	35.6	29.8	33.0
9/02/81 Expanded metal 0.035 2.5 kG, 7 m/s	32.7	46.4	15.0	13.4	17.8	30.0	----	----	31.9	----	15.4	20.3
9/30/81 Expanded metal 0.06 5.0 kG, 7 m/s	21.3	22.4	6.0	6.0	6.1	15.6	26.5	7.6	26.3	13.0	5.5	9.4
10/01/81 Expanded metal 0.06 2.5 kG, 7 m/s	22.4	24.4	9.1	7.4	9.7	16.7	28.0	10.7	20.3	13.1	10.0	11.8

operating conditions, as well as differences in penetration among the elements. Sodium, potassium, aluminum, and lead penetrations are, in general, much higher than overall mass penetration. Calcium, magnesium, iron, silica, and manganese penetrations are, in general, lower than overall mass penetration. Zinc and chromium penetrations are moderately higher than overall mass penetrations. That removal efficiencies of the alkaline metals are relatively poor and not particularly sensitive to varying magnetic field strengths is not unexpected. The earlier HGMS pilot plant tests on a sintering plant waste gas stream showed these metals to be significant contributors to the poor magnet performance. Since calcium, magnesium, silicon, and manganese show similar penetration to iron, it is presumed these elements may be chemically associated with the iron in the dust particles. Calcium and magnesium enter the electric arc process as fluxing agents and are principal constituents of the slag layer that forms on top of the molten iron as the refining operation proceeds. Manganese is an essential alloying element for steel and is introduced to the process through the scrap charge, as well as through additions of ferromanganese to the melt.

The fact that incomplete elemental separations occur in the magnetic filtering process suggests complex particle chemistry. One might expect that zinc and lead, both diamagnets (weakly repelled), would significantly penetrate the filter, and lead, in particular, does. While zinc penetration is higher than the overall penetration, enough zinc is apparently associated with iron in the particles to moderate its penetration.

Supporting data for the association of iron and zinc is provided in a paper by Keyser et al.[33] presented at the 1981 EPA Iron and Steel Pollution Abatement Symposium. The paper reports work done at Lehigh University on characterizing electric arc furnace dust. It found zinc and iron to be associated in particles labelled mixed ferrite. Some of these particles were found in both magnetic and non-magnetic fractions. Since some of the iron occurs in ferrite particles that are non-magnetic, this may be one explanation why iron penetration did not approach zero in these pilot plant tests. Further this Lehigh study found a considerable variation among the thirty-three samples from different plants as to the amount of zinc and iron occurring as magnetic and non-magnetic ferrite. This fact suggests that HGMF applied to other electric arc furnace waste gas streams might vary considerably in its overall performance.

Two sets of simultaneous inlet and outlet impactor runs were made with kapton substrates. The kapton substrates were used to permit analysis of the collected sample spots on each stage by x-ray fluorescence. The intent of these analyses was to examine the distribution of elements, particularly iron, by particle size. Figures 42 and 43 show the size distribution of iron and zinc at the inlet and outlet for two filter operating conditions. For the 2.5 kilogauss test run about 12 percent by weight of the inlet iron and zinc were below 1 μm in particle diameter. For the 5 kilogauss test run about 14 percent of the inlet iron and 21 percent of the inlet zinc were in particles below 1 μm in diameter. The outlet curves for both elements under both operating conditions show a finer elemental particle size distribution than at the inlet. This indicates that larger particle sizes for both elements are preferentially removed by the filter.

Figures 44 and 45, the elemental penetration curves for iron and zinc, clearly show this preference. These data suggest that in spite of the higher magnetic susceptability of iron, there is still a significant filter inefficiency caused by fine iron bearing particles as opposed to more coarse iron bearing particles. The HGMF efficiency was only 80 to 85 percent for iron at the 1 μm particle diameter. The shape of the iron elemental penetration curve is similar to the elemental penetration curve for zinc, a diamagnetic element. The association of these two elements in electric arc furnace dust particles (in both magnetic and non-magnetic fractions) may prevent achievement of high magnetic filter efficiency.

8.3 MODEL DISCUSSIONS

The theoretical HGMF model developed by Gooding[25] was used to determine how well the model would fit the experimental collection data.

In the model the particles are assumed to be spherical, uniformly distributed in the fluid stream, and moving at the same velocity as the fluid system of the collector. The basic element of the filter is assumed to be a clean, cylindrical wire of radius s, oriented so that its axis is perpendicular to the fluid flow as shown in Figure 46. The collision radius of the wire Y_c, is defined by the initial position of the particle whose trajectory just touches the wire.

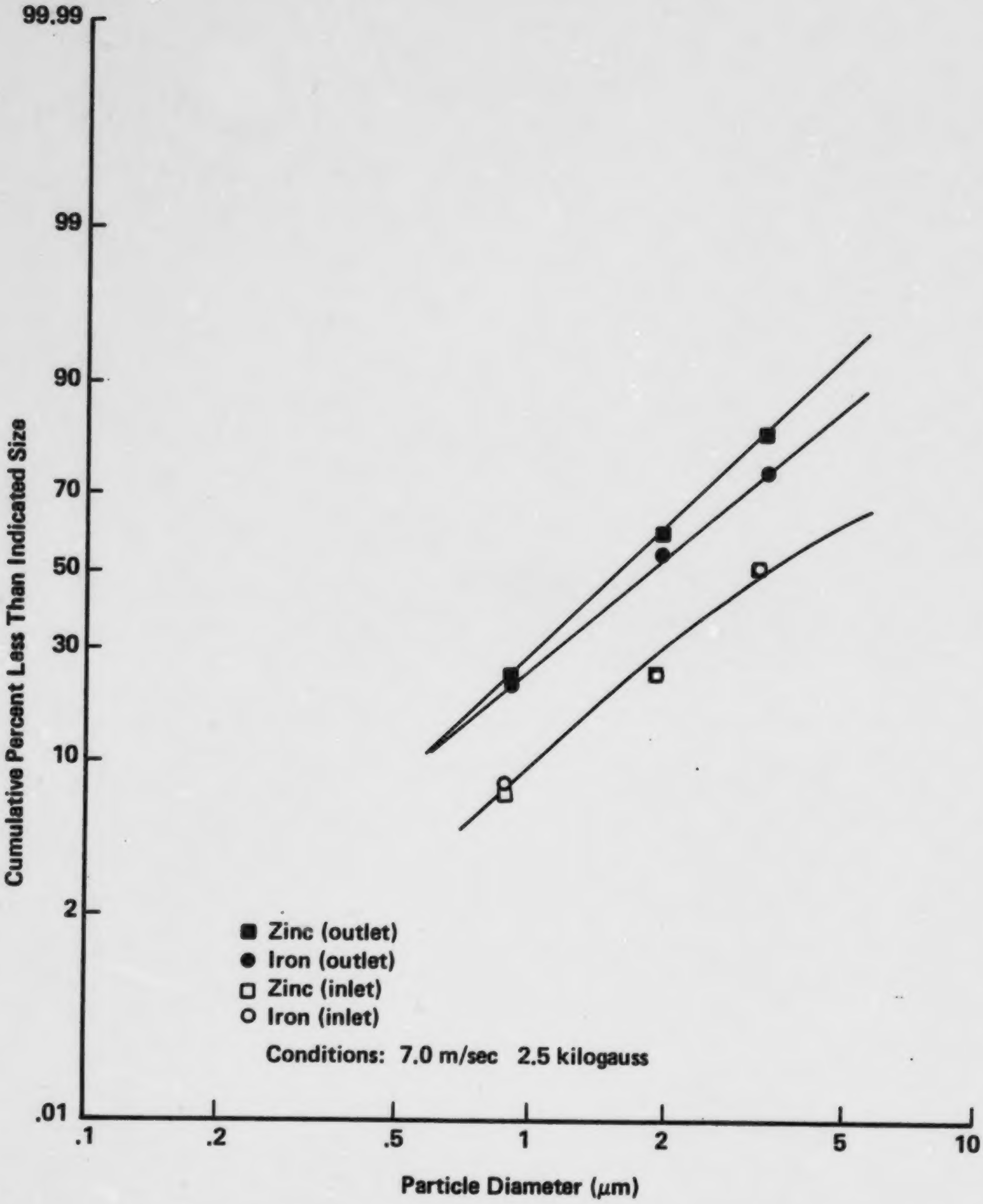

Figure 42. Georgetown Steel HGMF test—particle size elemental analysis, expanded metal matrix (packing density 0.06).

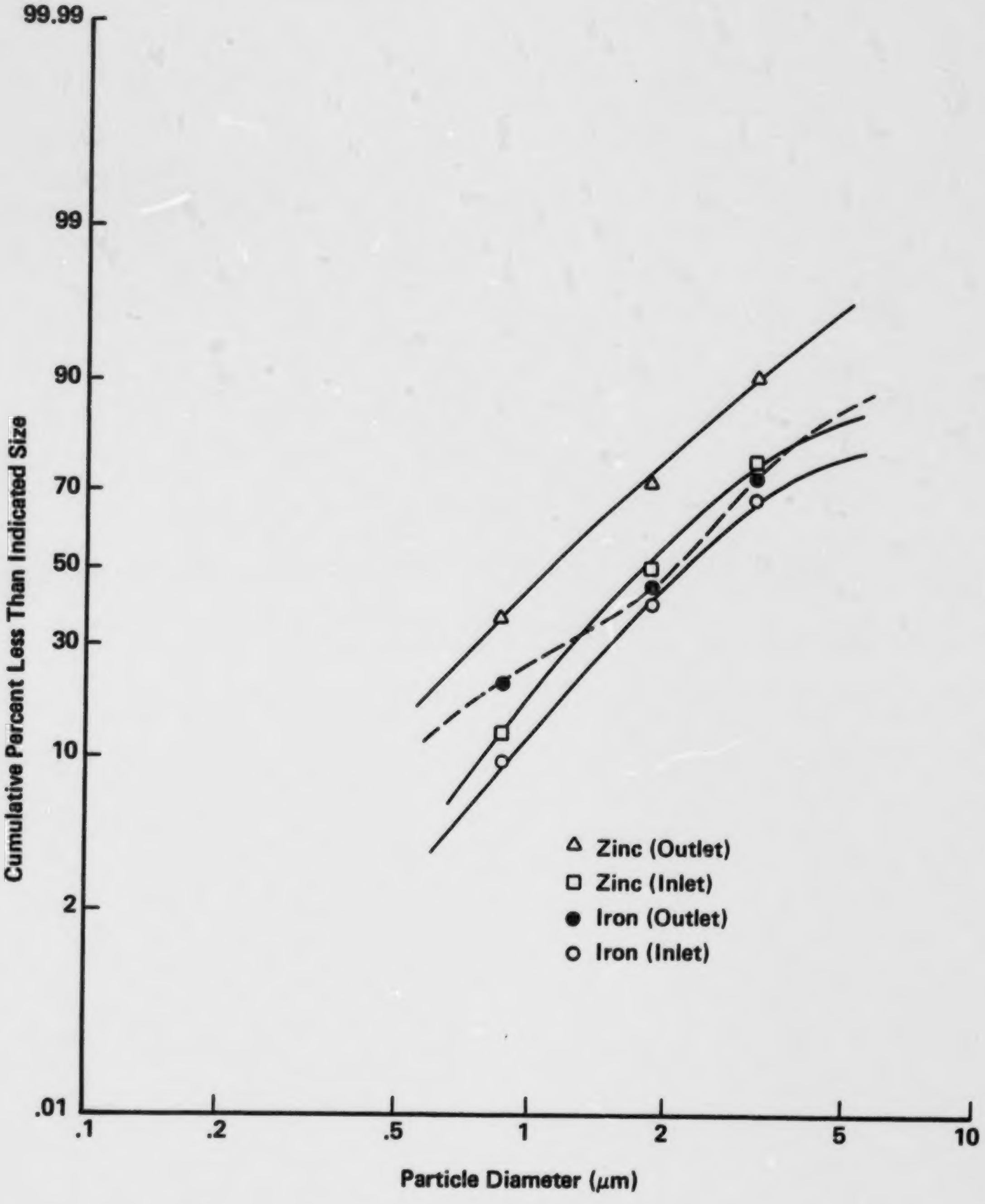

Figure 43. Georgetown Steel HGMF test—particle size elemental analysis, expanded metal matrix (packing density 0.06).

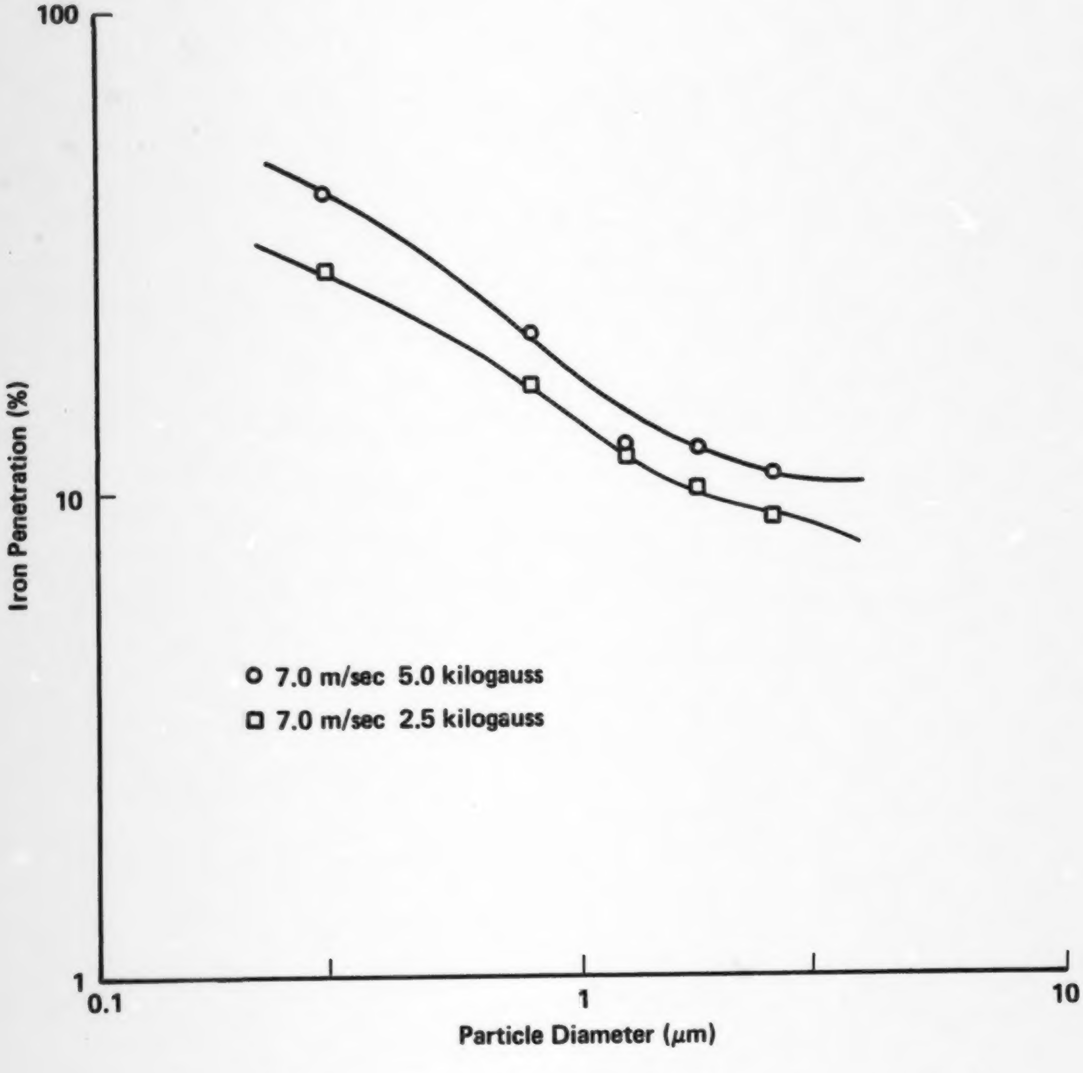

Figure 44. Georgetown Steel HGMF test—iron penetration vs. particle size (packing density 0.06).

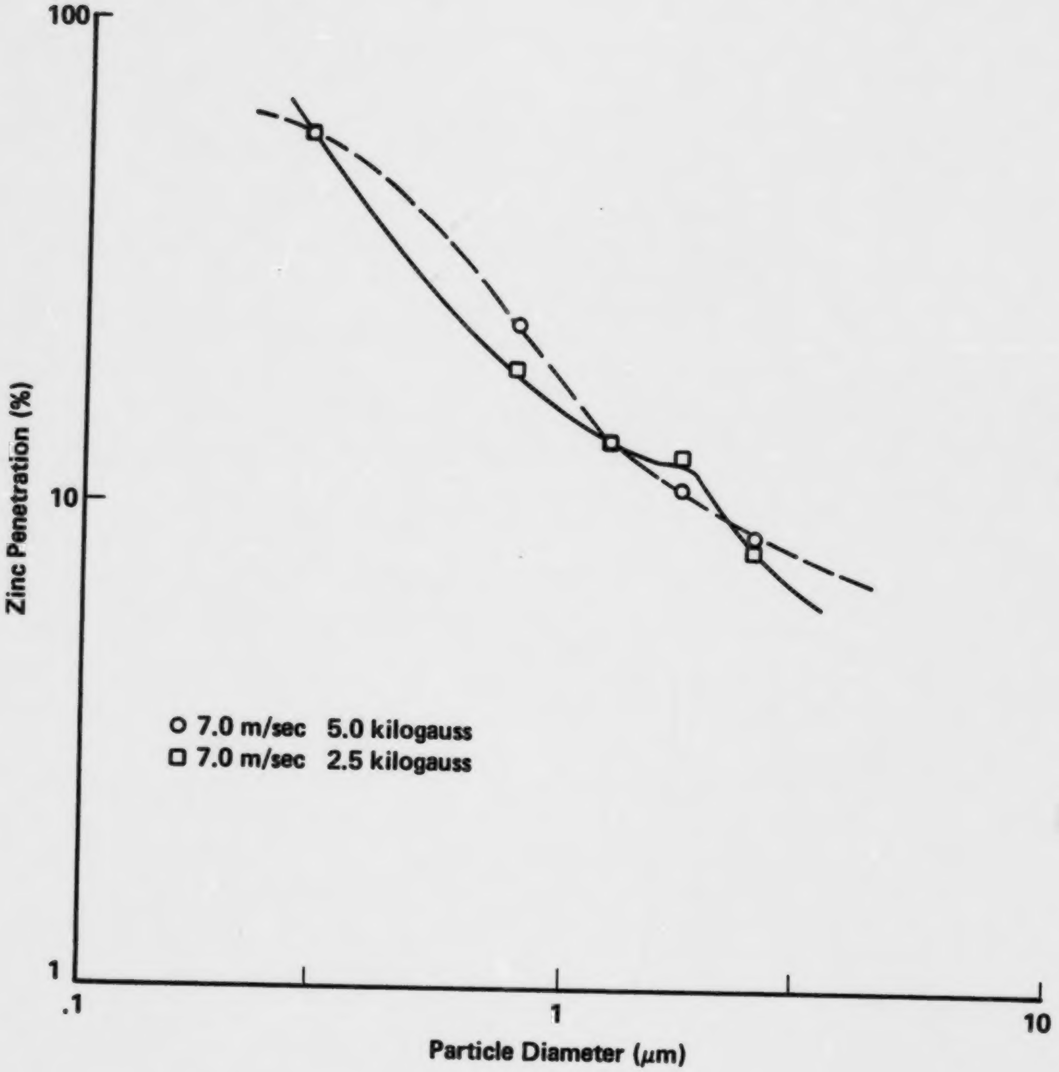

Figure 45. Georgetown Steel HGMF test—zinc penetration vs. particle size, expanded metal matrix (packing density 0.06).

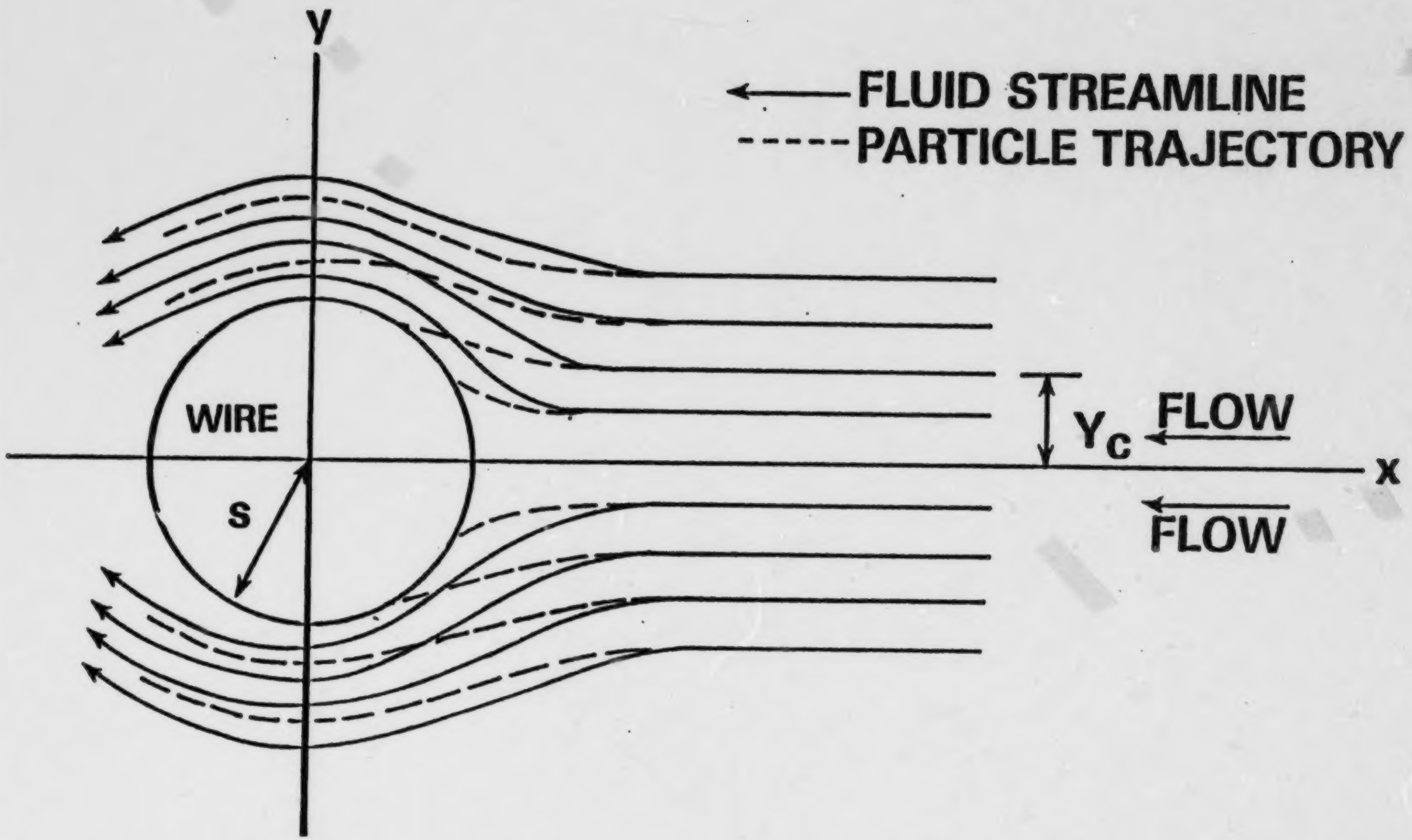
FLUID STREAMLINE
PARTICLE TRAJECTORY
y
x
WIRE
S
Y_c
FLOW
FLOW

Figure 46. Illustration of particle capture by a single wire.

The final predictive equation, as given earlier, is:

$$E = 1 - \exp\left[- \frac{4\,FL\,Y_c\,P}{\pi^2 S(1-F)^2}\right]$$

where P the reentrainment correction factor is defined as

$$P = a\,W^b K^c.$$

The reentrainment correction factor P is the probability of a particle adhering to the wire once it collides. A multiple regression analysis was conducted by Gooding on earlier data in order to correlate P with the previously defined dimensionless groups W and K. The results are given in Table 19.

The correlation values for the EAF dust calculated by Gooding did not work well when used with the Georgetown Steel test data so another regression analysis was conducted. Table 20 gives the results.

Figures 47 and 48 show the penetration versus particle size graphs for the actual data compared with the theoretical model. The agreement between the two runs and the model is fairly good until the particle diameter exceeds 1.0 μm at which point the agreement becomes very poor.

This could be due to the varying dust composition with particle size. There is no way in the model to account for varying dust composition and the resultant change in specific magnetization with particle size. More work will need to be done with the HGMF model and with dust analysis according to particle size before the model can be used confidently as a predictive tool.

8.4 DISCUSSION OF RESULTS

This pilot program was the first attempt at using a continuously cleaned magnetic filter unit on a gas stream as opposed to a liquid stream. While no long term continuous test was performed, the continuous cleaning system was capable of maintaining a stable pressure drop through the filter matrix at each of the velocity conditions over the period of performance characterization tests. In general these were one to two week periods with no actions taken to provide special extraordinary cleaning. Within the limitations of this experimental program the continuous cleaning system with compressed air satisfactorily maintained filter pressure drop.

TABLE 19. CORRELATION OF REENTRAINMENT CORRECTION

Data	Number of data points	Correlation	Correlation coefficient
BOF dust field-on	267	$P = 0.789 \frac{W^{0.087}}{K^{0.190}}$	0.727
BOF dust field-off	61	$P = 0.534\ K^{-0.317}$	0.669
EAF dust field-on	52	$P = 0.406 \frac{W^{0.013}}{K^{0.122}}$	0.634

TABLE 20. CORRELATION OF REENTRAINMENT CORRECTION FOR THE HGMF TESTS AT GEORGETOWN STEEL

Data	Number of data points	Correlation	Correlation coefficient
Steel wool & expanded metal	131	$p = 0.789 \frac{W^{0.048}}{K^{0.250}}$	0.516
Steel wool	53	$p = 0.280 \frac{W^{0.063}}{K^{0.136}}$	0.394
Expanded metal	77	$p = 0.449 \frac{W^{0.024}}{K^{0.307}}$	0.593

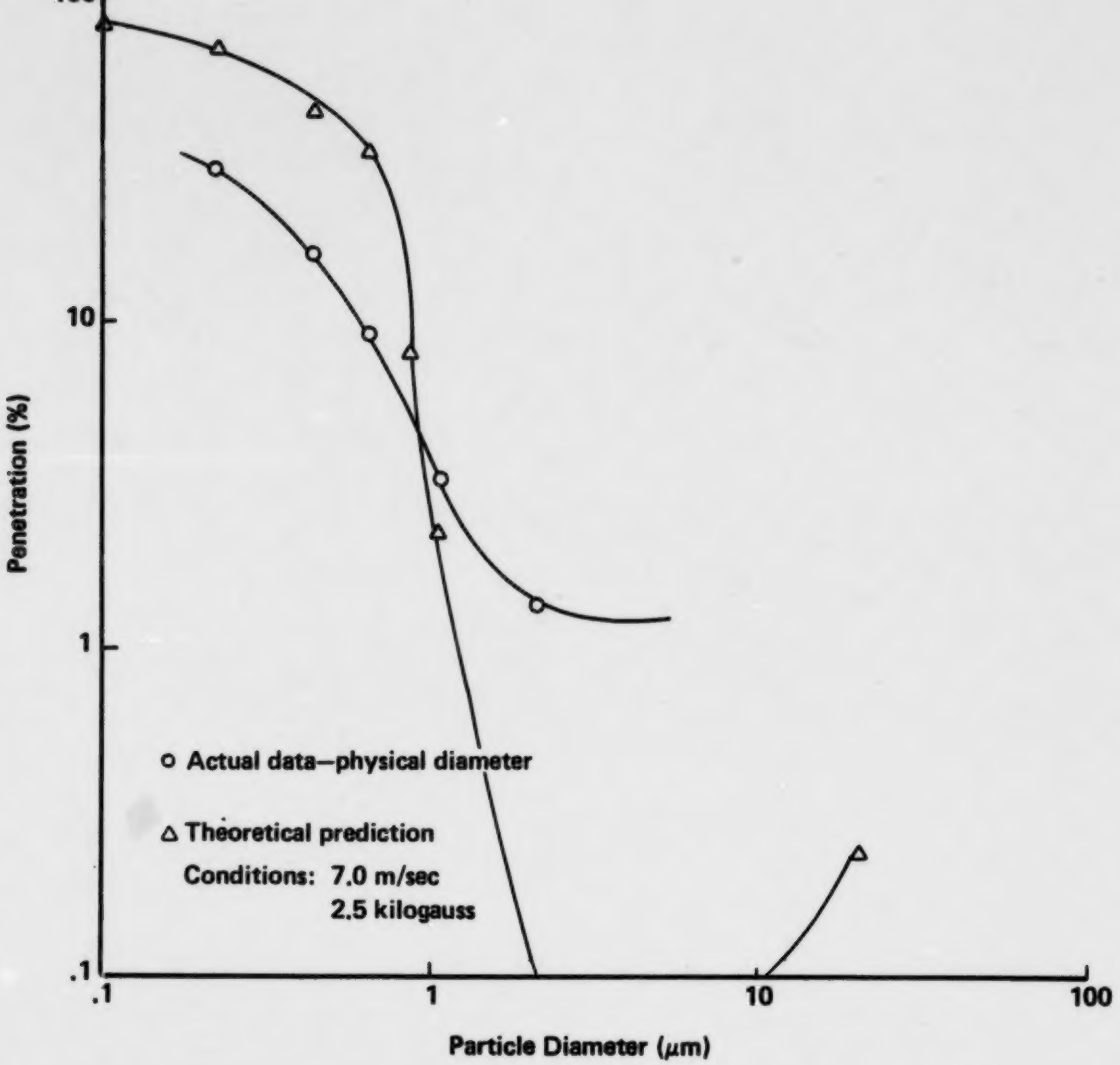

Figure 47. Georgetown Steel HGMF test—theoretical and actual penetration vs. particle size, expanded metal matrix (packing density 0.06).

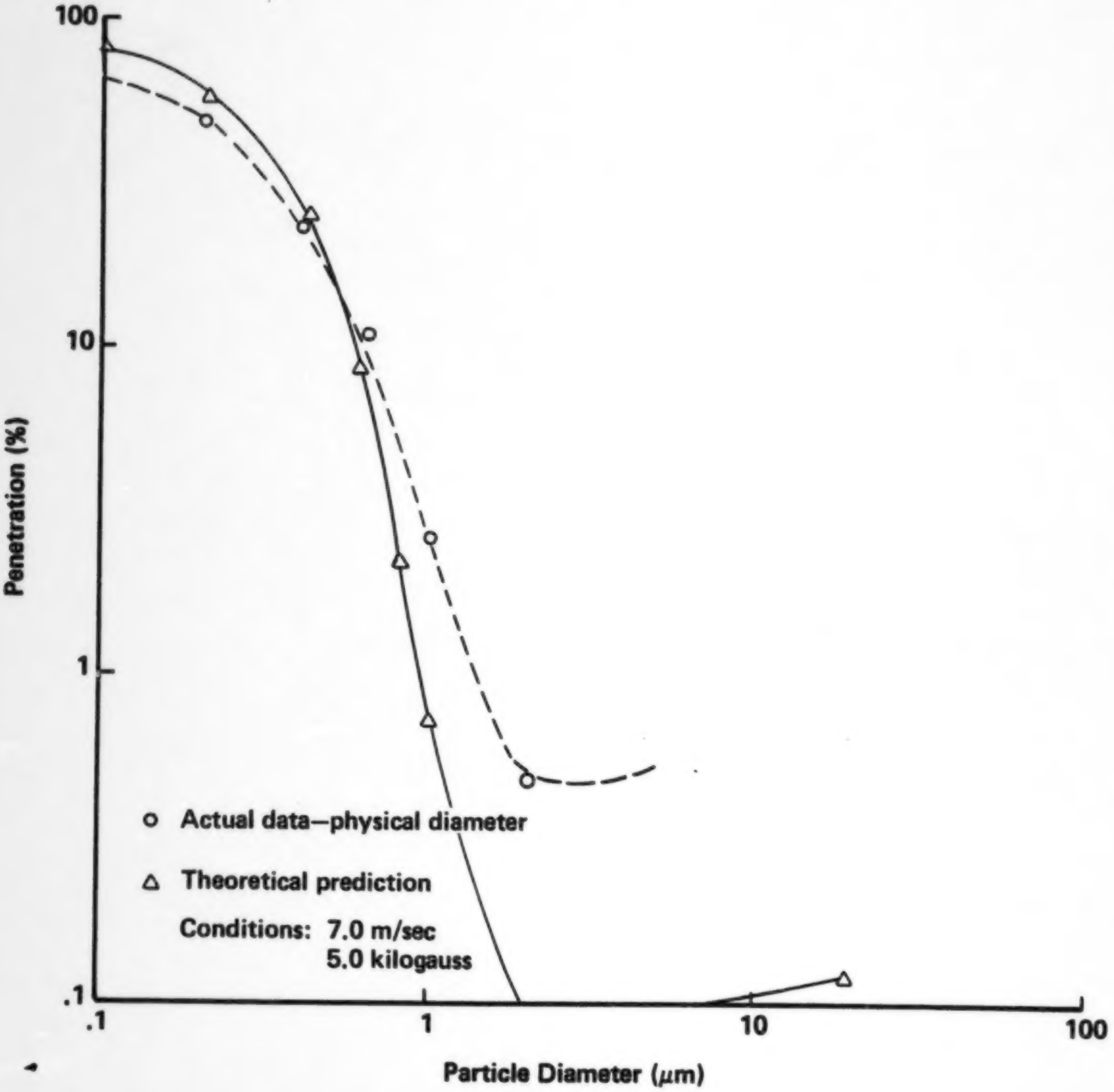

Figure 48. Georgetown Steel HGMF test—theoretical and actual penetration vs. particle size, expanded metal matrix (packing density 0.06).

The performance data discussed in Section 7.0 and statistical analyses discussed in Section 8.0 showed the best performance (efficiency) was achieved with an expanded metal matrix at 6 percent packing density. This best performance was achieved at a pressure drop lower than the second best performing matrix, steel wool. This test program was the first in the HGMF development program attempting to use an expanded metal matrix instead of steel wool. Given the better performance at lower pressure drop observed in the initial experiments, expanded metal matrices deserve further study.

For the given conditions of applied field, velocity (residence time), and inlet concentrations, the best overall efficiencies achieved were in the range of 94 to 96 percent with outlet concentrations in the range of 20 to 70 mg/m^3. The efficiency levels are much improved over those achieved in the previous pilot plant work on sinter plant emissions. The performance levels, however, are not competitive with conventional high efficiency control devices applied to electric arc furnaces. The New Source Performance Standard for electric arc furnaces limits particulate emissions to 12 mg/dsm^3. The HGMF outlet concentration in these tests were 2 to 6 times the required level. State standards for existing sources vary considerably e.g., Pennsylvania equivalent to 18 mg/dsm^3, Michigan equivalent to 130 mg/dsm^3. On a performance basis HGMF might have some limited retrofit potential.

Given that this pilot plant design was not an optimum design specifically for electric arc furnaces, one may question whether with design changes much better performance can be expected, i.e., can pentration be reduced by a factor of 2 or 6. One way to attempt an answer to this question is to examine the empirical data correlation (regression equation) for the 6 percent expanded metal case. The equation shows that outlet mass varied approximately as the 1.4 power of filter velocity. By halving the velocity (5 m/s to 2.5 m/s) one might expect to reduce penetration by a factor of 2.6. Increasing field strength above 5 kilogauss would not be nearly as effective in that outlet mass varies inversely as the 0.23 power of field strength. Reduction in filtering velocity is clearly the stronger effect, but halving the velocity requires doubling the filter area to treat a given volume of gas. This means the cost of the equipment will be significantly increased.

The theoretical model developed by Gooding suggests another way of improving performance. Instead of increasing residence time by reducing velocity, residence time may be increased by increasing the filter length in the direction of gas flow. This means of varying residence time could not be explored in the pilot plant. The theoretical model discussed in Section 8.3 suggests filter penetration is exponentially related to filter length. If the filter length were doubled, from 0.15 m to 0.30 m, penetration would be reduced by a factor of 1.6. Quadrupling the filter length would provide the needed reduction in penetration (a factor of 4) for the device to become competitive. However in addition to increasing the equipment costs there would be a severe energy penalty. Presumably the pressure drop across the magnetic filter would also quadruple.

The fractional penetration data shows the HGMF was not as effective on particles below 1 μm in diameter as on those above 1 μm. This behavior and the curve shapes shown in Section 8.2 are characteristic of conventional control devices. The leveling off and increase in penetration for particle sizes over 5 μm, apparently due to reentrainment, are often present in precipitator particle size versus penetration curves. In terms of fractional particle size penetration, it is not evident that any significant qualitative differences exist between HGMF and conventional control devices.

The magnetic analyses data reveal that the HGMF did not remove all of the magnetic material. The magnetic material penetrating the collector may do so because of insufficient residence time or due to reentrainment. The chemical analyses data reveal a significant amount of iron penetrated the filter, especially in the small particle size (below 1 μm) fraction. Penetration of the iron may be due to insufficient residence time and reentrainment. However, the recent report[33] indicating some iron in electric arc furnace dust to be present in a "non-magnetic" form (probably meaning not ferromagnetic) suggests a third mechanism for penetration. The HGMF's sensitivity to chemical composition of particles and their resulting magnetic susceptability is analagous to the effects of chemical composition on particle resistivity and electrostatic precipitator performance.

An alternative use for HGMF not explored in this study is to separate non-magnetic components of waste EAF dust from magnetic components, i.e. ferrous and non-ferrous. At present, EAF dust is classified as hazardous waste as a result of heavy metals contamination. Separation of the ferrous portion with minor contamination by zinc might permit its recycle to steelmaking, reducing the residue for disposal. With sufficient concentration of zinc, the non-ferrous portion might be sold to zinc refiners. The association of iron and zinc in non-magnetic particles identified in the study discussed above[33] suggests that this potential application of HGMF needs further study to determine the degree of separation achievable.

9.0 ECONOMICS

Approximate costs have been developed for four different options for particulate emission control of electric arc furnace (EAF) dust. The accuracy of these costs corresponds roughly to that of a study grade estimate (±30%) and are shown in Table 21. Although a best estimate is presented for both capital and annual expenses, it should be kept in mind that the absolute costs of the four options may depend on special process details, plant location, and material of construction. Consideration of these details was not within the scope of the estimate. However, the estimates were made for the following common base case:

Volumetric flow rate:	8,500 m^3/min @ 66° C
Inlet dust loading:	1,050 mg/sm^3
Outlet dust concentration:	12 mg/sm^3
Annual operation:	8,500 hr/yr

For purposes of the economic comparisons, it was assumed that HGMF performance could attain the outlet concentration needed to comply with the EAF NSPS, or 12 mg/dsm^3.

In addition, the following system parameters specific to each option were specified based on engineering judgment:

HGMF

	Superficial face velocity		
Flow velocity	7 m/s	5 m/s	2 m/s
ΔP_{HGMF}-cm H_2O	33.0	17.8	2.5
Total fan static ΔP, design	63.5	50.8	38.1
operating	50.8	38.1	25.4

TABLE 21. COSTS OF VARIOUS CONTROL OPTIONS FOR EAF PARTICULATE EMISSION $\$/m^3/s$

	Total capital costs	Total annualized costs 10 yr[1]	Total annualized costs 20 yr[1]	Direct operating costs[2]
HGMF[3]				
2 m/s	31.31	7.06	5.64	0.71
5 m/s	20.99	5.21	4.26	0.95
7 m/s	14.16	4.07	3.43	1.20
ESP	11.94[4]	3.43	2.89	1.01
FF	11.11	3.64	3.14	1.09
VS	17.58	8.11	7.31	4.55

[1] Total annual costs are computed for both 10 and 20 year capital recovery periods. The capital recovery factor for 10 years is .16275 and for 20 years is .11746.

[2] Direct operating costs include operation and maintenance labor, supervisory overhead, and utility costs. It does not include capital recovery charges or taxes, insurance, and administrative charges (taxes, insurance, and administration are computed at 4 percent of the total capital costs.)

[3] Values given for three separate face velocities.

[4] Capital costs for the ESP were calculated in four ways.

(a)	Ratio from reference (34) below using empirical factors	Cost = $\$11.50/am^3/s$
(b)	Itemized major equipment and cost factors	Cost = $10.47/am^3/s$
(c)	Escalate from reference (35)	Cost = $13.11/am^3/s$
(d)	Ratio from reference (34) using ".6 rule"	Cost = $13.13/am^3/s$

ESP

Migration velocity	4.6 cm/s
Specific collection area	100 $m^2/m^3/s$
ΔP_{ESP}	2.5 cm H_2O
Total fan static ΔP, design	5.9 cm H_2O
operating	3.9 cm H_2O

FABRIC FILTER

Air/cloth	1.0 cm/s
ΔP_{FF}	20.3 cm H_2O
Total fan static ΔP, design	50.8 cm H_2O
operating	38.1 cm H_2O

VENTURI SCRUBBER

L/G	93 ℓ/1,000 m^3
ΔP_{VS}	152 cm H_2O
Total fan static ΔP, design	203 cm H_2O
operating	191 cm H_2O
Water recycle ratio	0.9

The scope of the cost estimates includes flange to flange costs from the confluence of the particulate collection hoods (e.g., shell and canopy,) to the discharge of the clean air from the control device. For the venturi scrubber costs of sludge treatment equipment is also included. It is assumed that utilities are available at the plant site at the following rates:

Electricity	\$.05/kWh
Plant water	\$.066/1,000 ℓ
Cooling water	\$.026/1,000 ℓ
Compressed air	\$.706/1,000 m^3

9.1 CAPITAL COSTS

The total capital costs (TCC) were calculated using a modified Lang method, i.e., applying factors to the purchased equipment costs to account for direct and indirect installation costs.

A substantial amount of engineering judgment is used in formulating these factors. However, the relative order of these factors for the ESP, VS, and FF is consistent with other data.[36] These factors reflect the expense necessary to install and put into operation each control option. The ratio between installation costs and purchased equipment costs for HGMF was judged to be lower than for either the ESP or FF.

Table 21 shows that HGMF is more capital intensive than either the ESP or FF. Looking at the annualized costs, the venturi scrubber is not competitive with any of the other three options at the given conditions. Direct operating costs, which do not include the cost of capital over the life of the unit, are slightly higher for the HGMF at 7 m/s than for either the ESP or FF. However, the difference in both capital and direct operating costs among the HGMF, ESP, and FF is well within the probable error of the estimate (±30%). In addition, changes in labor and utility rates could alter the relative order of the direct operating costs. For example, if labor and maintenance material costs increased by 30 percent or if electricity were available at $.04 instead of $.05/kWh, the direct operating costs shown in Table 22 would result.

Thus, although the capital required for HGMF is relatively high, HGMF is cost competitive in direct operating costs both within the error associated with the estimate as well as under two possible scenarios which could be applicable to specific sites selected for HGMF. It is important to note that tax considerations are not part of this estimate. Investment tax credits and other tax incentives could offset some of the initially higher HGMF capital costs by reducing the total annualized costs of Table 21.

TABLE 22. DIRECT OPERATING COSTS

	I* $/am³/s	II** $/am³/s
HGMF 2 m/s	0.61	0.78
5 m/s	0.81	1.02
7 m/s	1.01	1.26
ESP	0.86	1.10
FF	0.94	1.19

* The result of changing electrical costs from $.05 to $.04 kWh.

**The result of a 30 percent increase in labor and maintenance material costs, electricity still at $.05/kWh.

10.0 REFERENCES

1. Obertueffer, J. A., "Magnetic Separation: A Review of Principles, Devices, and Applications," IEEE Trans. Magn., Mag-10, 223 (1974).

2. Kolm, H. H., J. A. Oberteuffer, and D. R. Kelland, "High Gradient Magnetic Separation," Sci. Am., 223, 47 (Nov. 1975).

3. Oder, R. R., "High Gradient Magnetic Separation Theory and Applications," IEEE Trans. Magn., Mag-12, 428 (1976).

4. Iannicelli, J., "New Developments in Magnetic Separation," IEEE Trans. Magn., Mag-12, 436 (1976).

5. Gooding, C. H., T. W. Sigmon, and L. K. Monteith, Application of High-Gradient Magnetic Separation to Fine Particle Control, PB 276-633/AS, National Technical Information Service, Springfield, VA (1977).

6. Kelland, D.R., "High Gradient Magnetic Separation Applied to Mineral Beneficiation, "IEEE Trans. Magn., Mag-9, 307(1973).

7. Murray, H.H., "Beneficiation of Selected Industrial Minerals and Coal by High Intensity Magnetic Separation," IEEE Trans. Magn., Mag-12, 498 (1976).

8. Kelland, D.R., and E. Maxwell, "Oxidized Taconite Beneficiation by Continuous High Gradient Magnetic Separation," IEEE Trans. Magn., Mag-11, 1582 (1975).

9. Ergun, S., and E.H. Bean, "Magnetic Separation of Pyrite from Coals," Report of Investigation No. 2718, U.S. Bureau of Mines, Pittsburgh, PA (1968).

10. Trindale, S.C., and H.H. Kolm, "Magnetic Desulfurization of Coal," IEEE Trans. Magn., Mag-9, 310 (1973).

11. Vives, D.L., L.J. Hirth, and W.H. Summerlin, "Direct Reduction and Magnetic Beneficiation of Alabama Brown Ore with Lignite," IEEE Trans. Magn., Mag-12, 490 (1976).

12. Maxwell, E., D.R. Kelland, and I.Y. Akoto, "High Gradient Magnetic Separation of Mineral Particulates from Solvent Refined Coal," IEEE Trns. Magn., Mag-12, 507 (1976).

13. Maxwell, E., I.S. Jacobs, and L.M. Levinson, Magnetic Separation of Mineral Matter from Coal Liquids, EPRI AF-508, Electric Power Research Institute, Palo Alto, CA (1977).

14. Liu, Y.A., G.E. Crow, C.J. Lin, and D.L. Vives, "A Pilot-Scale Study of High Gradient Magnetic Desulfurization of Solvent Refined Coal (SRC)," *IEEE Trans. Magn.*, *Mag-14*, (1978).

15. Maxwell, E., and D.R. Kelland, "High Gradient Magnetic Separation in Coal Desulfurization," *IEEE Trans. Magn.*, *Mag-14*, 482 (1978).

16. Hise, E.C., et. al. Separation of Dry Crushed Coal by High-Gradient Magnetic Separation. ORNL-5571, Oak Ridge National Laboratory, Oak Ridge, Tennessee, October 1979.

17. Mitchell, R., G. Bitton, and J.A. Oberteuffer, "High Gradient Magnetic Filtration of Magnetic and Non-Magnetic Contaminants from Water," *Separation and Purification Methods*, *4*, 267 (1975).

18. Petrakis, L., and P.F. Ahner, "High Gradient Magnetic Separations in Water Effluents," *IEEE Trans. Magn.*, *Mag-14*, 491 (1978).

19. Oberteuffer, J.A., I. Wechsler, P.G. Marston, and M.J. McNallan, "High Gradient Magnetic Filtration of Steel Mill Process and Waste Waters," *IEEE Trans. Magn.*, Mag-12, 428 (1976).

20. Harland, J.R., L. Nilsson, and M. Wallin, "Pilot-Scale High Gradient Magnetic Filtration of Steel Mill Wastewater," *IEEE Trans. Magn.*, *Mag-12*, 904 (1976).

21. DeLatour, C., and H.H. Kolm, "Magnetic Separation in Water Pollution Control-II," *IEEE Trans. Magn.*, *Mag-11*, 1570 (1975).

22. Yadidia, R., A. Abeliovich, and G. Belfort, "Algae Removal by High Gradient Magnetic Filtration," *Envr. Sci. and Tech.*, *11*, 913 (1977).

23. Melville, D., F. Paul, and S. Roath, "High Gradient Magnetic Separation of Red Cells from Whole Blood," *IEEE Trans. Magn.*, *Mag-11*, 1701 (1975).

24. Whitesides, G.M., C.L. Hill, and J. Brunie, "Magnetic Filtration of Small Heterogenous Catalyst Particles. Preparation of Ferrimagnetic Catalyst Supports," *Ind. Eng. Chem., Process Des. Dev.*, *15*, 226 (1976).

25. Gooding, C.H., *Pilot-Scale Field Tests of High-Gradient Magnetic Filtration*, EPA 600/7-80-037, U.S. Environmental Protection Agency, Research Triangle Park, NC (1980).

26. Friedlaender, F.J., et al. "Diamagnetic Particle Capture and Mineral Separation," *IEEE Trans. Magn.*, Mag-17, 2813 (1981).

27. Hardison, L.C., and C.A. Greathouse, *Air Pollution Control Technology and Costs in Nine Selected Area*, PB 222-746, National Technical Information Service, Springfield, VA (1972).

28. DeLatour, C., and H.H. Kolm, "Magnetic Separation in Water Pollution Control-II," *IEEE Trans. Magn.*, *Mag-11*, 1570 (1975).

29. Steiner, B.A., "Air Pollution Control in the Iron and Steel Industry," *International Metals Review*, No. 209, 171 (1978).

30. Jaasund, S.A., and M.R. Mazer, The Application of Wet Electrostatic Precipitators for the Control of Emissions from Three Metallurgical Processes," *Proceedings: Particulate Collection Problems Using ESP's in the Metallurgical Industry*, PB 274-017-AS, National Technical Information Service, Springfield, VA (1977).

31. Whitehead, C., "Design and Operating Experience with Electrostatic Precipitators on Electric Arc Furnaces," *Proceedings: Particulate Collection Problems Using ESP's in the Metallurgical Industry*, PB 274-017/AS, National Technical Information Service, Springfield, VA (1977).

32. Harris, D.B., *Procedures for Cascade Impactor Calibration and Operation in Process Streams*, PB 263-623/AS, National Technical Information Service, Springfield, VA (1977).

33. Keyser, N.H., et al., *Characterization, Recovery and Recycling of Electric Arc Furnace Dust*, Paper presented at the Symposium on Iron and Steel Pollution Abatement Technology for 1981, Chicago, Illinois, October 6-8, 1981.

34. Severson, S.D., F.A. Horney, D.S. Ensor, and G.R. Markowski, Economic Evaluation of Fabric Filtration versus Electrostatic Precipitation for Ultrahigh Particulate Collection Efficiency, FP-775, Research Project 834-1, prepared for EPRI by Stearns-Roger, Inc., (1978).

35. "ES&T Currents," Environmental Science & Technology, Vol. 12, No. 13, December 1978.

36. Neveril, R.B., *Capital and Operating Costs of Selected Air Pollution Control Systems*, EPA 450/5-80-002, U.S. Environmental Protection Agency, Research Triangle Park, NC (1978).